

1
2
3
4
5
6
7
8
9
10
11
12
13
14
15
16
17
18
19
20
21
22
23
24
25
26
27
28
29
30
31
32
33
34
35
36
37
38
39
40
41
42
43
44
45
46
47
48
49
50
51
52
53
54
55
56
57
58
59
60

	Felder, Eduard; Oncology, Nerviano Medical Sciences, Chemical Core Technologies Donati, Daniele; Oncology, Nerviano Medical Sciences, Medicinal Chemistry Montagnoli, Alessia; Oncology, Nerviano Medical Sciences, Cell Biology

SCHOLARONE™
Manuscripts

1
2
3
4
5
6
7
8
9
10
11
12
13
14
15
16
17
18
19
20
21
22
23
24
25
26
27
28
29
30
31
32
33
34
35
36
37
38
39
40
41
42
43
44
45
46
47
48
49
50
51
52
53
54
55
56
57
58
59
60

Discovery of 2-[1-(4,4-difluorocyclohexyl)piperidin-4-yl]-6-fluoro-3-oxo-2,3-dihydro-1H-isoindole-4-carboxamide (NMS-P118): a Potent, Orally Available and Highly Selective PARP-1 Inhibitor for Cancer Therapy

Gianluca Papeo,^{a} Helena Posteri,^a Daniela Borghi,^a Alina A. Busel,^b Francesco Caprera,^a Elena Casale,^a Marina Ciomei,^a Alessandra Cirila,^a Emiliana Corti,^a Matteo D'Anello,^a Marina Fasolini,^a Barbara Forte,^{a±} Arturo Galvani,^a Antonella Isacchi,^a Alexander Khvat,^b Mikhail Y. Krasavin,^{b,†} Rosita Lupi,^a Paolo Orsini,^a Rita Perego,^a Enrico Pesenti,^a Daniele Pezzetta,^c Sonia Rainoldi,^a Federico Riccardi-Sirtori,^a Alessandra Scolaro,^a Francesco Sola,^a Fabio Zuccotto,^{a±} Eduard R. Felder,^a Daniele Donati^a and Alessia Montagnoli^a*

^a Oncology, Nerviano Medical Sciences S.r.l., Viale Pasteur 10, 20014 Nerviano, Milan, Italy

^b Chemical Diversity Research Institute, Rabochaya St. 2 Khimki, Moscow Region, Russia
114401

^c Accelera S.r.l., Viale Pasteur 10, 20014 Nerviano, Milan, Italy

ABSTRACT

The nuclear protein poly(ADP-ribose) polymerase-1 (PARP-1) has a well-established role in the signaling and repair of DNA and is a prominent target in oncology, as testified by the number of candidates in clinical testing that unselectively target both PARP-1 and its closest isoform PARP-2. The goal of our program was to find a PARP-1 selective inhibitor that would potentially mitigate toxicities arising from cross-inhibition of PARP-2. Thus, an HTS campaign on the proprietary Nerviano Medical Sciences (NMS) chemical collection, followed by SAR optimization allowed us to discover 2-[1-(4,4-difluorocyclohexyl)piperidin-4-yl]-6-fluoro-3-oxo-2,3-dihydro-1*H*-isoindole-4-carboxamide (NMS-P118, **20by**). NMS-P118 proved to be a potent, orally available and highly selective PARP-1 inhibitor endowed with excellent ADME and pharmacokinetic profiles and high efficacy *in vivo* both as a single agent and in combination with temozolomide, in MDA-MB-436 and CAPAN-1 xenograft models, respectively. Co-crystal structures of **20by** with both PARP-1 and PARP-2 catalytic domain proteins allowed rationalization of the observed selectivity.

Introduction

The 113 KDa nuclear protein poly(ADP-ribose) polymerase-1 (PARP-1) is the most abundant and well-characterized member of the diphtheria toxin-like ADP-ribosyltransferase (ARTD) family of enzymes.¹ PARP-1 (*aka* ARTD-1) exerts its multifaceted biological roles^{2,3} through the construction of short-lived negatively charged ADP-ribose homopolymers [poly(ADP-ribose), PAR] either on PARP-1 itself (auto-modification) or on different acceptor proteins (hetero-modification). Transferral of monomer units to the growing poly(ADP-ribose) chain exploits the

1
2
3 intermediacy of a reactive oxonium ion species which, in turn, arises from the PARP-1-catalyzed
4 detachment of nicotinamide from nicotinamide adenine dinucleotide (NAD⁺).⁴ The well-
5 documented involvement of PARP-1 in the signaling and repair of DNA damage as well as its
6 over-activation in several pathological contexts, triggered a number of aggressive medicinal
7 chemistry programs aimed at the discovery of PARP-1 inhibitors, potentially useful in
8 therapeutic areas as diverse as stroke, cardiac ischemia, diabetes, inflammation and cancer.⁵
9 Presently, the primary focus of these efforts still concerns oncology, as testified by the
10 tremendous amount of pre-clinical and clinical data produced in the field.⁶ From an historical
11 perspective, PARP-1 inhibitors entered the arena as promising co-adjuvant components of
12 standard chemo- and radiotherapy regimens. Later, the discovery that tumor cell lines bearing
13 deficiencies or mutations in DNA-repair genes (e.g. BRCA1 or BRCA2) do not tolerate PARP-1
14 inhibition,⁷ fuelled the application of PARP inhibitors as single agent therapies in breast and
15 ovarian BRCA-mutated cancer settings. More recently, the discovery of new potential
16 combinative synergisms (e.g. PI3K,⁸ NAMPT⁹ and EGFR¹⁰ inhibitors) as well as the broadening
17 of “synthetic lethality” contexts (e.g. PTEN¹¹ and ATM¹² mutations, MSI colorectal cancer
18 phenotypes¹³ and Ewing’s sarcomas¹⁴) in which the inhibition of PARP-1 can be therapeutically
19 valuable has further raised interest in this target. Currently, eight PARP inhibitors are at different
20 stages of clinical investigation, targeting several tumors types either in combination or as single
21 agents.⁵ These clinical candidates, as well as all known pre-clinical PARP-1 inhibitors, were
22 designed to imitate the nicotinamide portion of NAD⁺, with which they compete for the
23 corresponding PARP-1 binding site. Accordingly, PARP-1 inhibitors are systematically endowed
24 with two peculiar nicotinamide-mimic motifs: (1) a rotationally constrained primary amide as,
25 for instance, in clinical candidates such as Veliparib (Abbott, Figure 1)¹⁵ and Niraparib
26 (Merck/Tesaro, Figure 1)¹⁶ or (2) an amide embedded in a ring as in Rucaparib (Pfizer/Clovis,
27
28
29
30
31
32
33
34
35
36
37
38
39
40
41
42
43
44
45
46
47
48
49
50
51
52
53
54
55
56
57
58
59
60

1
2
3 Figure 1),¹⁷ Olaparib (AstraZeneca, now marketed as Lynparza, Figure 1)¹⁸ and Talazoparib
4
5 (BioMarin, Figure 1).¹⁹ Within the PARP family of enzymes, none of these inhibitors selectively
6
7 inhibits PARP-1. For instance, all the clinical candidates and the vast majority of reported PARP
8
9 inhibitors also interact with PARP-2 (84% identity and 90% similarity within the PARP
10
11 signature motif^{2,3a}) with similar potencies, as recently independently described by Wahlberg²⁰
12
13 and ourselves.²¹ PARP-2 (*aka* ARTD-2)¹ is a 62 KDa nuclear protein and, like PARP-1, is
14
15 involved in DNA single strand break repair. However, its contribution to the total DNA damage
16
17 induced PARP activity is minimal (5 to 10%).²² Specifically, PARP-2 has been postulated to
18
19 participate in later steps of the DNA repair process, by recognizing gaps and flaps and by the
20
21 delayed and persistent accumulation at UV laser induced damaged sites.³ Moreover, PARP-2
22
23 depleted cells show increased sensitivity to ionizing radiation, indicating a role in the IR induced
24
25 DNA damage and suggesting a potential application for PARP-2 inhibitors in combination with
26
27 irradiation.²³ Aside from PARP-1 and -2 overlapping functions, as clearly demonstrated by the
28
29 embryonic lethality in double knockout mice, *PARP-2*^{-/-} single knockout mice show impaired
30
31 spermatogenesis, adipogenesis and thymopoiesis. These *PARP-2*^{-/-} mice furthermore suffer from
32
33 increased neuronal loss after ischemic damage and are more prone to develop pancreatitis
34
35 following chemical insult.²² In addition, loss of PARP-2 has recently been shown to shorten
36
37 erythrocytes lifespan and to impair differentiation of erythroid progenitors, leading to chronic
38
39 anemia.²⁴ As all these physiological functions of PARP-2 can potentially result in undesirable
40
41 side-effects following its inhibition, we reasoned that a potent and highly selective PARP-1
42
43 inhibitor, if equally efficacious in cancer therapy as are dual PARP-1/-2 one, might represent a
44
45 significant advancement in the field. Crucial data that prompted us to embark upon this strategy
46
47 were the findings of Bryant^{7a} and Sharp,²⁵ proving that PARP-1 genetic depletion is sufficient to
48
49 induce death of BRCA2- and BRCA1-deficient tumor cell lines respectively, together with the
50
51
52
53
54
55
56
57
58
59
60

1
2
3 feasibility of PARP-1 selective inhibitors (**1** and **2** (BYK204165), Figure 2),^{26,27} which were
4
5 however designed for different therapeutic applications and did not progress to clinical testing.
6
7 Herein we describe the synthesis and SAR investigation of isoindolinone-4-carboxamide
8
9 derivatives, leading to the discovery of 2-[1-(4,4-difluorocyclohexyl)piperidin-4-yl]-6-fluoro-3-
10
11 oxo-2,3-dihydro-1*H*-isoindole-4-carboxamide (NMS-P118, **20by**, Figure 2). NMS-P118 is a
12
13 potent ($K_D = 0.009 \mu\text{M}$) PARP-1 inhibitor, showing 150-fold selectivity over PARP-2 ($K_D = 1.39$
14
15 μM). NMS-P118 possesses excellent pharmacokinetic profile and nearly complete oral
16
17 bioavailability both in mice and rats. It proved to be highly efficacious *in vivo* both as single
18
19 agent in MDA-MB-436 human breast cancer tumors and in combination with temozolomide in
20
21 CAPAN-1 human pancreatic tumors growing as xenografts in the mouse. The compound is well
22
23 tolerated at highly efficacious doses and is endowed with an excellent ADME profile.
24
25
26
27
28
29

30 Chemistry

31
32
33 Two synthetic pathways were exploited to access the planned isoindolinone-4-carboxamide
34
35 derivatives. The first one capitalizes on an intramolecular Diels-Alder reaction as the key step
36
37 (Scheme 1A).²⁸ Thus furfural was initially subjected to a reductive amination protocol in the
38
39 presence of suitable amines (**6a-u**) by pre-forming the Schiff bases which were then reduced with
40
41 sodium borohydride. The corresponding properly functionalized furanylmethylamines (**7a-u**)
42
43 reacted with maleic anhydride in a two-step fashion, by first delivering the transient maleic acid
44
45 monoamide which then underwent an intramolecular Diels-Alder reaction. As anticipated,²⁹ the
46
47 process is highly stereoselective, with only the *exo*-isomer being detected in the reaction mixture.
48
49 The *exo*- tricyclic adducts (**8a-u**) were then dehydrated by exposure to concentrated aqueous
50
51 hydrochloric acid at reflux, followed by conversion of the resulting carboxylic acids (**9a-u**) into
52
53 the desired primary amides using the ammonium salt of hydroxybenzotriazole in the presence of
54
55
56
57
58
59
60

1
2
3 EDCI as the coupling agent (**10a-u**). Despite the lack of a common intermediate, the synthetic
4
5 sequence depicted in Scheme 1A is nonetheless straightforward, since isoindolinone precursors
6
7 (**7a-u**)-(**9a-u**) did not require any purification step. Further manipulation of the eastern portion of
8
9 the isoindolinone core was achieved (Scheme 1B) by elaboration of the piperidin-4-yl- moiety of
10
11 **11**³⁰ after debenylation of **10u**. Compound **11** was then subjected to either acylation with acyl
12
13 chlorides in pyridine or reductive alkylation in different conditions according to the carbonyl-
14
15 counterpart affording compound **12a-c** or **13a-ag** respectively. To further investigate SAR within
16
17 this chemical class, a second synthetic route to access benzo-substituted isoindolinone-4-
18
19 carboxamide analogues was pursued (Scheme 2). The key step of this alternative approach is the
20
21 *ortho* iodination of properly functionalized 2-methylbenzoic acids (**14a-d**) through C-H
22
23 activation, as described by Yu *et al.*³¹ Intermediates **15a-d** were then transformed into the
24
25 corresponding methyl esters **16a-d** before being subjected to a radical bromination at the benzylic
26
27 position. Crude benzyl bromides underwent a one pot nucleophilic displacement – ring closure
28
29 sequence^{28c, 30, 32} in the presence of easily accessible³³ amines (**17x-y**), thus yielding iodo-
30
31 isoindolinone intermediates **18**. A Rosenmund – von Braun protocol was subsequently applied to
32
33 efficiently replace the iodine atom with a cyano group. Finally, the resulting isoindolinone-4-
34
35 carbonitriles (**19**) were smoothly converted into the corresponding primary amides through a
36
37 recently disclosed³⁴ indium (III) chloride-catalyzed transfer of water from acetaldoxime in
38
39 refluxing toluene, producing compounds **20bx** and **20(a-d)y**.
40
41
42
43
44
45
46
47
48

49 Results and Discussion

50
51
52 By using our recently reported PARP-1 full length (FL) fluorescence polarization displacement
53
54 assay,²¹ a high throughput screening (HTS) campaign was conducted on the NMS proprietary
55
56 chemical collection. Two isoindolinone-4-carboxamide derivatives (**10a** and **10b**, Table 1)
57
58
59
60

1
2
3 emerged from this screening, possessing good biochemical activity on PARP-1 (each showing
4 $K_D = 0.09 \mu\text{M}$). The isoindolinone core is a known privileged scaffold for PARP inhibition,⁴
5
6 either as a feature embedded within a tetracyclic structure (**3**, Figure 2)³⁵ or also, after appropriate
7
8 linkage to adenosine, in NAD⁺-resembling compounds such as EB-47 (**4**, Figure 2).³² Such
9
10 inhibitors rely on the isoindolinone lactam moiety as a nicotinamide mimic. Subsequently,
11
12 Abbott disclosed a series of 2-substituted isoindolinone-4-carboxamide derivatives (e.g. **5**, Figure
13
14 2),³⁰ in which the carbonyl oxygen atom of the scaffold freezes the primary amide into its
15
16 biologically active conformation through an intramolecular hydrogen bond, according to the
17
18 alternative PARP-1 pharmacophore discussed above. All these compounds proved to be potent
19
20 dual PARP-1/-2 inhibitors.^{21,30}
21
22
23
24
25
26
27

28 The two low molecular weight compounds which emerged from our HTS campaign are highly
29
30 efficient ligands³⁶ of PARP-1 (**10a**: MW = 218 Da, Binding Efficiency Index (BEI) = 32.3,
31
32 Ligand Efficiency (LE) = 0.6; **10b**: MW = 248 Da, BEI = 28.4, LE = 0.54). Both compounds
33
34 exhibited the desired mechanism of action in HeLa cells, i.e. both were able to inhibit PARP-1
35
36 dependent PAR synthesis in cells at micromolar concentrations following H₂O₂-induced DNA
37
38 damage (PAR assay, Table 1). However, a fluorescence polarization displacement assay²¹ using
39
40 PARP-2 showed that both **10a** and **10b** also significantly bind this isoform (Table 1). Despite the
41
42 moderate cellular activity and the lack of selectivity, the high intrinsic potency of these two hits
43
44 deserved further investigation. The X-ray co-crystal structures of **10b** in complex with both
45
46 human PARP-1 (hPARP-1, Figure 3A) and human PARP-2 (hPARP-2, Figure 3B) catalytic
47
48 domains were solved in order to gain insight into the corresponding binding modes. As
49
50 anticipated,³⁰ the pseudo 7-membered ring, arising from a γ -turn-like intramolecular hydrogen
51
52 bond, locked the isoindolinone-4-carboxamide core into the *anti* conformation. This
53
54
55
56
57
58
59
60

1
2
3 intramolecular interaction minimizes negative entropic contribution to the binding energy
4
5 balance, and allows **10b** to establish the usual network of hydrogen bonds within the proteins'
6
7 catalytic domains (i.e. with Gly863 and Ser904 in hPARP-1 and with Gly429 and Ser470 in
8
9 hPARP-2) and π -stacking (with Tyr907 in hPARP-1 and Tyr473 in hPARP-2) of a prototypical
10
11 nicotinamide-mimic inhibitor.⁴ In order to corroborate the presence of an intramolecular
12
13 hydrogen bond not only in the crystal form, but also in solution, ¹HNMR spectra of **10b** in
14
15 solvents with different polarity were recorded (Figure 4). The chemical shift difference ($\Delta\delta =$
16
17 3.08 ppm) between the downfield intramolecularly bonded amide proton and the upfield non-
18
19 bonded one observed in a polar solvent such as DMSO-*d*₆ (Figure 4A) is fully consistent with
20
21 this kind of interaction.³⁷ As expected, this difference was further exacerbated ($\Delta\delta = 5.44$ ppm)
22
23 in a non polar solvent such as CDCl₃ (Figure 4B). These data were further consolidated by a
24
25 quantitative assessment³⁸ of the intramolecular hydrogen bond strength (See Supporting
26
27 Information for details). A closer inspection of the X-ray co-crystal structures of compound **10b**
28
29 revealed that the methoxypropyl- side chain did not actively participate in binding of the inhibitor
30
31 either to PARP-1 or to PARP-2, thus affording the possible opportunity of increasing PARP-1
32
33 potency by tailoring the substituent onto the lactam nitrogen atom. To this purpose, an overlay of
34
35 co-crystal structures of **10b** and the selective quinazolinone inhibitor **1** (PDB Code: 1UK0)
36
37 within hPARP-1 catalytic domain was analyzed (Figure 5). This exercise clearly ruled out the
38
39 possibility to achieve selectivity against PARP-2 by engaging contacts within the adenine-ribose
40
41 (AD) binding site,^{26a} as the substituents departing from **10b** and **1** point at different portions of
42
43 the protein (see gray arrows in Figure 5). Nevertheless, compounds dramatically different in
44
45 shape such as BYK204165 (**2**)²⁷ indicated that selectivity against PARP-2 might be achieved by
46
47 targeting regions of the PARP-1 catalytic domain other than the AD site. Thus, a systematic
48
49
50
51
52
53
54
55
56
57
58
59
60

1
2
3 exploration of this chemical class was undertaken alongside determination of compound
4 selection criteria, based on biochemical potency (PARP-1 $K_D \leq 0.1 \mu\text{M}^{21}$) and selectivity (PARP-
5 2 K_D /PARP-1 K_D *ratio* of about 100^{39}) thresholds. Inhibitors endowed with these features would
6 then be tested to quantify their ability to suppress H_2O_2 -induced PAR synthesis in HeLa cells,
7 which is exclusively PARP-1 dependent (PAR assay, see above). Derivatives possessing $\text{IC}_{50} \leq$
8 $0.1 \mu\text{M}$ in this cellular assay would be considered eligible for preclinical profiling. Good oral
9 bioavailability of the selected compounds was considered mandatory for further development.
10 After having established these cutoff criteria, HTS hits **10a** and **10b** were employed as a footprint
11 to design a first array of isoindolinones. This set of compounds was assembled by varying: (a) the
12 length of the aliphatic spacer connecting the nitrogen atom of the bicyclic core to the terminal
13 eastern substituent and (b) the nature of the eastern substituent itself. Results are reported in
14 Table 1. Thus, within the alkoxy-substituted series, shortening the spacer proved to be
15 detrimental in terms of biochemical potency, regardless of whether the alkoxy group was linear
16 or whether the oxygen atom was embedded in a cycle (compare **10c** and (\pm)-**10d** with **10b**). On
17 the contrary, a hydroxyethyl substituent (**10e**) restored potency but did not possess PARP-1 vs.
18 PARP-2 selectivity. The biochemical activity of phenyl-substituted derivatives increased one
19 order of magnitude upon going from benzyl (**10f**) to 2-phenylethyl (**10g**), with the latter being
20 unacceptably potent also against PARP-2. A further elongation of the spacer (**10h**) impacted
21 neither potency nor selectivity. By replacing the phenyl ring present in **10g** with a pyridin-2-yl
22 moiety (**10i**) an increase in potency, mainly against PARP-2, was observed, with a K_D on both
23 isoforms below the assay sensitivity limit.²¹ By capitalizing on this result, we then investigated a
24 series of isoindolinones encompassing differently substituted tertiary aliphatic amines located at
25 a variable distance from the scaffold. Both the morpholin-4-yl-ethyl- (**10j**) and the 1-piperidin-1-

1
2
3 yl-ethyl- (**10l**) derivatives showed a lower potency against PARP-1 than the corresponding higher
4
5 homologues (**10k** and **10m**). Furthermore, compounds **10k** and **10m** showed, respectively, 160-
6
7 fold and > 110-fold selectivity towards PARP-1 over PARP-2 and were thus also profiled in the
8
9 cellular PAR assay. While isoindolinone **10k** showed no significant inhibition of PAR synthesis
10
11 in cells, the IC₅₀ value of **10m**, although modest, prompted us to further decorate the piperidinyl
12
13 moiety in an effort to obtain more potent derivatives. The introduction of a 2,6-dimethyl
14
15 substitution (*cis*-**10n**), as well as an additional piperidinyl ring (**10o**) resulted in a dramatic drop
16
17 of activity. On the contrary, a lipophilic substituent such as a benzyl group in the 4 position of the
18
19 piperidinyl ring (**10p**) restored the biochemical potency on both enzymes. The
20
21 tetrahydroisoquinolin-2-yl-ethyl derivative (**10r**) proved to be more potent against PARP-1 and
22
23 more selective towards PARP-2 than the corresponding isomeric tetrahydroquinolin-2-yl-ethyl
24
25 substituted isoindolinone (**10q**). Unfortunately, **10r** showed negligible activity in the cellular
26
27 PAR assay. A further investigation was then conducted by moving the linker connecting the
28
29 isoindolinone core to the piperidinyl ring from the 1- to the 4 position of the latter. The resulting
30
31 derivatives were garnished with a lipophilic substituent onto the piperidinyl nitrogen atom,
32
33 affording compounds **10s** and **10t**. While derivative **10s** strongly inhibited PARP-1 but its
34
35 selectivity towards PARP-2 was below our arbitrary threshold, the corresponding regioisomer
36
37 **10t** showed high biochemical potency on the target, excellent selectivity and cellular activity.
38
39 Compound **10t** was then subjected to *in vitro* ADME profiling and pharmacokinetic analysis in
40
41 mice (Table 2). Disappointingly, despite the excellent solubility and good permeability, **10t**
42
43 showed high clearance *in vivo* (230 mL/min/kg) and negligible (< 1%) oral bioavailability thus
44
45 preventing any further development. The preliminary SAR information emerged from this first
46
47 cohort of isoindolinones underlines that a three- to four-carbon unit spacer between the bicyclic
48
49 core and a basic center generally delivers the most potent and selective PARP-1 inhibitors. This
50
51
52
53
54
55
56
57
58
59
60

1
2
3 observation prompted us to investigate the modulation of the potency and selectivity by
4 embedding the spacer into a piperidine ring, whose nitrogen was initially decorated with a benzyl
5 group (**10u**, Table 1). This lipophilic moiety was carefully chosen either because of its impact on
6 the inhibitory activity within the series (see **10p**, **10s** and **10t**, Table 1) and because it can be
7 easily replaced by standard chemistry (Scheme 1B). Compound **10u** proved to be quite potent
8 against PARP-1 and exceedingly selective. However, its ability in inhibiting the PARylation in
9 cells was trifling ($IC_{50} = 2 \mu M$). A second array of piperidin-4-yl substituted isoindolinones was
10 then synthesized in order both to implement the biochemical and cellular activity and the
11 pharmacokinetic profile of the inhibitor. Results are reported in Table 3. The mandatory
12 requirement of a basic nitrogen atom within this subseries was corroborated by the modest
13 biochemical potency against PARP-1 of amide derivatives such as **12a-c**. Linear or branched
14 alkyl substituted piperidine (**13a-e**) delivered potent unselective compounds with flat SAR, while
15 the presence of an oxygen atom within the aliphatic chain (**13f**) depressed the ability in inhibiting
16 the target. More SAR information was gathered by playing around the initially selected benzyl
17 substituent (**10u**). Thus, the introduction of a simple (electron donating) methyl substituent in the
18 *ortho*, *meta* and *para* position of the phenyl ring, respectively, afforded both biochemically
19 potent and selective compounds (**13g-i**) whose enzymatic activity (**13i** = **13h** > **13g**) did not
20 stringently mirror the cellular one (**13i** > **13g** > **13h**). Moderately deactivating groups such as
21 bromine (**13j-l**) again confirmed the positive impact of a *para* substitution (**13l**) on both
22 biochemical potency and selectivity, however with no significant activity in cells. Strong electron
23 withdrawing (**13m-o**) or donating (**13p**) groups generally worsened the inhibitor profile by
24 delivering poorly active (**13m**), poorly selective (**13o**) or compounds lacking cellular activity
25 (**13n** and **13p**). The replacement of the phenyl ring with a pyridine (**13q-s**) produced potent and
26 selective compounds and, in the case of the pyridin-2-ylmethyl derivative (**13s**), also with good
27
28
29
30
31
32
33
34
35
36
37
38
39
40
41
42
43
44
45
46
47
48
49
50
51
52
53
54
55
56
57
58
59
60

(despite still suboptimal) cellular activity. Biochemically potent PARP-1 inhibitors also emerged by replacing the phenyl ring with a five-membered heterocycle such as thiophene (**13t-u**), furan (**13v-z**) and pyrrole (**13aa-ab**). However, the pair of compounds (**13u** and **13ab**) which proved also to be selective against PARP-2 according to our screening criteria delivered disappointing results in PAR assay. Indole regioisomers (**13ac-ad**) behaved quite differently. While **13ac** was not selective enough for further profiling, the potent and selective 5-substituted regioisomer (**13ad**) displayed an excellent cellular activity. Finally, few isoindolinones decorated with non-aromatic rings directly linked to the piperidine moiety (**13ae-ag**) were investigated. Despite being both potent and exceedingly selective, the 4,4-difluorocyclohexyl⁴⁰ substituted isoindolinone (**13af**) proved to be four times more active in cellular assay than the corresponding tetrahydro-2H-pyran-4-yl derivative (**13ae**). On the contrary, 1,3-dioxolane-containing compound **13ag** showed only modest inhibitory activity against PARP-1. Having identified three compounds (**13i**, **13ad** and **13af**) possessing the suitable biochemical potency, selectivity and cellular activity, they were further profiled by analyzing their *in vitro* ADME and pharmacokinetic properties. Whereas permeability, plasma protein binding and HLM clearance data were, on average, quite similar between the compounds, isoindolinone **13af** showed a definitely higher solubility (Table 4). The PK profiles in mouse allowed selecting **13af** as the lead compound of this isoindolinones subset (Table 5). In fact, while **13i** demonstrated to possess low oral bioavailability (15%) and **13ad**, despite being orally available (80%), it is rapidly cleared from the body (110 mL/min/kg), **13af** proved to be suitable for oral administration (80%) with high exposure (21 μ Mh) and low clearance (17 mL/min/kg). With the proper arrangement of the right end portion of the inhibitor in hand, a final medicinal chemistry refinement was undertaken in the attempt to further improve **13af** cellular activity. The potency of **13af** in PAR assay was indeed suboptimal ($IC_{50} = 0.15$ μ M). The planned optimization was focused on the preparation of a handful of compounds

1
2
3 bearing small substituents on the phenyl ring of the isoindolinone bicyclic core, as the features of
4 the back wall of PARP-1 hosting the nicotinamide moiety prevents the introduction of large
5 groups.⁴ The biochemical and cellular activities of this set of inhibitors are reported in Table 6.
6
7
8 As none of the substituents introduced in the different positions of the aromatic ring are expected
9 to deliver any steric clash within the catalytic site of the protein, SAR rationalization has to be
10 found in the substituents' aptitude in modulating the stereoelectronic properties of the inhibitors.
11
12 Thus, the tremendous drop in biochemical activity of **20ay** against PARP-1 was attributed to the
13 loosening of the intramolecular hydrogen bond between the primary amide and the carbonyl
14 oxygen by the fluorine atom in position 5. This effect can be appreciated observing the small
15 chemical shift differences between the two amide protons in the ¹H NMR spectra of **20ay** (Table
16 7 and Supplementary Table 1),^{37,38} and is reasonably due to electron pair repulsion leading to
17 conformational destabilization where the fluorine atom and the carbonyl are coplanar. A
18 reduction in the intramolecular hydrogen bond strength, again measured as a decrease in the $\Delta\delta$
19 chemical shift between the two amide protons might also account for the lower inhibitory activity
20 displayed by the 7-fluoro isoindolinone **20cy** compared to **13af** (Table 7 and Supplementary
21 Table 1). On the other hand, in order to rationalize the high biochemical potency observed for
22 both the 6-fluoro **20by** and the corresponding 6-chloro derivative **20dy**, additional interactions
23 within the PARP-1 protein binding site were presumed (and later demonstrated, see below) to
24 counterbalance the substituent's negative impact on hydrogen bond strength (Table 7 and
25 Supplementary Table 1). Since **20by** was the most potent compound in PAR assay ($IC_{50} = 0.04$
26 μM), the replacement of fluorine- with chlorine atoms onto the cyclohexyl moiety⁴¹ was then
27 investigated by synthesizing compound **20bx** (Table 6). Isoindolinone **20bx** proved to be
28 biochemically potent, selective against PARP-2 (as were all tested examples belonging to this
29 subseries) and displayed an excellent activity in cells, thus demonstrating the importance of a
30
31
32
33
34
35
36
37
38
39
40
41
42
43
44
45
46
47
48
49
50
51
52
53
54
55
56
57
58
59
60

1
2
3 properly 4-substituted cyclohexyl moiety to deliver PARP-1 inhibitors effective at a cellular
4
5 level. In order to gain a deeper insight into **20by** selectivity profile, the compound was tested
6
7 against PARP-3 FL (*aka* ARTD-3; $K_D = 0.69 \mu\text{M}$),²¹ TNKS-1 catalytic domain (*aka* PARP-5a,
8
9 ARTD-5; $K_D > 10 \mu\text{M}$),²¹ sirtuin 1 (SIRT1; $IC_{50} > 10 \mu\text{M}$). Since clinical PARP inhibitors, such
10
11 as rucaparib and veliparib, show micromolar inhibitory activity also on some kinases,⁴²
12
13 compound **20by** was also tested on a panel of 56 different kinases to assess its selectivity ($IC_{50} >$
14
15 $10 \mu\text{M}$; see experimental section for details). Furthermore, to confirm the fluorescence
16
17 polarization displacement assay data, **20by**, along with **13af** and the (unselective) **13c** were also
18
19 tested against PARP-1 and PARP-2 catalytic domain by Surface Plasmon Resonance (SPR), an
20
21 independent binding assay.²¹ For comparative purposes, also the clinical candidates olaparib and
22
23 veliparib (Figure 1) were tested in this assay.²¹ SPR results are reported in Table 8. While **13c**, as
24
25 expected (Table 2), showed similar potency against both isoforms, isoindolinone **13af** exhibits a
26
27 PARP-1 $K_D = 0.016 \mu\text{M}$ and has approximately 75-fold less affinity for PARP-2. Finally,
28
29 compound **20by** proved to be a single digit nanomolar PARP-1 inhibitor ($K_D = 0.009 \mu\text{M}$), with
30
31 exquisite selectivity versus PARP-2 ($K_D = 1.39 \mu\text{M}$). Detailed kinetic parameters
32
33 (Supplementary Table 2) and kinetic analysis (Supplementary Figure 1) of this assay can be
34
35 found in Supporting Information. The approximately 30% decrease in mere efficiency of binding
36
37 (MW = 395 Da, BEI = 20.4, LE = 0.39), compared to the initial hits' efficiency (*vide supra*),
38
39 underscores the fact that late stage optimization of **20by** favoured modifications contributing to
40
41 the overall developability and bioactivity, not just focusing on molecular binding interactions
42
43 alone.
44
45
46
47
48
49
50
51
52

53
54 Compound **20by** was tested along with **13af** for the ability to inhibit proliferation of MDA-MB-
55
56 436, a triple negative (HER2/ER/PR –ve) breast cancer cell line carrying BRCA1 gene mutation.
57
58
59
60

1
2
3 The isoindolinone **20by** resulted about 4 times more potent compared to **13af**, with IC₅₀ of 0.14
4 and 0.6 μM respectively, reflecting the higher target inhibition in PAR assay. Cellular models
5
6 such as MCF7 and MIA-PACA that do not have BRCA mutations or HR defects were resistant to
7
8 both compounds with IC₅₀s >10 μM (Table 9). Aiming at rationalizing the high selectivity
9
10 against PARP-2 showed by **20by**, its X-ray co-crystal structures within the catalytic domains of
11
12 hPARP-1 (Figure 6A) and hPARP-2 (Figure 6B) were solved. As expected, the contacts
13
14 established by the isoindolinone-4-carboxamide core of **20by** mirrored those of **10b** (see Figure
15
16 3A and 3B). Additionally, the fluorine atom at position 6 fills a small cavity present in the
17
18 binding sites of both proteins (defined by Phe897, Ala898, Lys903 and Glu988 residues in
19
20 PARP-1 and by Phe463, Ala464, Lys469 and Glu558 residues in PARP-2) and interacts with the
21
22 backbone carbonyl of Phe897 in PARP-1 and Phe463 in PARP-2. The (4,4-
23
24 difluorocyclohexyl)piperidinyl- moiety points towards the donor loop and the α-helical bundle
25
26 domain, thus allowing the 4,4-difluorocyclohexyl ring to fill an induced pocket, to trigger the
27
28 rearrangement of α-helix 5, and to establish favorable hydrophobic interactions with a tyrosine
29
30 residue of the donor loop (Tyr889 in PARP-1 and Tyr455 in PARP-2). The slightly dissimilar
31
32 orientation of α-helix 5 in the two proteins, together with the presence of different residues
33
34 (Gln759 and Val762 in PARP-1 and Ile328 and Ser331 in PARP-2) may account for the
35
36 selectivity observed, as the induced pocket is larger in PARP-1 (Figure 6A) than in PARP-2
37
38 (Figure 6B). As a result, the 4,4-difluorocyclohexyl substituent is better accommodated in PARP-
39
40 1. The observation that α helix 5 is intrinsically closer to the active site in PARP-2 than in
41
42 PARP-1,⁴³ further supports the hypothesis that the aforementioned rearrangement is energetically
43
44 less favorable in PARP-2. In order to better characterize **20by**, experiments of cross species
45
46 metabolic stability in liver hepatocytes (Supplementary Table 3), cytochrome P450 inhibition
47
48
49
50
51
52
53
54
55
56
57
58
59
60

1
2
3 (Supplementary Table 4) and *in vitro* myelotoxicity across species (Supplementary Table 5), the
4
5 latter in comparison with olaparib (Figure 1), were performed. Compound **20by** proved to be
6
7 metabolically stable, it modestly inhibited two cytochrome P450 family members (CYP-2B6
8
9 IC₅₀: 8.15 μM; CYP-2D6 IC₅₀: 9.51 μM) out of eight isoforms tested. Its ability in hampering the
10
11 proliferation of bone marrow cells was from 5 to > 60 times lower than olaparib according to the
12
13 species.
14
15

16
17
18 Overall, compound **20by** appeared the most promising and was further progressed by evaluating
19
20 its ADME and pharmacokinetic parameters in mouse, which proved to be excellent (Table 10).
21
22 The compound showed high solubility and permeability, low *in vitro* and *in vivo* clearance and
23
24 complete oral bioavailability. The pharmacokinetic profile of **20by** in rat dosed iv at 10 mg/kg
25
26 and orally at 10 and 100 mg/kg (Table 10), mirrored that observed in mouse, with oral
27
28 bioavailability >65%, and linearity of exposure with dose.
29
30
31

32
33 To assess the *in vivo* anti-tumor activity of compound **20by** when used as single agent, we treated
34
35 nude mice bearing established subcutaneous MDA-MB-436 tumor xenografts (Figure 7). Oral
36
37 administration of compound **20by** for 28 days (once a day dose of 150 mg/kg) as a methocel
38
39 suspension significantly inhibited tumor growth, inducing complete response (tumor impalpable)
40
41 in all treated mice with no signs of toxicity or body weight loss. Six out of seven mice were still
42
43 tumor free one month after the end of treatment.
44
45
46

47
48 We also examined the effect of combining **20by** with temozolomide *in vivo*. Tumor growth of
49
50 subcutaneously implanted Capan-1 pancreatic xenografts was significantly inhibited when
51
52 animals were treated by oral administration of 100 mg/kg **20by** in combination with 50 mg/kg of
53
54 temozolomide. Even in the absence of significant anti tumor activity for the two compounds
55
56
57
58
59
60

1
2
3 given as single agent, **20by** strongly potentiated temozolomide, resulting in complete tumor
4 regressions in 3 out of 6 animals (Figure 8). Only a slight increase in body weight loss was
5
6 observed compared to the group treated with temozolomide alone.
7
8
9

10
11 To assess the *in vivo* pharmacodynamics of **20by**, Capan-1 xenograft-bearing mice received a
12 single oral administration of 100 mg/kg of compound. Tumors were harvested at 1, 2, 6 and 24
13 hours after treatment, and intra-tumor PAR levels were determined by ELISA. **20by** treatment
14 dramatically decreased intra-tumoral PAR levels at 1, 2 and 6 hours after administration,
15
16 confirming its expected mechanism of action also *in vivo*. Partial recovery of PAR levels was
17
18 observed at 24 hours (Figure 9).
19
20
21
22
23
24
25

26 Conclusion

27
28
29
30 PARP inhibitors currently undergoing clinical trials in oncology are unselective PARP-1/-2
31 inhibitors. Poly(ADP-ribose) polymerase-2 (PARP-2), the closest isoform of PARP-1, has a
32 number of reported physiological functions other than its subsidiary role in DNA repair. These
33 considerations inspired our efforts towards developing selective PARP-1 inhibitors as potentially
34 better tolerated drugs, especially in view of potential drug/drug combination settings. An HTS
35 campaign on our proprietary collection was performed, followed by an intensive medicinal
36 chemistry exploration around the resulting moderately potent, but unselective isoindolinone-4-
37 carboxamide hits **10a** and **10b**. Investigation of the substituent on the nitrogen atom of the bicyclic
38 core allowed the discovery of the selective **13af**, whose cellular activity and pharmacokinetic
39 properties were however still suboptimal. To further gain insight into the SAR of isoindolinone-
40 4-carboxamides, a completely different synthetic route was then implemented to access
41 derivatives modified on the aromatic ring of the bicyclic scaffold. These efforts successfully
42
43
44
45
46
47
48
49
50
51
52
53
54
55
56
57
58
59
60

1
2
3 culminated in the discovery of **20by** (NMS-P118), a potent and exceedingly selective PARP-1
4 inhibitor, whose unprecedented selectivity might reside in its distinct binding poses within the
5 catalytic domains of PARP-1 and PARP-2. NMS-P118 shows excellent ADME and
6 pharmacokinetic profiles, high oral availability in the mouse and rat and high efficacy both as a
7 single agent and in combination with temozolomide in BRCA1-mutated MDA-MB-436 and
8 BRCA-2 deficient CAPAN-1 human tumor xenograft models, respectively. NMS-P118 was
9 found to be less myelotoxic *in vitro* than olaparib (now marketed as Lynparza), a dual PARP-1/-2
10 inhibitor. NMS-P118 is, to our knowledge, the first PARP-1 selective inhibitor with
11 demonstrated anticancer activity as single agent, as well as in combination, and thus we provide
12 compelling proof-of-concept that the sole pharmacological inhibition of PARP-1 vs. PARP-2 is
13 sufficient for achieving high antitumor efficacy in BRCA deficient tumor settings.
14
15
16
17
18
19
20
21
22
23
24
25
26
27
28
29

30 **Experimental Section**

31
32 **1. Chemistry.** All solvents and reagents, unless otherwise stated, were high grade, commercially
33 available and were used without further purification. All experiments dealing with moisture-
34 sensitive compounds were conducted under dry nitrogen or argon. Organic solutions were
35 evaporated using a Heidolph WB 2001 rotary evaporator at 15-20 mmHg. Thin-layer
36 chromatography was performed on Merck silica gel 60 F₂₅₄ pre-coated plates. Flash
37 Chromatography was performed on silica gel (Merck grade 9395, 60A). All tested compounds,
38 reported in the present paper, possess a purity of at least 95% as determined by an HPLC-UV/MS
39 method. HPLC Analyses were performed on Waters XTerra RP18 (4,6 x 50 mm, 3.5 μm) column
40 using a Waters 2790 HPLC system equipped with a 996 Waters PDA detector and Micromass
41 ZQ single quadrupole mass spectrometer, equipped with an electrospray (ESI) ion source. Mobile
42 phase A was ammonium acetate 5 mM buffer (pH 5.5 with AcOH-acetonitrile 95:5), and Mobile
43
44
45
46
47
48
49
50
51
52
53
54
55
56
57
58
59
60

1
2
3 phase B was water-acetonitrile (5:95). Gradient from 10 to 90% B in 8 minutes, hold 90% B 2
4
5 minutes. UV detection at 220 nm and 254 nm. Flow rate 1 mL/min. Injection volume 10 μ L. Full
6
7 scan mass spectra were recorded in the mass range of 100-800 amu. Capillary voltage was 2.5
8
9 KV; source temperature was 120 $^{\circ}$ C; cone was 10 V. Mass are given as m/z ratio. When
10
11 necessary, compounds were purified by preparative HPLC on a Waters Symmetry C18 (19 x 50
12
13 mm, 5 μ m) column or on a Waters XTerra RP 18 (30 x 150 mm, 5 μ m) column using a Waters
14
15 preparative HPLC 600 equipped with a 996 Waters PDA detector and a Micromass ZMD single
16
17 quadrupole mass spectrometer, electrospray ionization (positive ion mode). Mobile phase A was
18
19 water-0.01% TFA, and mobile phase B was acetonitrile. Gradient from 10 to 90% B in 8
20
21 minutes, hold 90% B 2 minutes. Flow rate 20 mL/min. Alternatively, mobile phase A was water-
22
23 0.1% NH_4OH , and mobile phase B was acetonitrile. Gradient from 10 to 100% B in 8 minutes,
24
25 hold 100% B 2 minutes. Flow rate 20 mL/min. ^1H -NMR spectra were recorded at 28 $^{\circ}$ C on a
26
27 Varian INOVA 400 spectrometer operating at 400.5 MHz for ^1H and equipped with 5 mm
28
29 $^1\text{H}\{^{15}\text{N}, ^{31}\text{P}\}$ z axis PFG Indirect Detection Probe, at 25 $^{\circ}$ C on a Varian INOVA 500
30
31 spectrometer operating at 499.75 MHz for ^1H and equipped with 5 mm $^1\text{H}\{^{13}\text{C}, ^{15}\text{N}\}$ z axis PFG
32
33 Indirect Detection Probe and on a Varian Mercury 300 spectrometer operating at 300.5 MHz for
34
35 ^1H and equipped with 5mm PFG autoswitchable $^1\text{H}, ^{19}\text{F}, ^{13}\text{C} ^{31}\text{P}$ probe. Spectra were recorded in
36
37 DMSO- d_6 or CDCl_3 . Chemical shifts were referenced with respect to the residual solvent signal
38
39 (DMSO- d_6 : 2.50 ppm, CDCl_3 : 7.27 ppm). Data are reported as follows: chemical shift (δ),
40
41 multiplicity (s = singlet, d = doublet, t = triplet, q = quartet, bs = broad signal, td = triplet of
42
43 doublets, dd = doublet of doublets, ddd = doublet of doublets of doublets, m = multiplet),
44
45 coupling constants (Hz), and number of protons. As formerly reported,⁴⁴ ESI(+) high-resolution
46
47 mass spectra (HRMS) were obtained on a Q-ToF Ultima (Waters, Manchester, UK) mass
48
49 spectrometer directly connected with an Agilent 1100 micro-HPLC system (Palo Alto, US).
50
51
52
53
54
55
56
57
58
59
60

1
2
3 **1-benzyl-N-(furan-2-ylmethyl)piperidin-4-amine (7u)**. An equimolar solution of furan-2-
4
5
6
7
8
9
10
11
12
13
14
15
16
17
18
19
20
21
22
23
24
25
26
27
28
29
30
31
32
33
34
35
36
37
38
39
40
41
42
43
44
45
46
47
48
49
50
51
52
53
54
55
56
57
58
59
60
carbaldehyde (4.8 g, 50 mmol) and 1-benzylpiperidin-4-amine **6u** (9.5 g, 50 mmol) in dioxane (30 mL) was heated to reflux for 8 hours by employing a Dean-Stark apparatus. The reaction mixture was concentrated under vacuum and rinsed with ethanol (1000 mL). Sodium borohydride (2.08 g, 55 mmol) was added and the mixture was left overnight at room temperature. Then it was diluted with water and extracted with diethyl ether. The organic phase was dried over anhydrous sodium sulfate and concentrated under reduced pressure to give the title compound, employed in the following steps without any further purification.

2-(1-benzylpiperidin-4-yl)-1-oxo-1,2,3,6,7,7a-hexahydro-3a,6-epoxyisoindole-7-carboxylic acid (8u). To a solution of **7u** (13.3 g, 50 mmol) in tetrahydrofuran (140 mL) maleic anhydride (4.9 g, 50 mmol) was added. The reaction mixture was refluxed for 6 hours and stirred overnight at room temperature. The precipitate solid obtained was filtered, washed with diethyl ether and dried to give the desired compound as a white solid. ESI(+) MS: m/z 369 (MH^+).

2-(1-benzylpiperidin-4-yl)-3-oxo-2,3-dihydro-1H-isoindole-4-carboxylic acid (9u). Compound **8u** (18.4 g, 50 mmol) was dissolved in 37% hydrochloric acid (150 mL) and the solution was refluxed for 3 hours. The solvent was removed under reduced pressure to afford the resulting crude as hydrochloride salt. HRMS (ESI+): calcd. for $C_{21}H_{23}N_2O_3^+$ [$M + H$] $^+$ 351.1703; found 351.1706.

2-(1-benzylpiperidin-4-yl)-3-oxo-2,3-dihydro-1H-isoindole-4-carboxamide (10u).

To a solution of **9u** (19.3 g, 50 mmol) in N,N-dimethylformamide (300 mL) hydroxybenzotriazole ammonium salt (15.2 g, 100 mmol), 1-ethyl-3-(3'-dimethylamino)carbodiimide hydrochloric acid salt (19.2 g, 100 mmol) and triethylamine (17 mL, 200 mmol) were added. The reaction mixture was stirred at room temperature overnight. The solvent was removed under reduced pressure and the residue was dissolved in ethyl acetate.

1
2
3
4
5
6
7
8
9
10
11
12
13
14
15
16
17
18
19
20
21
22
23
24
25
26
27
28
29
30
31
32
33
34
35
36
37
38
39
40
41
42
43
44
45
46
47
48
49
50
51
52
53
54
55
56
57
58
59
60

The solution was washed with 15% ammonium hydroxide and the organic phase was dried over anhydrous sodium sulfate and concentrated in vacuo. The crude was purified by flash chromatography (dichloromethane/methanol 97:3) to afford the title compound (3.5 g, 20% over four steps) as a white solid. ^1H NMR (400 MHz, $\text{DMSO-}d_6$) δ 10.72 (bs, 1H), 8.20 (dd, $J = 7.4$, 1.5 Hz, 1H), 7.76 (dd, $J = 7.4$, 1.5 Hz, 1H), 7.71 (dd, $J = 7.4$, 7.4 Hz, 1H), 7.66 (bs, 1H), 7.36 - 7.30 (m, 4H), 7.30 - 7.20 (m, 1H), 4.56 (s, 2H), 4.11 - 4.00 (m, 1H), 3.51 (s, 2H), 2.96 - 2.88 (m, 2H), 2.15 - 2.03 (m, 2H), 1.90 - 1.70 (m, 4H). HRMS (ESI+): calcd. for $\text{C}_{21}\text{H}_{24}\text{N}_3\text{O}_2^+$ $[\text{M} + \text{H}]^+$ 350.1863; found 350.1874

Compounds 10a-t. By employment of the above-described procedure and using the suitably substituted amine **6a-t**, compounds **10a-t** were obtained.

3-oxo-2-propyl-2,3-dihydro-1H-isoindole-4-carboxamide (10a). ^1H NMR (400 MHz, $\text{DMSO-}d_6$) δ 10.76 (bs, 1H), 8.20 (d, $J = 7.6$ Hz, 1H), 7.76 (d, $J = 7.3$ Hz, 1H), 7.72 (dd, $J = 7.6$, 7.3 Hz, 1H), 7.66 (bs, 1H), 4.57 (s, 2H), 3.56 - 3.51 (m, 2H), 1.71 - 1.61 (m, 2H), 0.89 (t, $J = 7.3$ Hz, 3H). HRMS (ESI+): calcd. for $\text{C}_{12}\text{H}_{15}\text{N}_2\text{O}_2^+$ $[\text{M} + \text{H}]^+$ 219.1128; found 219.1122.

2-(3-methoxypropyl)-3-oxo-2,3-dihydro-1H-isoindole-4-carboxamide (10b). ^1H NMR (400 MHz, $\text{DMSO-}d_6$) δ 10.75 (bs, 1H), 8.21 (d, $J = 7.7$ Hz, 1H), 7.77 (d, $J = 7.3$ Hz, 1H), 7.72 (dd, $J = 7.7$, 7.3 Hz, 1H), 7.67 (bs, 1H), 4.58 (s, 2H), 3.66 - 3.60 (m, 2H), 3.40 - 3.36 (m, 2H), 3.24 (s, 3H), 1.92 - 1.84 (m, 2H). HRMS (ESI+): calcd. for $\text{C}_{13}\text{H}_{17}\text{N}_2\text{O}_3^+$ $[\text{M} + \text{H}]^+$ 249.1234; found 249.1232.

2-(2-methoxyethyl)-3-oxo-2,3-dihydro-1H-isoindole-4-carboxamide (10c). ^1H NMR (400 MHz, $\text{DMSO-}d_6$) δ 10.68 (bs, 1H), 8.20 (dd, $J = 7.5$, 1.3 Hz, 1H), 7.77 (dd, $J = 7.6$, 1.3 Hz, 1H), 7.72 (dd, $J = 7.6$, 7.5 Hz, 1H), 7.67 (bs, 1H), 4.61 (s, 2H), 3.75 (t, $J = 5.3$ Hz, 2H), 3.60 (t, $J =$

5.3 Hz, 2H), 3.28 (s, 3H). HRMS (ESI+): calcd. for $C_{12}H_{15}N_2O_3^+$ $[M + H]^+$ 235.1077; found 235.1083.

3-oxo-2-(tetrahydrofuran-2-ylmethyl)-2,3-dihydro-1*H*-isoindole-4-carboxamide (\pm -10d). 1H

NMR (400 MHz, DMSO- d_6) δ 10.66 (bs, 1H), 8.20 (dd, $J = 7.5, 1.3$ Hz, 1H), 7.77 (dd, $J = 7.6, 1.3$ Hz, 1H), 7.72 (dd, $J = 7.6, 7.5$ Hz, 1H), 7.67 (bs, 1H), 4.71 – 4.58 (m, 2H), 4.14 – 4.07 (m, 1H), 3.84 – 3.76 (m, 1H), 3.73 – 3.55 (m, 3H), 1.93 – 2.02 (m, 1H), 1.88 - 1.77 (m, 2H), 1.63 - 1.53 (m, 1H). HRMS (ESI+): calcd. for $C_{14}H_{17}N_2O_3^+$ $[M + H]^+$ 261.1234; found 261.1242.

2-(2-hydroxyethyl)-3-oxo-2,3-dihydro-1*H*-isoindole-4-carboxamide (10e). 1H NMR (400

MHz, DMSO- d_6) δ 10.77 (bs, 1H), 8.21 (dd, $J = 7.4, 1.2$ Hz, 1H), 7.77 (dd, $J = 7.6, 1.2$ Hz, 1H), 7.72 (dd, $J = 7.6, 7.4$ Hz, 1H), 7.66 (bs, 1H), 4.87 (t, $J = 5.2$ Hz, 1H), 4.63 (s, 2H), 3.70 – 3.60 (m, 4H). HRMS (ESI+): calcd. for $C_{11}H_{13}N_2O_3^+$ $[M + H]^+$ 221.0921; found 221.0919.

2-benzyl-3-oxo-2,3-dihydro-1*H*-isoindole-4-carboxamide (10f). 1H NMR (400 MHz, DMSO-

d_6) δ 10.59 (bs, 1H), 8.22 - 8.17 (m, 1H), 7.75 - 7.69 (m, 3H), 7.40 - 7.28 (m, 5H), 4.79 (s, 2H), 4.47 (s, 2H). HRMS (ESI+): calcd. for $C_{16}H_{15}N_2O_2^+$ $[M + H]^+$ 267.1128; found 267.1120.

3-oxo-2-(2-phenylethyl)-2,3-dihydro-1*H*-isoindole-4-carboxamide (10g). 1H NMR (400 MHz,

DMSO- d_6) δ 10.68 (bs, 1H), 8.19 (dd, $J = 7.3, 1.6$ Hz, 1H), 7.74 (dd, $J = 7.6, 1.6$ Hz, 1H), 7.70 (dd, $J = 7.6, 7.3$ Hz, 1H), 7.66 (bs, 1H), 7.32 - 7.25 (m, 4H), 7.23 - 7.18 (m, 1H), 4.49 (s, 2H), 3.85 – 3.80 (m, 2H), 3.00 - 2.94 (m, 2H). HRMS (ESI+): calcd. for $C_{17}H_{17}N_2O_2^+$ $[M + H]^+$ 281.1285; found 281.1295.

3-oxo-2-(3-phenylpropyl)-2,3-dihydro-1*H*-isoindole-4-carboxamide (10h). 1H NMR (400

MHz, DMSO- d_6) δ 10.74 (bs, 1H), 8.21 (dd, $J = 7.4, 1.5$ Hz, 1H), 7.78 - 7.75 (m, 1H), 7.75 - 7.70 (m, 1H), 7.67 (bs, 1H), 7.31 - 7.24 (m, 4H), 7.20 - 7.15 (m, 1H), 4.59 (s, 2H), 3.64 – 3.59

(m, 2H), 2.67 - 2.60 (m, 2H), 2.01 - 1.92 (m, 2H). HRMS (ESI+): calcd. for $C_{18}H_{19}N_2O_2^+$ [M + H]⁺ 295.1441; found 295.1433.

3-oxo-2-[2-(pyridin-2-yl)ethyl]-2,3-dihydro-1*H*-isoindole-4-carboxamide (10i). ¹H NMR (400 MHz, DMSO-*d*₆) δ 10.66 (bs, 1H), 8.48 (ddd, *J* = 4.9, 1.8, 1.0 Hz, 1H), 8.19 (dd, *J* = 7.4, 1.5 Hz, 1H), 7.75 (dd, *J* = 7.6, 1.5 Hz, 1H), 7.73 - 7.68 (m, 2H), 7.65 (bs, 1H), 7.32 (td, *J* = 7.8, 1.0 Hz, 1H), 7.23 (ddd, *J* = 7.5, 4.9, 1.0 Hz, 1H), 4.52 (s, 2H), 3.98 - 3.93 (m, 2H), 3.15 - 3.10 (m, 2H). HRMS (ESI+): calcd. for $C_{16}H_{16}N_3O_2^+$ [M + H]⁺ 282.1237; found 282.1243.

2-[2-(morpholin-4-yl)ethyl]-3-oxo-2,3-dihydro-1*H*-isoindole-4-carboxamide (10j).

¹H NMR (400 MHz, DMSO-*d*₆) δ 10.73 (bs, 1H), 8.20 (dd, *J* = 7.5, 1.3 Hz, 1H), 7.78 (dd, *J* = 7.6, 1.3 Hz, 1H), 7.72 (dd, *J* = 7.6, 7.5 Hz, 1H), 7.66 (bs, 1H), 4.64 (s, 2H), 3.71 (t, *J* = 6.2 Hz, 2H), 3.57 - 3.52 (m, 4H), 2.59 (t, *J* = 6.2 Hz, 2H), 2.46 - 2.41 (m, 4H). HRMS (ESI+): calcd. for $C_{15}H_{20}N_3O_3^+$ [M + H]⁺ 290.1499; found 290.1507.

2-[3-(morpholin-4-yl)propyl]-3-oxo-2,3-dihydro-1*H*-isoindole-4-carboxamide (10k). ¹H NMR (400 MHz, DMSO-*d*₆) δ 10.76 (bs, 1H), 8.20 (dd, *J* = 7.5, 1.2 Hz, 1H), 7.76 (dd, *J* = 7.6, 1.2 Hz, 1H), 7.71 (dd, *J* = 7.6, 7.5 Hz, 1H), 7.65 (bs, 1H), 4.58 (s, 2H), 3.61 (t, *J* = 7.1 Hz, 2H), 3.53 - 3.47 (m, 4H), 2.37 - 2.29 (m, 6H), 1.85 - 1.76 (m, 2H). HRMS (ESI+): calcd. for $C_{16}H_{22}N_3O_3^+$ [M + H]⁺ 304.1656; found 304.1664.

3-oxo-2-[2-(piperidin-1-yl)ethyl]-2,3-dihydro-1*H*-isoindole-4-carboxamide (10l).

¹H NMR (400 MHz, DMSO-*d*₆) δ 10.75 (bs, 1H), 8.20 (dd, *J* = 7.7, 1.2 Hz, 1H), 7.78 (dd, *J* = 7.4, 1.2 Hz, 1H), 7.72 (dd, *J* = 7.7, 7.4 Hz, 1H), 7.66 (bs, 1H), 4.63 (s, 2H), 3.68 (t, *J* = 6.3 Hz, 2H), 2.54 (t, *J* = 6.3 Hz, 2H), 2.43 - 2.36 (m, 4H), 1.50 - 1.42 (m, 4H), 1.41 - 1.32 (m, 2H). HRMS (ESI+): calcd. for $C_{16}H_{22}N_3O_2^+$ [M + H]⁺ 288.1707; found 288.1712.

3-oxo-2-[3-(piperidin-1-yl)propyl]-2,3-dihydro-1H-isoindole-4-carboxamide hydrochloride

(10m). ^1H NMR (400 MHz, DMSO- d_6) δ 10.58 (bs, 1H), 8.93 (bs, 1H), 8.21 (dd, $J = 7.6, 1.1$ Hz, 1H), 7.80 (dd, $J = 7.4, 1.1$ Hz, 1H), 7.74 (dd, $J = 7.6, 7.4$ Hz, 1H), 7.71 (bs, 1H), 4.59 (s, 2H), 3.66 (t, $J = 6.6$ Hz, 2H), 3.50 – 3.40 (m, 2H), 3.13 - 3.03 (m, 2H), 2.92 - 2.78 (m, 2H), 2.09 – 1.98 (m, 2H), 1.85 – 1.75 (m, 2H), 1.73 – 1.52 (m, 3H), 1.43 – 1.28 (m, 1H). HRMS (ESI+): calcd. for $\text{C}_{17}\text{H}_{24}\text{N}_3\text{O}_2^+ [\text{M} + \text{H}]^+$ 302.1863; found 302.1865.

cis-2-[3-(2,6-dimethylpiperidin-1-yl)propyl]-3-oxo-2,3-dihydro-1H-isoindole-4-carboxamide

(cis-10n). ^1H NMR (400 MHz, DMSO- d_6) δ 10.58 (bs, 1H), 8.72 (bs, 1H), 8.21 (dd, $J = 7.5, 1.2$ Hz, 1H), 7.80 (dd, $J = 7.6, 1.2$ Hz, 1H), 7.74 (dd, $J = 7.6, 7.5$ Hz, 1H), 7.70 (bs, 1H), 4.63 (s, 2H), 3.72 – 3.64 (m, 2H), 3.35 – 3.20 (m partially overlapped by water signal, 4 H), 2.06 – 1.93 (m, 2H), 1.89 – 1.80 (m, 2H), 1.54 – 1.43 (m, 4H), 1.25 (d, $J = 6.3$ Hz, 6H). HRMS (ESI+): calcd. for $\text{C}_{19}\text{H}_{28}\text{N}_3\text{O}_2^+ [\text{M} + \text{H}]^+$ 330.2176; found 330.2176.

2-[3-(1,4'-bipiperidin-1'-yl)propyl]-3-oxo-2,3-dihydro-1H-isoindole-4-carboxamide

dihydrochloride (10o). ^1H NMR (400 MHz, DMSO- d_6) δ 10.58 (bs, 1H), 9.38 (bs, 2H), 8.21 (dd, $J = 7.6, 1.2$ Hz, 1H), 7.80 (d, $J = 7.5, 1\text{H}$), 7.75 (dd, $J = 7.6, 7.5$ Hz, 1H), 7.72 (bs, 1H), 4.59 (s, 2H), 3.70 – 2.82 (m, 13H), 2.30 – 1.30 (m, 12H). HRMS (ESI+): calcd. for $\text{C}_{22}\text{H}_{33}\text{N}_4\text{O}_2^+ [\text{M} + \text{H}]^+$ 385.2598; found 385.2611.

2-[3-(4-benzylpiperidin-1-yl)propyl]-3-oxo-2,3-dihydro-1H-isoindole-4-carboxamide (10p).

^1H NMR (400 MHz, DMSO- d_6) δ 10.78 (bs, 1H), 8.21 (dd, $J = 7.4, 1.3$ Hz, 1H), 7.76 (dd, $J = 7.5, 1.3$ Hz, 1H), 7.72 (dd, $J = 7.5, 7.4$ Hz, 1H), 7.65 (bs, 1H), 7.28 – 7.23 (m, 2H), 7.19 – 7.13 (m, 1H), 7.12 – 7.09 (m, 2H), 4.56 (s, 2H), 3.62 – 3.56 (m, 2H), 2.87 – 2.74 (m, 2H), 2.41 (d, $J = 6.8$ Hz, 2H), 2.33 – 2.22 (m, 2H), 1.82 – 1.70 (m, 4H), 1.52 – 1.37 (m, 3H), 1.11 – 0.99 (m, 2H). HRMS (ESI+): calcd. for $\text{C}_{24}\text{H}_{30}\text{N}_3\text{O}_2^+ [\text{M} + \text{H}]^+$ 392.2333; found 392.2346.

2-[2-(3,4-dihydroquinolin-1(2H)-yl)ethyl]-3-oxo-2,3-dihydro-1H-isoindole-4-carboxamide

(10q). ^1H NMR (400 MHz, DMSO- d_6) δ 10.68 (bs, 1H), 8.20 (dd, $J = 7.6, 1.3$ Hz, 1H), 7.77 (dd, $J = 7.4, 1.3$ Hz, 1H), 7.72 (dd, $J = 7.6, 7.4$ Hz, 1H), 7.69 (bs, 1H), 6.97 – 6.92 (m, 1H), 6.88 – 6.85 (m, 1H), 6.75 - 6.70 (m, 1H), 6.49 – 6.44 (m, 1H), 4.65 (s, 2H), 3.78 – 3.73 (m, 2H), 3.58 – 3.53 (m, 2H), 3.34 - 3.28 (m overlapped by water signal, 2H), 2.69 – 2.65 (m, 2H), 1.88 - 1.80 (m, 2H). HRMS (ESI+): calcd. for $\text{C}_{20}\text{H}_{22}\text{N}_3\text{O}_2^+$ $[\text{M} + \text{H}]^+$ 336.1707; found 336.1692.

2-[2-(3,4-dihydroisoquinolin-2(1H)-yl)ethyl]-3-oxo-2,3-dihydro-1H-isoindole-4-carboxamide (10r).

^1H NMR (400 MHz, DMSO- d_6) δ 10.75 (bs, 1H), 8.19 (dd, $J = 7.6, 1.2$ Hz, 1H), 7.76 (dd, $J = 7.7, 1.2$ Hz, 1H), 7.69 (dd, $J = 7.7, 7.6$ Hz, 1H), 7.66 (bs, 1H), 7.11 – 7.00 (m, 4H), 4.65 (s, 2H), 3.81 (t, $J = 6.2$ Hz, 2H), 3.65 (s, 2H), 2.82 – 2.73 (bs, 6H). HRMS (ESI+): calcd. for $\text{C}_{20}\text{H}_{22}\text{N}_3\text{O}_2^+$ $[\text{M} + \text{H}]^+$ 336.1707; found 336.1722.

2-[[1-(4-methylbenzyl)piperidin-4-yl]methyl]-3-oxo-2,3-dihydro-1H-isoindole-4-

carboxamide (10s). ^1H NMR (400 MHz, DMSO- d_6) δ 10.72 (bs, 1H), 8.20 (dd, $J = 7.4, 1.6$ Hz, 1H), 7.77 – 7.74 (m, 1H), 7.74 – 7.69 (m, 1H), 7.66 (bs, 1H), 7.20 – 7.07 (m, 4H), 4.57 (s, 2H), 3.46 (d, $J = 7.2$ Hz, 2H), 3.39 (s, 2H), 2.82 - 2.72 (m, 2H), 2.27 (s, 3H), 1.95 – 1.82 (m, 2H), 1.82 – 1.68 (m, 1H), 1.65 - 1.53 (m, 2H), 1.30 – 1.16 (m, 2H). HRMS (ESI+): calcd. for $\text{C}_{23}\text{H}_{28}\text{N}_3\text{O}_2^+$ $[\text{M} + \text{H}]^+$ 378.2176; found 378.2183.

2-[[1-(3-methylbenzyl)piperidin-4-yl]methyl]-3-oxo-2,3-dihydro-1H-isoindole-4-

carboxamide (10t). ^1H NMR (400 MHz, DMSO- d_6) δ 10.72 (bs, 1H), 8.20 (dd, $J = 7.3, 1.5$ Hz, 1H), 7.77 – 7.73 (m, 1H), 7.73 – 7.69 (m, 1H), 7.66 (bs, 1H), 7.20 – 7.15 (m, 1H), 7.11 - 7.00 (m, 3H), 4.57 (s, 2H), 3.46 (d, $J = 7.3$ Hz, 2H), 3.39 (s, 2H), 2.80 - 2.74 (m, 2H), 2.28 (s, 3H), 1.94 –

1
2
3 1.85 (m, 2H), 1.83 – 1.70 (m, 1H), 1.62 - 1.54 (m, 2H), 1.29 – 1.18 (m, 2H). HRMS (ESI+):
4
5 calcd. for $C_{23}H_{28}N_3O_2^+$ $[M + H]^+$ 378.2176; found 378.2188.
6
7

8 **3-oxo-2-(piperidin-4-yl)-2,3-dihydro-1H-isoindole-4-carboxamide hydrochloride (11).** A
9
10 solution of **10u** (1.3 g, 3.72 mmol) in acetic acid (100ml) in the presence of Pd/C 10% (260 mg)
11
12 was hydrogenated at 50 psi for 8 hours. The mixture was filtered over a pad of celite and the
13
14 solution was concentrated to afford the title compound (900 mg, 93%). 1H NMR (400 MHz,
15
16 DMSO- d_6) δ 10.58 (bs, 1H), 8.82 (bs, 1H), 8.59 (bs, 1H), 8.21 (dd, $J = 7.5, 1.1$ Hz, 1H), 7.82
17
18 (dd, $J = 7.6, 1.1$ Hz 1H), 7.75 (dd, $J = 7.6, 7.5$ Hz, 1H), 7.71 (bs, 1H), 4.56 (s, 2H), 4.32 - 4.45
19
20 (m, 1H), 3.46 - 3.36 (m overlapped by water signal, 2H), 3.17 – 3.04 (m, 2H), 2.09 – 1.92 (m,
21
22 4H). HRMS (ESI+): calcd. for $C_{14}H_{18}N_3O_2^+$ $[M + H]^+$ 260.1394; found 260.1398.
23
24
25

26 **2-[1-(cyclopropylcarbonyl)piperidin-4-yl]-3-oxo-2,3-dihydro-1H-isoindole-4-carboxamide**
27
28 **(12b).** To a solution of **11** (60 mg, 0.23 mmol) in pyridine (2 ml) cyclopropanecarbonyl chloride
29
30 (26.4 mg, 0.25 mmol) was added. After stirring at 60 °C for 8 hours the solvent was removed
31
32 under reduced pressure and the crude was purified by flash chromatography
33
34 (dichloromethane/methanol 95:5) to give the desired compound (32 mg, 40%). 1H NMR (400
35
36 MHz, DMSO- d_6) δ 10.70 (bs, 1H), 8.21 (dd, $J = 7.2, 1.6$ Hz, 1H), 7.78 - 7.75 (m, 1H), 7.75 -
37
38 7.71 (m, 1H), 7.69 (bs, 1H), 4.57 (s, 2H), 4.60 – 4.38 (m, 2H), 4.40 – 4.30 (m, 1H), 3.40 – 3.19
39
40 (m partially overlapped by water signal, 1H), 2.76 – 2.65 (m, 1H), 2.07 – 2.00 (m, 1H), 1.97 –
41
42 1.54 (m, 4H), 0.83 – 0.67 (m, 4H). HRMS (ESI+): calcd. for $C_{18}H_{22}N_3O_3^+$ $[M + H]^+$ 328.1656;
43
44 found 328.1669.
45
46
47
48

49
50 Compounds **12a-12c**. Operating in an analogous way but employing suitably substituted starting
51
52 material, the following compounds were obtained:
53
54

55 **2-(1-acetylpiperidin-4-yl)-3-oxo-2,3-dihydro-1H-isoindole-4-carboxamide (12a).** 1H NMR
56
57 (400 MHz, DMSO- d_6) δ 10.69 (bs, 1H), 8.21 (dd, $J = 7.3, 1.5$ Hz, 1H), 7.78 - 7.75 (m, 1H), 7.75
58
59
60

1
2
3
4
5
6
7
8
9
10
11
12
13
14
15
16
17
18
19
20
21
22
23
24
25
26
27
28
29
30
31
32
33
34
35
36
37
38
39
40
41
42
43
44
45
46
47
48
49
50
51
52
53
54
55
56
57
58
59
60

– 7.70 (m, 1H), 7.69 (bs, 1H), 4.55 (s, 2H), 4.58 - 4.49 (m, 1H), 4.36 - 4.26 (m, 1H), 3.99 - 3.91 (m, 1H), 3.15 - 3.25 (m, 1H), 2.70 - 2.60 (m, 1H), 2.04 (s, 3H), 1.90 - 1.70 (m., 3H), 1.68 - 1.55 (m, 1H). HRMS (ESI+): calcd. for $C_{16}H_{20}N_3O_3^+$ $[M + H]^+$ 302.1499; found 302.1506.

2-[1-(cyclohexylcarbonyl)piperidin-4-yl]-3-oxo-2,3-dihydro-1H-isoindole-4-carboxamide

(12c). 1H NMR (400 MHz, DMSO- d_6) δ 10.69 (bs, 1H), 8.21 (dd, $J = 7.2, 1.7$ Hz, 1H), 7.77 - 7.70 (m, 2H), 7.69 (bs, 1H), 4.62 - 4.50 (m, 1H), 4.56 (s, 2H), 4.37 - 4.27 (m, 1H), 4.13 - 4.02 (m, 1H), 3.24 - 3.10 (m, 1H), 2.71 - 2.57 (m, 2H), 1.93 - 1.50 (m, 8H), 1.47 - 1.09 (m, 6H). HRMS (ESI+): calcd. for $C_{21}H_{28}N_3O_3^+$ $[M + H]^+$ 370.2125; found 370.2117.

2-[1-(4,4-difluorocyclohexyl)piperidin-4-yl]-3-oxo-2,3-dihydro-1H-isoindole-4-carboxamide

(13af). To a suspension of **11** (56 mg, 0.19 mmol) in dichloromethane (2 mL) 4,4-difluorocyclohexanone (37.5 mg, 0.28 mmol) sodium acetate (32 mg, 0.38 mmol) and methanol (0.3 mL) were added. The resulted solution was stirred at room temperature for 5 hours. Then sodium cyanoborohydride was added and the mixture was stirred overnight. Solvents were removed under reduce pressure and the residue was dissolved in dichloromethane and washed twice with water. The organic phase was dried over anhydrous sodium sulfate and concentrated in vacuo and the residue was purified by flash chromatography (dichloromethane/methanol 95:5) to give the title compound (33 mg, 45%). 1H NMR (400 MHz, DMSO- d_6) δ 10.73 (bs, 1 H), 8.20 (dd, $J = 7.4, 1.5$ Hz, 1H), 7.77 - 7.74 (m, 1H), 7.74 - 7.69 (m, 1H), 7.66 (bs, 1H), 4.55 (s, 2H), 4.09 - 3.95 (m., 1H), 3.00 - 2.90 (m, 2H), 2.66 - 2.44 (m overlapped by DMSO signal, 1H), 2.35 - 2.23 (m, 2H), 2.10 - 1.96 (m, 2H), 1.94 - 1.70 (m, 8H), 1.61 - 1.47 (m, 2H). HRMS (ESI+): calcd. for $C_{20}H_{26}F_2N_3O_2^+$ $[M + H]^+$ 378.1988; found 378.1982.

Compounds **13a-13ag**. Operating in an analogous way but employing suitably substituted starting material, the following compounds were obtained:

1
2
3 **2-(1-methylpiperidin-4-yl)-3-oxo-2,3-dihydro-1*H*-isoindole-4-carboxamide (13a).** ¹H NMR
4
5 (400 MHz, DMSO-*d*₆) δ 10.73 (bs, 1H), 8.21 (dd, *J* = 7.5, 1.2 Hz, 1H), 7.77 (dd, *J* = 7.6, 1.2 Hz,
6
7 1H), 7.73 (dd, *J* = 7.6, 7.5 Hz, 1H), 7.67 (bs, 1H), 4.56 (s, 2H), 4.06 – 3.98 (m, 1H), 2.91 - 2.85
8
9 (m, 2H), 2.21 (s, 3H), 2.06 – 1.97 (m, 2H), 1.88 - 1.78 (m, 2H), 1.78 - 1.70 (m, 2H). HRMS
10
11 (ESI+): calcd. for C₁₅H₂₀N₃O₂⁺ [M + H]⁺ 274.1550; found 274.1557.

12
13
14 **2-(1-ethylpiperidin-4-yl)-3-oxo-2,3-dihydro-1*H*-isoindole-4-carboxamide (13b).** ¹H NMR
15
16 (400 MHz, DMSO-*d*₆) δ 10.73 (bs, 1H), 8.20 (dd, *J* = 7.5, 1.5 Hz, 1H), 7.77 (dd, *J* = 7.6, 1.5 Hz,
17
18 1H), 7.72 (dd, *J* = 7.6, 7.5 Hz, 1H), 7.66 (bs, 1H), 4.55 (s, 2H), 4.09 – 3.98 (m, 1H), 3.01 - 2.95
19
20 (m, 2H), 2.36 (q, *J* = 7.1 Hz, 2H), 2.02 - 1.95 (m, 2H), 1.85 – 1.72 (m, 4H), 1.01 (t, *J* = 7.1 Hz,
21
22 3H). HRMS (ESI+): calcd. for C₁₆H₂₂N₃O₂⁺ [M + H]⁺ 288.1707; found 288.1707.

23
24
25 **3-oxo-2-[1-(propan-2-yl)piperidin-4-yl]-2,3-dihydro-1*H*-isoindole-4-carboxamide (13c).** ¹H
26
27 NMR (400 MHz, DMSO-*d*₆) δ 10.74 (bs, 1H), 8.21 (dd, *J* = 7.5, 1.3 Hz, 1H), 7.77 (dd, *J* = 7.6,
28
29 1.3 Hz, 1H), 7.72 (dd, *J* = 7.6, 7.5 Hz, 1H), 7.67 (bs, 1H), 4.56 (s, 2H), 4.10 – 3.96 (m, 1H), 2.96
30
31 – 2.84 (m, 2H), 2.80 – 2.68 (m, 1H), 2.30 – 2.18 (m, 2H), 1.83 – 1.69 (m, 4H), 0.99 (d, *J* = 6.1
32
33 Hz, 6H). HRMS (ESI+): calcd. for C₁₇H₂₄N₃O₂⁺ [M + H]⁺ 302.1863; found 302.1862.

34
35
36 **2-[1-(2-methylpropyl)piperidin-4-yl]-3-oxo-2,3-dihydro-1*H*-isoindole-4-carboxamide (13d).**
37
38 ¹H NMR (400 MHz, DMSO-*d*₆) δ 10.73 (bs, 1H), 8.20 (dd, *J* = 7.4, 1.5 Hz, 1H), 7.76 (d, *J* = 7.5
39
40 Hz, 1H), 7.72 (dd, *J* = 7.5, 7.4 Hz, 1H), 7.66 (bs, 1H), 4.56 (s, 2H), 4.08 – 3.98 (m, 1H), 2.96 –
41
42 2.89 (m, 2H), 2.06 (d, *J* = 6.2 Hz, 2H), 2.04 – 1.95 (m, 2H), 1.87 – 1.70 (m, 5H), 0.87 (d, *J* = 6.6
43
44 Hz, 6H). HRMS (ESI+): calcd. for C₁₈H₂₆N₃O₂⁺ [M + H]⁺ 316.2020; found 316.2020.

45
46
47 **2-[1-(cyclopropylmethyl)piperidin-4-yl]-3-oxo-2,3-dihydro-1*H*-isoindole-4-carboxamide**
48
49 **(13e).** ¹H NMR (400 MHz, DMSO-*d*₆) δ 10.73 (bs, 1H), 8.20 (dd, *J* = 7.5, 1.2 Hz, 1H), 7.77 (dd,
50
51 *J* = 7.6, 1.2 Hz, 1H), 7.72 (dd, *J* = 7.6, 7.5 Hz, 1H), 7.66 (bs, 1H), 4.56 (s, 2H), 4.10 – 3.97 (m,
52
53 1H), 3.13 - 3.04 (m, 2H), 2.21 (d, *J* = 6.3 Hz, 2H), 2.10 - 2.00 (m, 2H), 1.90 - 1.71 (m, 4H), 0.90
54
55
56
57
58
59
60

1
2
3 - 0.80 (m, 1H), 0.50 - 0.44 (m, 2H), 0.12 - 0.06 (m, 2H). HRMS (ESI+): calcd. for $C_{18}H_{24}N_3O_2^+$
4
5
6 $[M + H]^+$ 314.1863; found 314.1860.

7
8 **2-[1-(2-methoxyethyl)piperidin-4-yl]-3-oxo-2,3-dihydro-1H-isoindole-4-carboxamide (13f).**

9
10 1H NMR (400 MHz, DMSO- d_6) δ 10.73 (bs, 1H), 8.20 (dd, $J = 7.6, 1.3$ Hz, 1H), 7.76 (dd, $J =$
11
12 7.4, 1.3 Hz, 1H), 7.71 (dd, $J = 7.6, 7.4$ Hz, 1H), 7.66 (bs, 1H), 4.55 (s, 2H), 4.08 – 3.97 (m, 1H),
13
14 3.44 (t, $J = 5.8$ Hz, 2H), 3.24 (s, 3H), 3.02 - 2.95 (m, 2H), 2.53 – 2.47 (m overlapped by DMSO
15
16 signal, 2H), 2.14 – 2.06 (m, 2), 1.86 – 1.69 (m, 4H). HRMS (ESI+): calcd. for $C_{17}H_{24}N_3O_2^+$ $[M +$
17
18 $H]^+$ 318.1812; found 318.1811.

19
20
21 **2-[1-(2-methylbenzyl)piperidin-4-yl]-3-oxo-2,3-dihydro-1H-isoindole-4-carboxamide (13g).**

22
23 1H NMR (400 MHz, DMSO- d_6) δ 10.73 (bs, 1H), 8.20 (dd, $J = 7.3, 1.6$ Hz, 1H), 7.78 - 7.75 (m,
24
25 1H), 7.75 - 7.70 (m, 1H), 7.67 (bs, 1 H), 7.28 – 7.23 (m, 1H), 7.19 – 7.12 (m, 3H), 4.57 (s, 2 H),
26
27 4.14 - 4.02 (m, 1H), 3.47 (s, 2H), 2.96 - 2.88 (m, 2H), 2.35 (s, 3 H), 2.19 - 2.10 (m, 2 H), 1.88 –
28
29 1.73 (m, 4H). HRMS (ESI+): calcd. for $C_{22}H_{26}N_3O_2^+$ $[M + H]^+$ 364.2020; found 364.2034.

30
31
32 **2-[1-(3-methylbenzyl)piperidin-4-yl]-3-oxo-2,3-dihydro-1H-isoindole-4-carboxamide (13h).**

33
34 1H NMR (400 MHz, DMSO- d_6) δ 10.73 (bs, 1H), 8.21 (dd, $J = 7.3, 1.4$ Hz, 1H), 7.77 (dd, $J =$
35
36 7.4, 1.4 Hz, 1H), 7.72 (dd, $J = 7.4, 7.3$ Hz, 1H), 7.67 (bs, 1H), 7.25 – 7.19 (m, 1H), 7.16 - 7.05
37
38 (m, 3H), 4.58 (s, 2H), 4.13 – 4.00 (m, 1H), 3.47 (s, 2H), 2.98 - 2.87 (m, 2H), 2.32 (s, 3H), 2.13 -
39
40 2.04 (m, 2H), 1.90 - 1.72 (m, 4H). HRMS (ESI+): calcd. for $C_{22}H_{26}N_3O_2^+$ $[M + H]^+$ 364.2020;
41
42 found 364.2031.

43
44
45 **2-[1-(4-methylbenzyl)piperidin-4-yl]-3-oxo-2,3-dihydro-1H-isoindole-4-carboxamide (13i).**

46
47
48 1H NMR (400 MHz, DMSO- d_6) δ 10.73 (bs, 1H), 8.20 (dd, $J = 7.3, 1.5$ Hz, 1H), 7.77 (dd, $J =$
49
50 7.4, 1.5 Hz, 1H), 7.72 (dd, $J = 7.4, 7.3$ Hz, 1H), 7.67 (bs, 1 H), 7.23 - 7.18 (m, 2H), 7.16 - 7.12
51
52 (m, 2H), 4.57 (s, 2H), 4.11 – 4.00 (m, 1H), 3.46 (s, 2H), 2.96 - 2.88 (m, 2H), 2.30 (s, 3H), 2.12 -
53
54 (m, 2H), 1.90 - 1.72 (m, 4H). HRMS (ESI+): calcd. for $C_{22}H_{26}N_3O_2^+$ $[M + H]^+$ 364.2020;
55
56 found 364.2031.

2.03 (m, 2H), 1.88 - 1.71 (m, 4H). HRMS (ESI+): calcd. for $C_{22}H_{26}N_3O_2^+$ $[M + H]^+$ 364.2020; found 364.2033.

2-[1-(2-bromobenzyl)piperidin-4-yl]-3-oxo-2,3-dihydro-1H-isoindole-4-carboxamide (13j).

1H NMR (400 MHz, DMSO- d_6) δ 10.73 (bs, 1H), 8.21 (dd, $J = 7.3, 1.5$ Hz, 1H), 7.77 (dd, $J = 7.4, 1.5$ Hz, 1H), 7.73 (dd, $J = 7.4, 7.3$ Hz, 1H), 7.68 (bs, 1H), 7.62 (dd, $J = 7.9, 1.0$ Hz, 1H), 7.52 (dd, $J = 7.7, 1.3$ Hz, 1H), 7.40 (td, $J = 7.5, 1.0$ Hz, 1H), 7.23 (td, $J = 7.5, 1.3$ Hz, 1H), 4.58 (s, 2H), 4.15 - 4.05 (m, 1H), 3.60 (s, 2H), 3.00 - 2.92 (m, 2H), 2.29 - 2.19 (m, 2H), 1.91 - 1.75 (m, 4H). HRMS (ESI+): calcd. for $C_{21}H_{23}BrN_3O_2^+$ $[M + H]^+$ 428.0968; found 428.0974.

2-[1-(3-bromobenzyl)piperidin-4-yl]-3-oxo-2,3-dihydro-1H-isoindole-4-carboxamide (13k).

1H NMR (400 MHz, DMSO- d_6) δ 10.72 (bs, 1H), 8.21 (dd, $J = 7.3, 1.5$ Hz, 1H), 7.77 (dd, $J = 7.4, 1.5$ Hz, 1H), 7.73 (dd, $J = 7.4, 7.3$ Hz, 1H), 7.67 (bs, 1H), 7.54 (s, 1H), 7.49 - 7.45 (m, 1H), 7.37 - 7.30 (m, 2H), 4.58 (s, 2H), 4.12 - 4.00 (m, 1H), 3.53 (s, 2H), 2.95 - 2.88 (m, 2H), 2.17 - 2.08 (m, 2H), 1.91 - 1.74 (m, 4H). HRMS (ESI+): calcd. for $C_{21}H_{23}BrN_3O_2^+$ $[M + H]^+$ 428.0968; found 428.0975.

2-[1-(4-bromobenzyl)piperidin-4-yl]-3-oxo-2,3-dihydro-1H-isoindole-4-carboxamide (13l).

1H NMR (400 MHz, DMSO- d_6) δ 10.72 (bs, 1H), 8.21 (dd, $J = 7.4, 1.3$ Hz, 1H), 7.76 (dd, $J = 7.4, 1.3$ Hz, 1H), 7.72 (dd, $J = 7.4, 7.4$ Hz, 1H), 7.67 (bs, 1H), 7.53 (d, $J = 8.3$ Hz, 2H), 7.30 (d, $J = 8.3$ Hz, 2H), 4.57 (s, 2H), 4.12 - 4.01 (m, 1H), 3.49 (s, 2H), 2.94 - 2.87 (m, 2H), 2.16 - 2.06 (m, 2H), 1.90 - 1.71 (m, 4H). HRMS (ESI+): calcd. for $C_{21}H_{23}BrN_3O_2^+$ $[M + H]^+$ 428.0968; found 428.0983.

3-oxo-2-{1-[2-(trifluoromethyl)benzyl]piperidin-4-yl}-2,3-dihydro-1H-isoindole-4-

carboxamide (13m). 1H NMR (400 MHz, DMSO- d_6) δ 10.73 (bs, 1H), 8.21 (dd, $J = 7.6, 1.5$ Hz, 1H), 7.85 - 7.81 (m, 1H), 7.79 - 7.66 (m, 5H), 7.51 - 7.46 (m, 1H), 4.59 (s, 2H), 4.15 - 4.05 (m,

1
2
3
4
5
6
7
8
9
10
11
12
13
14
15
16
17
18
19
20
21
22
23
24
25
26
27
28
29
30
31
32
33
34
35
36
37
38
39
40
41
42
43
44
45
46
47
48
49
50
51
52
53
54
55
56
57
58
59
60

1H), 3.68 (s, 2H), 2.95 - 2.89 (m, 2H), 2.24 - 2.16 (m, 2H), 1.92 - 1.75 (m, 4H). HRMS (ESI+):
calcd. for C₂₂H₂₃F₃N₃O₂⁺ [M + H]⁺ 418.1737; found 418.1745.

3-oxo-2-{1-[3-(trifluoromethyl)benzyl]piperidin-4-yl}-2,3-dihydro-1H-isoindole-4-

carboxamide (13n). ¹H NMR (400 MHz, DMSO-*d*₆) δ 10.72 (bs, 1H), 8.21 (dd, *J* = 7.4, 1.5 Hz, 1H), 7.77 (dd, *J* = 7.5, 1.5 Hz, 1H), 7.73 (dd, *J* = 7.5, 7.4 Hz, 1H), 7.70 - 7.56 (m, 5H), 4.59 (s, 2H), 4.13 - 4.03 (m, 1H), 3.63 (s, 2H), 2.96 - 2.89 (m, 2H), 2.20 - 2.10 (m, 2H), 1.91 - 1.74 (m, 4H). HRMS (ESI+): calcd. for C₂₂H₂₃F₃N₃O₂⁺ [M + H]⁺ 418.1737; found 418.1749.

3-oxo-2-{1-[4-(trifluoromethyl)benzyl]piperidin-4-yl}-2,3-dihydro-1H-isoindole-4-

carboxamide (13o). ¹H NMR (400 MHz, DMSO-*d*₆) δ 10.71 (bs, 1H), 8.20 (dd, *J* = 7.4, 1.3 Hz, 1H), 7.76 (dd, *J* = 7.6, 1.2 Hz, 1H), 7.74 - 7.68 (m, 3H), 7.67 (bs, 1H), 7.57 (d, *J* = 7.9 Hz, 2H), 4.57 (s, 2H), 4.12 - 4.02 (m, 1H), 3.61 (s, 2H), 2.96 - 2.88 (m, 2H), 2.19 - 2.10 (m, 2H), 1.91 - 1.72 (m, 4H). HRMS (ESI+): calcd. for C₂₂H₂₃F₃N₃O₂⁺ [M + H]⁺ 418.1737; found 418.1740.

2-{1-[4-(dimethylamino)benzyl]piperidin-4-yl}-3-oxo-2,3-dihydro-1H-isoindole-4-

carboxamide (13p). ¹H NMR (400 MHz, DMSO-*d*₆) δ 10.72 (bs, 1H), 8.19 (dd, *J* = 7.4, 1.3 Hz, 1H), 7.76 (dd, *J* = 7.5, 1.3 Hz, 1H), 7.71 (t, *J* = 7.5, 7.4 Hz, 1H), 7.66 (bs, 1H), 7.11 (d, *J* = 8.4 Hz, 2H), 6.69 (d, *J* = 8.4 Hz, 2H), 4.55 (s, 2H), 4.09 - 3.98 (m, 1H), 3.36 (s, 2H), 2.96 - 2.86 (m, 2H), 2.87 (s, 6H), 2.06 - 1.97 (m, 2H), 1.86 - 1.70 (m, 4H). HRMS (ESI+): calcd. for C₂₃H₂₉N₄O₂⁺ [M + H]⁺ 393.2285; found 393.2293.

3-oxo-2-[1-(pyridin-4-ylmethyl)piperidin-4-yl]-2,3-dihydro-1H-isoindole-4-carboxamide

(13q). ¹H NMR (400 MHz, DMSO-*d*₆) δ 10.72 (bs, 1H), 8.54 - 8.51 (m, 2H), 8.21 (dd, *J* = 7.5, 1.4 Hz, 1H), 7.78 (dd, *J* = 7.6, 1.4 Hz, 1H), 7.73 (t, *J* = 7.6, 7.5 Hz, 1H), 7.68 (bs, 1H), 7.37 - 7.34 (m, 2H), 4.58 (s, 2H), 4.13 - 4.03 (m, 1H), 3.56 (s, 2H), 2.95 - 2.88 (m, 2H), 2.20 - 2.11 (m, 2H), 1.93 - 1.74 (m, 4H). HRMS (ESI+): calcd. for C₂₀H₂₃N₄O₂⁺ [M + H]⁺ 351.1816; found 351.1817.

3-oxo-2-[1-(pyridin-3-ylmethyl)piperidin-4-yl]-2,3-dihydro-1H-isoindole-4-carboxamide

(13r). ¹H NMR (400 MHz, DMSO-*d*₆) δ 10.71 (bs, 1H), 8.52 (s, 1H), 8.48 (d, *J* = 4.8 Hz, 1H), 8.20 (dd, *J* = 7.4, 1.3 Hz, 1H), 7.77 – 7.71 (m, 3H), 7.66 (bs, 1H), 7.37 (dd, *J* = 7.7, 4.8 Hz, 1H), 4.56 (s, 2H), 4.11 – 4.01 (m, 1H), 3.55 (s, 2H), 2.96 - 2.87 (m, 2H), 2.19 – 2.07 (m, 2H), 1.89 - 1.70 (m, 4H). HRMS (ESI⁺): calcd. for C₂₀H₂₃N₄O₂⁺ [M + H]⁺ 351.1816; found 351.1822.

3-oxo-2-[1-(pyridin-2-ylmethyl)piperidin-4-yl]-2,3-dihydro-1H-isoindole-4-carboxamide

(13s). ¹H NMR (400 MHz, DMSO-*d*₆) δ 10.73 (bs, 1H), 8.51 (d, *J* = 4.8 Hz, 1H), 8.21 (dd, *J* = 7.4, 1.3 Hz, 1H), 7.83 - 7.75 (m, 2H), 7.73 (dd, *J* = 7.4, 7.4 Hz, 1H), 7.67 (bs, 1H), 7.47 (d, *J* = 7.8 Hz, 1H), 7.28 (dd, *J* = 6.8, 4.8 Hz, 1H), 4.58 (s, 2H), 4.14 - 4.03 (m, 1H), 3.65 (s, 2H), 3.00 – 2.02 (m, 2H), 2.26 - 2.14 (m, 2H), 1.93 - 1.73 (m, 4H). HRMS (ESI⁺): calcd. for C₂₀H₂₃N₄O₂ [M + H]⁺ 351.1816; found 351.1815.

3-oxo-2-[1-(thiophen-2-ylmethyl)piperidin-4-yl]-2,3-dihydro-1H-isoindole-4-carboxamide

(13t). ¹H NMR (400 MHz, DMSO-*d*₆) δ 10.72 (bs, 1H), 8.21 (dd, *J* = 7.4, 1.5 Hz, 1H), 7.77 (dd, *J* = 7.5, 1.5 Hz, 1H), 7.72 (dd, *J* = 7.5, 7.4 Hz, 1H), 7.67 (bs, 1H), 7.46 - 7.42 (m, 1H), 7.00 – 6.97 (m, 2H), 4.58 (s, 2H), 4.11 - 4.01 (m, 1H), 3.73 (s, 2H), 3.03 – 2.96 (m, 2H), 2.16 - 2.08 (m, 2H), 1.88 – 1.74 (m, 4H). HRMS (ESI⁺): calcd. for C₁₉H₂₂N₃O₂S⁺ [M + H]⁺ 356.1427; found 356.1430.

3-oxo-2-[1-(thiophen-3-ylmethyl)piperidin-4-yl]-2,3-dihydro-1H-isoindole-4-carboxamide

(13u). ¹H NMR (400 MHz, DMSO-*d*₆) δ 10.73 (bs, 1H), 8.21 (dd, *J* = 7.3, 1.3 Hz, 1H), 7.75 (dd, *J* = 7.4, 1.3 Hz, 1H), 7.72 (dd, *J* = 7.4, 7.3 Hz, 1H), 7.67 (bs, 1H), 7.49 (m, 1H), 7.33 (s, 1H), 7.08 (d, *J* = 4.6 Hz, 1H), 4.57 (s, 2H), 4.10 – 3.99 (m, 1H), 3.53 (s, 2H), 2.98 - 2.90 (m, 2H), 2.12 - 2.02 (m, 2H), 1.90 - 1.72 (m, 4H). HRMS (ESI⁺): calcd. for C₁₉H₂₂N₃O₂S⁺ [M + H]⁺ 356.1427; found 356.1432.

2-[1-(furan-2-ylmethyl)piperidin-4-yl]-3-oxo-2,3-dihydro-1*H*-isoindole-4-carboxamide

(**13v**). ¹H NMR (400 MHz, DMSO-*d*₆) δ 10.71 (bs, 1H), 8.19 (dd, *J* = 7.4, 1.3 Hz, 1H), 7.76 (dd, *J* = 7.5, 1.3 Hz, 1H), 7.71 (dd, *J* = 7.5, 7.4 Hz, 1H), 7.66 (bs, 1H), 7.59 (s, 1H), 6.41 (dd, *J* = 2.4, 1.8 Hz, 1H), 6.30 (d, *J* = 2.4 Hz, 1H), 4.55 (s, 2H), 4.06 – 3.97 (m, 1H), 3.53 (s, 2H), 2.97 – 2.89 (m, 2H), 2.15 – 2.07 (m, 2H), 1.87 – 1.70 (m, 4H), HRMS (ESI⁺): calcd. for C₁₉H₂₂N₃O₃⁺ [M + H]⁺ 340.1656; found 340.1651.

2-[1-(furan-3-ylmethyl)piperidin-4-yl]-3-oxo-2,3-dihydro-1*H*-isoindole-4-carboxamide

(**13z**). ¹H NMR (400 MHz, DMSO-*d*₆) δ 10.73 (bs, 1H), 8.21 (dd, *J* = 7.6, 1.5 Hz, 1H), 7.76 (dd, *J* = 7.4, 1.5 Hz, 1H), 7.72 (dd, *J* = 7.6, 7.4 Hz, 1H), 7.67 (bs, 1H), 7.62 (s, 1H), 7.58 (s, 1H), 6.45 (s, 1H), 4.56 (s, 2H), 4.11 – 3.98 (m, 1H), 3.37 (s, 2H), 3.02 – 2.91 (m, 2H), 2.09 – 1.99 (m, 2H), 1.88 – 1.71 (m, 4H). HRMS (ESI⁺): calcd. for C₁₉H₂₂N₃O₃⁺ [M + H]⁺ 340.1656; found 340.1649.

3-oxo-2-[1-(1*H*-pyrrol-2-ylmethyl)piperidin-4-yl]-2,3-dihydro-1*H*-isoindole-4-carboxamide

(**13aa**). ¹H NMR (400 MHz, DMSO-*d*₆) δ 10.73 (bs, 1H), 10.65 (bs, 1H), 8.20 (dd, *J* = 7.4, 1.3 Hz, 1H), 7.77 (dd, *J* = 7.6, 1.3 Hz, 1H), 7.72 (dd, *J* = 7.6, 7.4 Hz, 1H), 7.67 (bs, 1H), 6.65 (s, 1H), 5.96 – 5.92 (m, 1H), 5.89 (s, 1H), 4.55 (s, 2H), 4.11 – 3.97 (m, 1H), 3.44 (s, 2H), 2.99 – 2.88 (m, 2H), 2.08 – 1.97 (m, 2H), 1.86 – 1.71 (m, 4H). HRMS (ESI⁺): calcd. for C₁₉H₂₃N₄O₂⁺ [M + H]⁺ 339.1816; found 339.1812.

2-{1-[(1-methyl-1*H*-pyrrol-2-yl)methyl]piperidin-4-yl}-3-oxo-2,3-dihydro-1*H*-isoindole-4-

carboxamide (13ab). ¹H NMR (400 MHz, DMSO-*d*₆) δ 10.72 (bs, 1H), 8.19 (dd, *J* = 7.3, 1.5 Hz, 1H), 7.75 (dd, *J* = 7.4, 1.2 Hz, 1H), 7.71 (dd, *J* = 7.4, 7.3 Hz, 1H), 7.66 (bs, 1H), 6.67 – 6.65 (m, 1H), 5.89 – 5.85 (m, 2H), 4.55 (s, 2H), 4.10 – 4.00 (m, 1H), 3.61 (s, 3H), 3.41 (s, 2H), 2.98 – 2.89 (m, 2H), 2.07 – 1.97 (m, 2H), 1.80 – 1.70 (m, 4H). HRMS (ESI⁺): calcd. for C₂₀H₂₅N₄O₂⁺ [M + H]⁺ 353.1972; found 353.1984.

2-[1-(1*H*-indol-4-ylmethyl)piperidin-4-yl]-3-oxo-2,3-dihydro-1*H*-isoindole-4-carboxamide

(13ac). ¹H NMR (400 MHz, DMSO-*d*₆) δ 11.06 (bs, 1H), 10.74 (bs, 1H), 8.20 (dd, *J* = 7.4, 1.5 Hz, 1H), 7.75 (dd, *J* = 7.5, 1.2 Hz, 1H), 7.72 (dd, *J* = 7.5, 7.4 Hz, 1H), 7.67 (bs, 1H), 7.35 – 7.28 (m, 2H), 7.08 – 7.02 (m, 1H), 6.99 – 6.94 (m, 1H), 6.61 (s, 1H), 4.57 (s, 2H), 4.13 – 4.02 (m, 1H), 3.75 (s, 2H), 3.04 – 2.96 (m, 2H), 2.19 – 2.09 (m, 2H), 1.89 – 1.71 (m, 4H). HRMS (ESI⁺): calcd. for C₂₃H₂₅N₄O₂⁺ [M + H]⁺ 389.1972; found 389.1983.

2-[1-(1*H*-indol-5-ylmethyl)piperidin-4-yl]-3-oxo-2,3-dihydro-1*H*-isoindole-4-carboxamide

(13ad). ¹H NMR (400 MHz, DMSO-*d*₆) δ 11.01 (bs, 1H), 10.73 (bs, 1H), 8.20 (dd, *J* = 7.3, 1.5 Hz, 1H), 7.75 (dd, *J* = 7.4, 1.5 Hz, 1H), 7.71 (dd, *J* = 7.4, 7.3 Hz, 1H), 7.66 (bs, 1H), 7.46 (s, 1H), 7.34 (d, *J* = 8.2 Hz, 1H), 7.33 – 7.28 (m, 1H), 7.07 (dd, *J* = 8.2, 1.3 Hz, 1H), 6.40 – 6.37 (m, 1H), 4.56 (s, 2H), 4.10 – 4.00 (m, 1H), 3.56 (s, 2H), 3.00 – 2.92 (m, 2H), 2.13 – 2.02 (m, 2H), 1.87 – 1.71 (m, 4H). HRMS (ESI⁺): calcd. for C₂₃H₂₅N₄O₂⁺ [M + H]⁺ 389.1972; found 389.1970.

3-oxo-2-[1-(tetrahydro-2*H*-pyran-4-yl)piperidin-4-yl]-2,3-dihydro-1*H*-isoindole-4-

carboxamide (13ae). ¹H NMR (400 MHz, DMSO-*d*₆) δ 10.74 (bs, 1H), 8.20 (dd, *J* = 7.6, 1.5 Hz, 1H), 7.76 (dd, *J* = 7.4, 1.5 Hz, 1H), 7.71 (dd, *J* = 7.6, 7.4 Hz, 1H), 7.66 (bs, 1H), 4.55 (s, 2H), 4.07 – 3.98 (m, 1H), 3.92 – 3.85 (m, 2H), 3.35 – 3.24 (m partially overlapped by water signal, 2H), 3.04 – 2.96 (m, 2H), 2.47 – 2.42 (m partially overlapped by DMSO signal, 1H), 2.29 – 2.19 (m, 2H), 1.81 – 1.65 (m, 6H), 1.50 – 1.38 (m, 2H). HRMS (ESI⁺): calcd. for C₁₉H₂₆N₃O₃⁺ [M + H]⁺ 344.1969; found 344.1962.

2-[1-(1,4-dioxaspiro[4.5]dec-8-yl)piperidin-4-yl]-3-oxo-2,3-dihydro-1*H*-isoindole-4-

carboxamide (13ag). ¹H NMR (400 MHz, DMSO-*d*₆) δ 10.74 (bs, 1H), 8.20 (dd, *J* = 7.4, 1.5 Hz, 1H), 7.76 (dd, *J* = 7.6, 1.5 Hz, 1H), 7.71 (dd, *J* = 7.6, 7.4 Hz, 1H), 7.66 (bs, 1H), 4.55 (s, 2H), 4.05 – 3.95 (m, 1H), 3.86 – 3.80 (m, 4H), 2.97 – 2.89 (m, 2H), 2.44 – 2.34 (m, 1H), 2.33 –

1
2
3 2.23 (m, 2H), 1.80 – 1.37 (m, 12H). HRMS (ESI+): calcd. for $C_{22}H_{30}N_3O_4^+$ $[M + H]^+$ 400.2231;
4
5 found 400.2229.
6
7

8 **4-Fluoro-2-iodo-6-methyl-benzoic acid (15b).** A mixture of 4-fluoro-2-methyl-benzoic acid
9
10 **14b** (20.00 g, 0.130 mol), iodobenzene diacetate (50.15 g, 0.156 mol), iodine (39.52 g, 0.156
11
12 mol) and palladium(II) acetate (1.46 g, 0.006 mol) in N,N-dimethylformamide (360 mL) was
13
14 degassed by cycling vacuum and nitrogen three times and was then heated for 18 hours at 100°C
15
16 internal temperature, under argon. The resulting dark mixture was cooled to room temperature,
17
18 diluted with methyl-tert-butylether (200 mL) and treated with a solution of sodium metabisulfite
19
20 (250 g) in water (500 mL) under efficient stirring. Then, this yellow colored mixture was
21
22 acidified by slowly adding conc. hydrochloric acid (130 mL). The aqueous layer was separated
23
24 and extracted twice with methyl-tert-butylether (mL100 x 2). The combined organic extracts
25
26 were treated with a solution of sodium hydroxide pellets (80 g) in water (300 mL) under stirring.
27
28 The organic layer containing only iodobenzene was discarded, while the aqueous layer was added
29
30 with sodium chloride, cooled to ice temperature and brought to pH = 1 with conc. hydrochloric
31
32 acid (130 mL). From this aqueous medium the product was extracted with methyl-tert-butylether
33
34 (100 mL x 3) and the combined extracts were dried over Na_2SO_4 and finally concentrated under
35
36 reduced pressure affording the title compound (30.5 g, 84%) as brown solid. This raw material
37
38 was used in the next step without purification. 1H NMR (300 MHz, $CDCl_3$) δ 7.45 (dd, $J_{HH} = 2.4$
39
40 Hz, $J_{HF} = 7.9$, 1H), 6.96 (dd, $J_{HH} = 2.4$ Hz, $J_{HF} = 9.1$, 1H), 2.46 (s, 3H). ESI(+) MS: m/z 281
41
42 (MH^+).
43
44
45
46
47
48

49
50 **Compounds 15a, 15c, 15d.** Operating in an analogous way, but employing suitably substituted
51
52 starting material the following compounds was obtained:
53
54
55
56
57
58
59
60

1
2
3 **3-fluoro-2-iodo-6-methylbenzoic acid (15a).** ^1H NMR (400 MHz, DMSO- d_6) δ 13.69 (bs, 1H),
4 7.30 (dd, $J_{\text{HH}} = 8.9$ Hz, $J_{\text{HF}} = 5.6$ Hz, 1H), 7.19 (dd, $J_{\text{HH}} = 8.9$ Hz, $J_{\text{HF}} = 8.2$ Hz, 1H), 2.27 (s,
5 3H). ESI(+) MS: m/z 281 (MH^+).
6
7
8
9

10 **3-fluoro-6-iodo-2-methylbenzoic acid (15c).** ^1H NMR (400 MHz, DMSO- d_6) δ 7.71 (dd, $J_{\text{HH}} =$
11 9.0 Hz, $J_{\text{HF}} = 5.0$ Hz, 1H), 7.04 (dd, $J_{\text{HH}} = 9.0$ Hz, $J_{\text{HF}} = 9.3$ Hz, 1H), 2.20 (d, $J_{\text{HF}} = 2.2$ Hz, 3H).
12 ESI(+) MS: m/z 281 (MH^+).
13
14
15
16

17 **4-chloro-2-iodo-6-methylbenzoic acid (15d).** ^1H NMR (400 MHz, DMSO- d_6) δ 7.83 – 7.81 (m,
18 1H), 7.47 – 7.45 (m, 1H), 2.25 (s, 3H). ESI(+) MS: m/z 297 (MH^+).
19
20
21

22 **4-Fluoro-2-iodo-6-methyl-benzoic acid methyl ester (16b).** To a solution of **15b** (30.05 g,
23 0.109 mol) in N,N-dimethylformamide (300 mL) was added anhydrous potassium carbonate
24 (22.0 g, 0.16 mol) under efficient magnetic stirring. After 15 minutes methyl p-toluenesulfonate
25 (30.7 g, 0.16 mol) was added. The brown suspension was stirred at room temperature for 2 hours.
26 Potassium acetate (12.4 g, 0.13 mol) was then added to destroy the unreacted methyl p-
27 toluenesulfonate and the mixture was stirred overnight. The thick reaction mixture was diluted
28 with methyl-tert-butylether (100 mL) and washed with water (600 mL); the aqueous layer was
29 separated and extracted twice with methyl-tert-butylether (70 mL x 2). The combined organic
30 extracts were washed with brine (50 mL), dried over Na_2SO_4 and concentrated under reduced
31 pressure to a solid residue. This material was purified by flash chromatography (n-hexane/ethyl
32 acetate 9:1), affording the desired compound (26.2 g, 81%) as colorless oil. ^1H NMR (400 MHz,
33 DMSO- d_6) δ 7.63 (dd, $J_{\text{HH}} = 2.4$ Hz, $J_{\text{HF}} = 8.3$ Hz, 1H), 7.25 (dd, $J_{\text{HH}} = 2.4$ Hz, $J_{\text{HF}} = 9.6$ Hz,
34 1H), 3.86 (s, 3H), 2.27 (s, 3H). ESI(+) MS: m/z 295 (MH^+).
35
36
37
38
39
40
41
42
43
44
45
46
47
48
49
50
51

52 **Compounds 16a, 16c, 16d.** Operating in an analogous way, but employing suitably substituted
53 starting material the following compounds was obtained:
54
55
56
57
58
59
60

1
2
3 **Methyl 3-fluoro-2-iodo-6-methylbenzoate (16a).** ^1H NMR (400 MHz, DMSO- d_6) δ 7.29 (dd,
4
5 $J_{\text{HH}} = 8.4$ Hz, $J_{\text{HF}} = 5.2$ Hz, 1H), 7.25 (dd, $J_{\text{HH}} = 8.4$ Hz, $J_{\text{HF}} = 8.0$ Hz, 1H), 3.89 (s, 3H), 2.24 (s,
6
7 3H). ESI(+) MS: m/z 295 (MH^+).
8
9

10 **Methyl 3-fluoro-6-iodo-2-methylbenzoate (16c).** ^1H NMR (400 MHz, DMSO- d_6) δ 7.75 (dd,
11
12 $J_{\text{HH}} = 8.7$ Hz, $J_{\text{HF}} = 5.0$ Hz, 1H), 7.11 (dd, $J_{\text{HH}} = 8.7$ Hz, $J_{\text{HF}} = 9.5$ Hz 1H), 3.89 (s, 3H), 2.16 (d,
13
14 $J_{\text{HF}} = 2.3$ Hz, 3H). ESI(+) MS: m/z 295 (MH^+).
15
16

17 **Methyl 4-chloro-2-iodo-6-methylbenzoate (16d).** ^1H NMR (400 MHz, DMSO- d_6) δ 7.82 (m,
18
19 1H), 7.46 (m, 1H), 3.87 (s, 3H), 2.25 (s, 3H). ESI(+) MS: m/z 311 (MH^+).
20
21

22 **2-[1-(4,4-difluorocyclohexyl)piperidin-4-yl]-5-fluoro-7-iodo-2,3-dihydro-1H-isoindol-1-one**
23 **(18by).** To a solution of **16b** (2.2 g, 7.5 mmol) in methyl pivalate (13 mL), N-bromosuccinimide
24
25 (2.2 g, 12.3 mmol) and benzoylperoxide (146 mg, 0.78 mmol) were added. The reaction mixture
26
27 was stirred at 85°C under nitrogen atmosphere for 3 hours. Crude was filtered on Gooch and
28
29 washed with toluene. Volatiles were evaporated and the residue was dissolved in acetonitrile (21
30
31 mL). Triethylamine (2.8 mL, 20.4 mmol) and **17y** (1.5 g, 6.8 mmol) were added and the reaction
32
33 mixture was stirred at 90°C for 4 hours. Crude was diluted with dichloromethane and washed
34
35 with 15% ammonium hydroxide. Organic phase was dried over sodium sulfate, filtered and
36
37 evaporated. Column chromatography (dichloromethane/ethanol: 95/5) afforded title compound
38
39 (1.9 g, 58%). ^1H NMR (400 MHz, DMSO- d_6) δ 7.80 (dd, $J_{\text{HH}} = 2.2$ Hz, $J_{\text{HF}} = 8.9$ Hz, 1H), 7.51
40
41 (dd, $J_{\text{HH}} = 2.2$ Hz, $J_{\text{HF}} = 8.3$ Hz, 1H), 4.37 (s, 2H), 4.02 – 3.89 (m, 1H), 2.99 – 2.88 (m, 2H), 2.54
42
43 – 2.45 (m overlapped by DMSO signal, 1H), 2.33 – 2.21 (m, 2H), 2.10 – 1.97 (m, 2H), 1.90 –
44
45 1.67 (m, 8H), 1.61 – 1.47 (m, 2H). HRMS (ESI+): calcd. for $\text{C}_{19}\text{H}_{23}\text{F}_3\text{IN}_2\text{O}^+$ $[\text{M} + \text{H}]^+$ 479.0802;
46
47 found 479.0803.
48
49
50
51
52
53

54
55 **Compounds 18ay, 18cy and 18dy.** Operating in an analogous way, but employing suitably
56
57 substituted starting material the following compounds was obtained:
58
59
60

2-[1-(4,4-difluorocyclohexyl)piperidin-4-yl]-6-fluoro-7-iodo-2,3-dihydro-1H-isoindol-1-one

(18ay). ^1H NMR (400 MHz, DMSO- d_6) δ 7.57 (dd, $J_{\text{HH}} = 8.2$ Hz, $J_{\text{HF}} = 4.6$ Hz, 1H), 7.45 (dd, $J_{\text{HH}} = 8.2$ Hz, $J_{\text{HF}} = 8.4$ Hz, 1H), 4.36 (s, 2H), 4.02 – 3.92 (m, 1H), 2.98 – 2.90 (m, 2H), 2.54 – 2.45 (m overlapped by DMSO signal, 1H), 2.32 – 2.22 (m, 2H), 2.10 – 1.96 (m, 2H), 1.91 – 1.69 (m, 8H), 1.60 – 1.48 (m, 2H). HRMS (ESI+): calcd. for $\text{C}_{19}\text{H}_{22}\text{F}_3\text{IN}_2\text{O}^+$ $[\text{M} + \text{H}]^+$ 479.0802; found 479.0790.

2-[1-(4,4-Difluorocyclohexyl)piperidin-4-yl]-4-fluoro-7-iodo-2,3-dihydro-1H-isoindol-1-one

(18cy). ^1H NMR (400 MHz, DMSO- d_6) δ 7.92 (dd, $J_{\text{HH}} = 8.5$ Hz, $J_{\text{HF}} = 4.5$ Hz, 1H), 7.24 (dd, $J_{\text{HH}} = 8.5$ Hz, $J_{\text{HF}} = 8.7$ Hz, 1H), 4.47 (s, 2H), 4.01 – 3.90 (m, 1H), 2.97 – 2.90 (m, 2H), 2.54 – 2.45 (m overlapped by DMSO signal, 1H), 2.31 – 2.22 (m, 2H), 2.11 – 1.93 (m, 2H), 1.92 – 1.67 (m, 8H), 1.61 – 1.48 (m, 2H). HRMS (ESI+): calcd. for $\text{C}_{19}\text{H}_{23}\text{F}_3\text{IN}_2\text{O}^+$ $[\text{M} + \text{H}]^+$ 479.0802; found 479.0804.

2-[1-(4,4-Difluorocyclohexyl)piperidin-4-yl]-5-chloro-7-iodo-2,3-dihydro-1H-isoindol-1-one

(18dy). ESI(+) MS: m/z 495 (MH+). After HPLC-MS analysis, compound **18dy** was submitted to the next step without further purification and ^1H -NMR characterization.

2-[1-(4,4-difluorocyclohexyl)piperidin-4-yl]-6-fluoro-3-oxo-2,3-dihydro-1H-isoindole-4-

carbonitrile (19by). **18by** (1.9 g, 3.97 mmol) and copper(I) cyanide (534 mg, 5.96 mmol) were dissolved in N,N-dimethylformamide (16 mL) and the resulted solution was refluxed under nitrogen atmosphere for 3 hours. The solvent was removed under reduced pressure and the residue was diluted with dichloromethane and washed with 15% ammonium hydroxide. Organic phase was dried over sodium sulfate, filtered and evaporated. Column chromatography (dichloromethane/ethanol: 95/5) afforded title compound (1.28 g, 86%). ^1H NMR (400 MHz, DMSO- d_6) δ 7.95 (dd, $J_{\text{HH}} = 2.2$ Hz, $J_{\text{HF}} = 9.2$ Hz, 1H), 7.83 (dd, $J_{\text{HH}} = 2.2$ Hz, $J_{\text{HF}} = 8.3$ Hz, 1H), 4.49 (m, 2H), 3.98 – 3.89 (m, 1H), 2.98 – 2.86 (m, 2H), 2.51 – 2.41 (m overlapped by

DMSO signal, 1H), 2.33 – 2.19 (m, 2H), 2.07 – 1.92 (m, 2H), 1.90 – 1.64 (m, 8H), 1.58 – 1.43 (m, 2H). HRMS (ESI+): calcd. for C₂₀H₂₃F₃N₃O⁺ [M + H]⁺ 378.1788; found 378.1782.

Compounds 19ay, 19cy and 19dy. Operating in an analogous way, but employing suitably substituted starting material the following compounds was obtained:

2-[1-(4,4-difluorocyclohexyl)piperidin-4-yl]-5-fluoro-3-oxo-2,3-dihydro-1H-isoindole-4-

carbonitrile (19ay). ¹H NMR (400 MHz, DMSO-*d*₆) δ 7.98 (dd, *J*_{HH} = 8.5 Hz, *J*_{HF} = 4.6 Hz, 1H), 7.74 (dd, *J*_{HH} = 8.5 Hz, *J*_{HF} = 9.8 Hz, 1H), 4.51 (s, 2H), 4.02 – 3.92 (m, 1H), 2.97 - 2.90 (m, 2H), 2.54 – 2.45 (m overlapped by DMSO signal, 1H), 2.34 – 2.23 (m, 2H), 2.11 – 1.96 (m, 2H), 1.93 – 1.67 (m, 8H), 1.61 – 1.48 (m, 2H). HRMS (ESI+): calcd. for C₂₀H₂₃F₃N₃O⁺ [M + H]⁺ 378.1788; found 378.1779.

7-Fluoro-2-[1-(4,4-difluorocyclohexyl)piperidin-4-yl]-3-oxo-2,3-dihydro-1H-isoindole-4-

carbonitrile (19cy). ¹H NMR (400 MHz, DMSO-*d*₆) δ 8.05 (dd, *J*_{HH} = 8.5 Hz, *J*_{HF} = 4.3 Hz, 1H), 7.65 (dd, *J*_{HH} = 8.5 Hz, *J*_{HF} = 8.7 Hz, 1H), 4.62 (s, 2H), 4.02 – 3.92 (m, 1H), 2.97 - 2.90 (m, 2H), 2.54 – 2.45 (m overlapped by DMSO signal, 1H), 2.34 – 2.24 (m, 2H), 2.11 – 1.96 (m, 2H), 1.93 – 1.67 (m, 8H), 1.61 – 1.48 (m, 2H). ESI(+) MS: *m/z* 378 (MH⁺).

6-Chloro-2-[1-(4,4-difluorocyclohexyl)piperidin-4-yl]-3-oxo-2,3-dihydro-1H-isoindole-4-

carbonitrile (19dy). ¹H NMR (400 MHz, DMSO-*d*₆) δ 8.15 (d, *J* = 1.8 Hz, 1H), 8.06 (d, *J* = 1.8 Hz, 1H), 4.52 (s, 2H), 4.01 – 3.91 (m, 1H), 2.97 – 2.90 (m, 2H), 2.55 – 2.44 (m overlapped by DMSO signal, 1H), 2.33 – 2.22 (m, 2H), 2.10 – 1.96 (m, 2H), 1.92 – 1.69 (m, 8H), 1.63 – 1.46 (m, 2H). HRMS (ESI+): calcd. for C₂₀H₂₃ClF₂N₃O⁺ [M + H]⁺ 394.1492; found 394.1502.

2-[1-(4,4-Difluorocyclohexyl)-piperidin-4-yl]-6-fluoro-3-oxo-2,3-dihydro-1H-isoindole-4-

carboxamide (20by). To a solution of **19by** (2.81 g; 7.44 mmol) in toluene (28 mL) acetaldoxime (4.4 g; 74.4 mmol) and indium(III) chloride (82 mg; 0.37 mmol) were added at

1
2
3 room temperature. The resulting solution was heated at reflux for 1 hour, then concentrated under
4
5 reduced pressure. The residue was taken-up with water, isopropanol and dichloromethane. The
6
7 organic layer was separated and finally concentrated under reduced pressure. The resulting crude
8
9 was crystallized from ethanol delivering, after drying, the desired compound (1.82 g, 62%) as a
10
11 white solid. ^1H NMR (400 MHz, $\text{DMSO-}d_6$) δ 10.77 (bs, 1H), 7.89 (dd, $J_{\text{HH}} = 2.6$ Hz, $J_{\text{HF}} = 10.9$
12
13 Hz, 1H), 7.85 (bs, 1H), 7.66 (dd, $J_{\text{HH}} = 2.6$ Hz, $J_{\text{HF}} = 7.7$ Hz, 1H), 4.56 (s, 2H), 4.04 – 3.94 (m,
14
15 1H), 2.98 – 2.91 (m, 2H), 2.53 – 2.45 (m, overlapped by DMSO signal, 1H), 2.32 – 2.22 (m, 2H),
16
17 2.10 – 1.96 (m, 2H), 1.92 – 1.67 (m, 8H), 1.60 – 1.48 (m, 2H). HRMS (ESI+): calcd. for
18
19 $\text{C}_{20}\text{H}_{25}\text{F}_3\text{N}_3\text{O}_2^+$ $[\text{M} + \text{H}]^+$ 396.1894; found 396.1890.

20
21
22
23
24
25 **Compounds 20ay, 20cy and 20dy.** Operating in an analogous way, but employing suitably
26
27 substituted starting material the following compounds was obtained:

28
29 **2-[1-(4,4-difluorocyclohexyl)piperidin-4-yl]-5-fluoro-3-oxo-2,3-dihydro-1H-isoindole-4-**

30
31 **carboxamide (20ay).** ^1H NMR (400 MHz, $\text{DMSO-}d_6$) δ 7.86 (bs, 1H), 7.62 (bs, 1H), 7.59 (dd,
32
33 $J_{\text{HH}} = 8.4$ Hz, $J_{\text{HF}} = 4.5$ Hz, 1H), 7.44 (dd, $J_{\text{HH}} = 8.4$ Hz, $J_{\text{HF}} = 9.6$ Hz, 1H), 4.42 (s, 2H), 3.99 –
34
35 3.89 (m, 1H), 2.97 – 2.90 (m, 2H), 2.53 – 2.45 (m overlapped by DMSO signal, 1H), 2.32 – 2.23
36
37 (m, 2H), 2.10 – 1.96 (m, 2H), 1.91 – 1.66 (m, 8H), 1.61 – 1.46 (m, 2H). HRMS (ESI+): calcd. for
38
39 $\text{C}_{20}\text{H}_{25}\text{F}_3\text{N}_3\text{O}_2^+$ $[\text{M} + \text{H}]^+$ 396.1894; found 396.1884.

40
41
42
43 **2-[1-(4,4-difluorocyclohexyl)piperidin-4-yl]-7-fluoro-3-oxo-2,3-dihydro-1H-isoindole-4-**

44
45 **carboxamide (20cy).** ^1H NMR (400 MHz, $\text{DMSO-}d_6$) δ 10.55 (bs, 1H), 8.26 (dd, $J_{\text{HH}} = 8.8$ Hz,
46
47 $J_{\text{HF}} = 5.2$ Hz, 1H), 7.71 (bs, 1H), 7.57 (dd, $J_{\text{HH}} = 8.8$ Hz, $J_{\text{HF}} = 8.4$ Hz, 1H), 4.63 (s, 2H), 4.06 –
48
49 3.95 (m, 1H), 2.99 – 2.91 (m, 2H), 2.56 – 2.44 (m overlapped by DMSO signal, 1H), 2.34 – 2.22
50
51 (m, 2H), 2.09 – 1.97 (m, 2H), 1.93 – 1.71 (m, 8H), 1.61 – 1.48 (m, 2H). HRMS (ESI+): calcd. for
52
53 $\text{C}_{20}\text{H}_{25}\text{F}_3\text{N}_3\text{O}_2^+$ $[\text{M} + \text{H}]^+$ 396.1894; found 396.1900.

1
2
3
4 **6-chloro-2-[1-(4,4-difluorocyclohexyl)piperidin-4-yl]-3-oxo-2,3-dihydro-1*H*-isoindole-4-**
5 **carboxamide (20dy).** ¹H NMR (400 MHz, DMSO-*d*₆) δ 10.68 (bs, 1H), 8.12 (d, *J* = 2.1 Hz, 1H),
6 7.89 (d, *J* = 2.1 Hz, 1H), 7.86 (bs, 1H), 4.56 (s, 2H), 4.05 – 3.95 (m, 1H), 2.98 – 2.91 (m, 2H),
7 2.54 – 2.45 (m overlapped by DMSO signal, 1H), 2.32 – 2.23 (m, 2H), 2.10 – 1.97 (m, 2H), 1.91
8 – 1.68 (m, 8H), 1.61 – 1.48 (m, 2H). HRMS (ESI⁺): calcd. for C₂₀H₂₅ClF₂N₃O₂⁺ [M + H]⁺
9 412.1598; found 412.159

17 **2. Biochemistry.**

18
19
20 **2.1 Protein Production.** PARP-1 full length (FL) and catalytic domain (CD), PARP-2 FL and
21 CD, PARP-3 FL and TNKS-1 CD were prepared as previously described.²¹

22
23
24 **2.2 Fluorescence Polarization Displacement Assay.** Fluorescence polarization displacement
25 assay on PARP-1 FL, PARP-2 FL, PARP-3 FL and TNKS-1 CD was performed as reported.²¹

26
27
28 **2.3 Surface Plasmon Resonance Binding Assay.** Surface Plasmon resonance binding assay on
29 PARP-1 CD and on PARP-2 CD was conducted as previously reported.²¹

30
31
32 **2.4 Kinase Assay.** Compound **20by** was profiled as previously described⁴⁵ on 56 different
33 kinases (ABL, ACK1, AKT1, ALK, AUR1, AUR2, BRK, BUB1, CDC7/DBF4, CDK2/CYCA,
34 CHK1, CK2, EEF2K, EGFR1, ERK2, EphA2, FAK, FGFR1, FLT3, GSK3beta, Haspin, IGFR1,
35 IKK2, IR, JAK1, JAK2, JAK3, KIT, LCK, LYN, MAPKAPK2, MELK, MET, MNK2, MPS1,
36 MST4, NEK6, NIM1, P38alpha, PAK4, PDGFRb, PDK1, PERK, PIM1, PIM2, PKAalpha,
37 PKCbeta, PLK1, RET, SULU1, Syk, TLK2, TRKA, TYK2, VEGFR2, ZAP70). The IC₅₀ values
38 were found to be >10 μM for all enzymes tested.

39
40
41 **2.5 HTS Campaign.** See ref. (21) for HTS experimental details.

52 **3. Cell Biology.**

53
54
55 **3.1 PAR Assay.** Cellular activity of PARP-1 inhibitors was assessed by measuring the inhibition
56 of the hydrogen peroxide induced PAR formation in HeLa cells (ECACC). Cellular PAR levels
57
58
59
60

1
2
3 were measured by immunocytochemistry, and quantified using an ArrayScan vTi instrument
4
5 (Cellomics Thermo Scientific).
6

7
8 Studies were performed as follows: 6000 cells/well were seeded in 96 well plates (Perkin Elmer)
9
10 in MEM/10% FCS and incubated for 24 hours at 37 °C, 5% carbon dioxide. Test compounds
11
12 were then added at the required concentration for 30 minutes. DNA damage was then induced by
13
14 adding hydrogen peroxide at the concentration of 0.1 mM for 15 minutes. Concentration curves
15
16 were prepared in MEM/10% FCS from compound stocks in DMSO, and final DMSO
17
18 concentration was 0.002% (v/v). Duplicate wells for each concentration point were prepared with
19
20 a typical highest compound concentration of 20 μ M and serial dilution 1:3. Plates were dried and
21
22 fixed adding cold methanol-acetone (70:30) solution for 15 minutes at room temperature, fixing
23
24 solution was aspirated and wells were air dried for 5 minutes and then dehydrated in PBS. Non-
25
26 specific binding sites were blocked by incubating wells for 30 minutes in PBS containing 5%
27
28 (w/v) FBS 0.05% Tween 20. Wells were then incubated for 1 hour at room temperature in PBS
29
30 containing anti PAR mouse monoclonal antibody (Anti-PAR, Mouse mAb 10H, Tulip Cat N°
31
32 1020) diluted 1:200 in blocking solution. After 3 washes in PBS, wells incubated in PBS (w/v)
33
34 5% FBS 0.05% Tween 20 containing 2 μ g/mL Cy2-conjugated Goat anti mouse secondary
35
36 antibody (Amersham Pharmacia Biotech cat. N° PA 42002) (Absorption maximum 489 nm
37
38 fluorescence maximum 506 nm) and 1 μ g/mL DAPI (4',6-diamidino-2-phenylindole dilactate,
39
40 absorption maximum 359 nm fluorescence maximum 461 nm, Sigma cat. N° D9564). After
41
42 washing further 3 times in PBS, cellular PAR immunoreactivity was assessed using the
43
44 ArrayScan vTi instrument, with a Zeiss 10X 0.5 N.A. objective, and applying the CytoNucTrans
45
46 V3 algorithm (Cellomics/Thermo Fisher) with a XF100 filter. At least 10 fields, corresponding to
47
48 at least 900 cells, were read for each well. Compound IC₅₀s were derived from sigmoidal
49
50 interpolation functions of experimental data using GraphPad Prism software.
51
52
53
54
55
56
57
58
59
60

1
2
3 **3.2 Colony Forming Assay.** Inhibition of cell proliferation was evaluated as follows: cells were
4 seeded at a density of 600 cells/cm² in RPMI medium, supplemented with 10% FBS. After 24
5 hours, medium was replaced with same containing increasing serial dilutions of inhibitor starting
6 from a highest concentration of 10 μ M. After ten days, cells were fixed and stained with crystal
7 violet. Colonies were counted using Infrared Scanner (Odyssey Li-Cor). All the experiments
8 were performed in duplicate. IC₅₀ was calculated using the GraphPad Prism® Software.⁴⁶

9
10
11 **4. X-ray Crystallographic Data.** Crystals of the catalytic domain of hPARP-1 in complex with
12 compound **10b** and **20by** were grown at 4 °C using the vapor diffusion method from a solution of
13 2 M ammonium sulfate, 2% Peg 400 and 0.1 M Tris pH 8. Before crystallization, the protein was
14 concentrated at 10 mg/mL in a buffer containing: 50 mM Tris-HCl pH 8.0, 150 mM sodium
15 chloride, 10% glycerol, 14 mM β -mercaptoethanol and 0.1% β -octylglucoside. Compounds **10b**
16 and **20by** were added to the protein solution at a final concentration of 0.5 mM. Small co-crystals
17 of **10b** grew in a few days and were optimized using streak seeding. On the contrary, the catalytic
18 domain of hPARP-1 in complex with **20by** crystallized only after several months, giving a
19 different crystal form (space group of hPARP-1-**20by** crystal is I222, while for hPARP-1-**10b**
20 crystal is C2). For data collection, crystals were cryoprotected in a mother liquor solution
21 containing 30% glycerol and frozen in liquid nitrogen. Crystals of the catalytic domain of
22 hPARP-2 in complex with compounds **10b** and **20by** were obtained at 4 °C by the vapor
23 diffusion method (hanging drops), mixing equal volumes of a protein solution (10 mg/mL of
24 protein in 50 mM TrisHCl pH 8.5, 150 mM sodium chloride and 0.5 mM dithiothreitol (DTT)
25 containing either **10b** or **20by** at a final concentration of 0.5 mM) and the reservoir solution
26 consisting of 25% PEG 4000, 0.2 M magnesium chloride and 0.1 M TrisHCl pH 8.5. Addition of
27 0.1% β -octylglucoside and streak seeding improved the quality and reproducibility of the
28 crystals. Crystals were further transferred to a cryoprotectant solution (reservoir solution
29
30
31
32
33
34
35
36
37
38
39
40
41
42
43
44
45
46
47
48
49
50
51
52
53
54
55
56
57
58
59
60

1
2
3 supplemented with 30% glycerol) and frozen in liquid nitrogen. Diffraction data for the different
4
5 complexes were collected at ESRF (Grenoble, France). Data were indexed and integrated using
6
7 Mosflm and Scala,^{47,48} structures were refined with Refmac^{48,49} and model building was
8
9 performed with Coot.⁵⁰ All structures have been deposited to the Protein Data Bank (PDB) with
10
11 accession codes: 4ZZX, 4ZZY, 4ZZZ and 5A00.
12
13

14 **5. ADME Data.**

15
16
17 **5.1 Solubility.** Solubility at pH = 7 was measured as previously reported.⁵¹
18

19
20 **5.2 Cell Permeability.** PAMPA permeability assay was performed as described.⁵¹
21

22
23 **5.3 Plasma Protein Binding.** Plasma protein binding was evaluated according to the
24
25 methodology already described.⁵²
26

27
28 **5.4 Intrinsic Clearance in Human Liver Microsomes (HLM).** Metabolic stability in the
29
30 presence of human liver microsomes was assessed as reported.⁵¹
31

32
33 **5.5 Intrinsic Clearance in Rat Hepatocytes.** Clearance determination in rat hepatocytes was
34
35 performed as previously described.⁵¹
36

37 **6. In Vivo Pharmacokinetic Studies.**

38
39 All procedures adopted for housing and handling of animals were in strict compliance with
40
41 Italian and European guidelines for Laboratory Animal Welfare and the protocols were approved
42
43 by IRB.
44

45
46 **6.1 Pharmacokinetics in Mouse.** The pharmacokinetic profile and the oral bioavailability of the
47
48 compounds have been investigated in mouse (Balb,Nu/Nu, Harlan, Italy) in *ad hoc*
49
50 pharmacokinetic studies. The compounds were formulated for intravenous bolus administration
51
52 as follows: 5% tween 80 in 5% dextrose for **13i**; PEG 400 in 5% dextrose for **13ad**; 10% tween
53
54 80 in 5% dextrose for **13af** and **20by**. Oral administration was performed using the compounds
55
56 formulated in 0.5% methylcellulose. A single administration at the dose of 10 mg/kg was given
57
58
59
60

1
2
3 and three male animals for each route were used. All blood samples were taken from retro-orbital
4 vein at 5 minutes, 30 minutes, 1 hour, 3 hours, 6 hours, 24 hours after intravenous administration
5 and 15 minutes, 30 minutes, 1 hour, 3 hours, 6 hours, 24 hours after oral administration. Plasma
6 samples were prepared by plasma proteins precipitation adding 200 μL of acetonitrile to 20 μL of
7 plasma in a 96 well plate. After capping and vortex mixing, the plate was centrifuged for 15
8 minutes at 4000 rpm. The supernatant was considered as final extract and injected onto the LC-
9 MS/MS system (UHPLC system: Waters Acquity using BEH HILIC 50*2.1 mm 1.7 μm
10 analytical column; MS instrument: Waters TQD equipped with electrospray ion source operating
11 in positive ion mode). Lower limit of quantification is 5.0 ng/mL, upper limit of quantification is
12 5000 ng/mL. Pharmacokinetic analysis was performed with WinNonlin software (version 5.2.1)
13 using a non-compartmental method (linear trapezoidal rule and linear regression analysis of
14 natural log-transformed plasma concentrations vs. time data). Oral bioavailability (F) was
15 calculated from the ratio of average oral to IV (intravenous) dose-normalized plasma AUC
16 values.
17

18
19
20
21
22
23
24
25
26
27
28
29
30
31
32
33
34
35
36 **6.2 Pharmacokinetics in Rat.** The pharmacokinetic profile and the oral bioavailability of the
37 compounds have been investigated in rat (Sprague Dawley, Charles River Laboratories, Italy) in
38 *ad hoc* pharmacokinetic studies. Compound **20by** was formulated for intravenous bolus
39 administration in 20% DMSO + 40% PEG 400 in 5% dextrose. Oral administration was
40 performed using a **20by** suspension in 0.5% methylcellulose. A single administration at the dose
41 of 10 mg/kg for each route and a single oral administration at the dose of 100 mg/kg were given.
42
43
44
45
46
47
48
49
50
51
52
53
54
55
56
57
58
59
60
60 Three male animals for each study were used. All blood samples were taken by means of a
cannula implanted in the superior vena cava *via* the jugular vein at 5 minutes, 30 minutes, 1 hour,
3 hours, 6 hours and 24 hours after intravenous administration and 15 minutes, 30 minutes, 1
hour, 3 hours, 6 hours and 24 hours after oral administration. Plasma samples were prepared by

1
2
3 plasma proteins precipitation adding 200 μL of acetonitrile to 20 μL of plasma in a 96 well plate.
4
5 After capping and vortex mixing, the plate was centrifuged for 15 minutes at 3700 rpm at 6 $^{\circ}\text{C}$.
6
7 The supernatant was considered as final extract and injected onto the LC-MS/MS system (HPLC
8
9 system: Hewlett Packard 1100 series using Zorbax SB CN 75*4.6 mm 3.5 μm analytical column;
10
11 MS instrument: MDS/SCIEX 4000QTRAP equipped with TURBO ION SPRAY source
12
13 operating in positive ion mode. Lower limit of quantification is 4.3 ng/mL, upper limit of
14
15 quantification is 1030 ng/mL. Pharmacokinetic analysis was performed with Watson package
16
17 (version 6.4.0.04) and Excel spreadsheet (Microsoft Inc., Seattle, USA) using a non-
18
19 compartmental method (linear trapezoidal rule and linear regression analysis of natural log-
20
21 transformed plasma concentrations vs. time data). Absolute bioavailability (F) was calculated
22
23 from the ratio of average oral to IV (intravenous) dose-normalized plasma AUC (area under
24
25 curve) values.
26
27
28
29
30

31 **7. *In Vivo* Pharmacology.**

32
33
34 **7.1 20by Anti-tumor activity as single agent.** The anti-tumor activity of compound **20by** was
35
36 investigated in femal athymic nu/nu mice carrying subcutaneously MDA-MB-436 triple negative
37
38 BRCA-1 mutated breast cancer. When tumors reached an average volume of $\sim 150 \text{ mm}^3$, mice
39
40 were randomized into various treatment groups, and were treated orally, once a day for 28
41
42 consecutive days, with **20by** (150 mg/kg) or empty vehicle (1% Tween80 in methocel). Median
43
44 tumor volume of seven mice per group was determined by caliper and was plotted over time to
45
46 monitor tumor growth (first day of treatment is day 21).
47
48
49

50
51 **7.2 20by Anti-tumor activity in combination with temozolomide (TMZ).** In a combination
52
53 study with temozolomide, **20by** was administered to male athymic nu/nu mice carrying
54
55 subcutaneously implanted Capan-1 pancreatic cancer cells, orally once daily for 12 days at the
56
57
58
59
60

1
2
3 dose of 100 mg/kg, starting on day 9. Temozolomide was administered in glucosate at a dosage
4
5 of 50 mg/kg for 5 days starting from day 11.
6
7

8 **8. *In vivo* pharmacodynamics.** Tumors of animals treated with a single oral administration of
9
10 **20by** (100 mg/kg) were harvested at 2, 4, 8 and 24 hours, homogenized in PBS and extracted
11
12 with lysis buffer. Levels of PAR in the tumor lysates were determined by ELISA. Plates were
13
14 first coated with anti-PAR monoclonal antibody (Tulip) for 2 hours at 37 °C and then washed
15
16 with PBS 0.1% Tween20. After blocking, 10 mg of tumor lysates were added to the plate in
17
18 triplicate and left overnight at 4 °C in PBS 2%BSA and 0.5% SDS. The day after the plates were
19
20 washed and the polyclonal primary antibody anti-PAR (Trevigen) was added, diluted 1:2000 in
21
22 PBS 2% BSA and mouse serum 1:500. Two hours later the plates were washed with PBS 0.1%
23
24 Tween20 and incubated with the secondary antibody anti-HRP (Amersham) diluted 1:1000 in the
25
26 same buffer as for the primary antibody. The substrate Supersignal ELISA Pico was then added
27
28 after washes and the plates were read at 425 nm.
29
30
31
32
33

34 ASSOCIATED CONTENT

35
36
37
38 **Supporting Information.** Quantitative assessment of the intramolecular hydrogen bond strength
39
40 of selected isoindolinones. Detailed kinetic parameters and kinetic analysis of surface plasmon
41
42 resonance binding assay. Experimental details concerning *in vitro* evaluation of cross species
43
44 metabolism, cytochrome P450 inhibition and mielotoxicity of compound **20by**. This material is
45
46 available free of charge via the Internet at <http://pubs.acs.org>.
47
48
49
50

51 AUTHOR INFORMATION

52 53 54 55 **Corresponding Author** 56 57 58 59 60

*To whom correspondence should be addressed. Phone +39-0331581537.

Fax: +39-0331581347. E-mail: gianluca.papeo@nervianoms.com.

Present Addresses

[‡] College of Life Sciences, University of Dundee, Dow Street Dundee, DD1 5EH, Scotland, UK

[‡] Institute of Chemistry, St. Petersburg State University, 26 Universitetskiy Prospekt, Peterhof
198504, Russian Federation

Acknowledgment

The authors gratefully acknowledge the technical skill and support of the Experimental Therapy Team, the Biochemical Screening Group and Analytical Chemistry Department of NMS.

Abbreviations

AD, adenine-ribose; ADME, absorption, distribution, metabolism, excretion; ARTD, ADP-ribosyltransferase diphtheria toxin-like; ATM, ataxia telangiectasia mutated; AUC, area under the plasma concentration versus time curve up to the last detectable concentration; BEI, binding efficiency index; BRCA, breast cancer susceptibility gene; BSA, bovine serum albumine; CD, catalytic domain; CL, plasma clearance; C_{max} , maximum plasma concentration; DAPI, 4',6-diamidino-2-phenylindole; DTT, dithiothreitol; EGFR, epidermal growth factor receptor; ELISA, enzyme-linked immunosorbent assay; ER, estrogen receptor; F , oral bioavailability; FBS, fetal bovine serum; FCS, fetal calf serum; FL, full length; HER2, human epidermal growth factor receptor 2; HLM, human liver microsomes; HR, homologous recombination; HRP, horseradish peroxidase; HTS, high-throughput screening; LE, ligand efficiency; MEM, minimum essential medium; MSI, microsatellite instability; NAD^+ , nicotinamide adenine dinucleotide; NAMPT,

1
2
3 nicotinamide phosphoribosyltransferase; PAR, poly(ADP-ribose); PARP, poly(ADP-ribose)
4
5 polymerase; PBS, phosphate buffered saline; PEG, polyethylene glycol; PI3K,
6
7 phosphatidylinositol-3-kinase; PR, progesterone receptor; PTEN, phosphatase and tensin
8
9 homolog; RPMI, Roswell Park Memorial Institute (culture medium); SAR, structure-activity
10
11 relationship; SDS, sodium dodecyl sulfate; SEM, standard error of measurement; SIRT1, sirtuin
12
13 1; $t_{1/2}$, terminal half life; TNKS-1, tankyrase-1; V_{ss} , volume of distribution at steady state.
14
15
16
17
18
19
20
21
22
23
24
25
26
27
28
29
30
31
32
33
34
35
36
37
38
39
40
41
42
43
44
45
46
47
48
49
50
51
52
53
54
55
56
57
58
59
60

References

- (1) Hottiger, M. O.; Hassa, P. O.; Lüscher, B.; Schöler, H.; Koch-Nolte, F. Toward a unified nomenclature for mammalian ADP-ribosyltransferases. *Trends in Biochem. Sci.* **2010**, *35*, 208-219.
- (2) Krishnakumar, R.; Kraus, W. L. The PARP side of the nucleus: molecular actions, physiological outcomes, and clinical targets. *Mol. Cell* **2010**, *39*, 8-24.
- (3) (a) Yelamos, J.; Farres, J.; Lacuna, L.; Ampurdanes, C.; Martin-Caballero, J. PARP-1 and PARP-2: new players in tumour development. *Am. J. Cancer Res.* **2011**, *1*, 328-346; (b) Ryu, K. W.; Kim, D.-S.; Kraus, W. L. New Facets in the Regulation of Gene Expression by ADP-Ribosylation and Poly(ADP-ribose) Polymerases. *Chem. Rev.* **2015**, *115*, 2453-2481.
- (4) Ferraris, D. V. Evolution of Poly(ADP-ribose) Polymerase-1 (PARP-1) Inhibitors. From concept to clinic. *J. Med. Chem.* **2010**, *53*, 4561-4584.
- (5) Curtin, N.; Szabo, C. Therapeutic applications of PARP inhibitors: anticancer therapy and beyond. *Mol. Aspects Med.* **2013**, *34*, 1217-1256.
- (6) (a) Penning, T. D. Small-molecule PARP modulators – Current status and future therapeutic potential. *Curr. Opin. Drug Discov. Devel.* **2010**, *13*, 577-586; (b) Jones, P. Development of poly(ADP-Ribose)polymerase (PARP) inhibitors in oncology. *Annu. Rep. Med. Chem.* **2010**, *45*, 229-243; (c) Kummar, S.; Chen, A.; Parchment, R. E.; Kinders, R. J.; Ji, J.; Tomaszewski, J. E.; Doroshow, J. H. Advances in using PARP inhibitors to treat cancer. *BMC Med.* **2012**, *10*, 25; (d) Curtin, N. J. Poly(ADP-ribose) polymerase (PARP) and PARP inhibitors. *Drug Discov. Today: Dis. Model* **2012**, *9*, e51-e58; (e) Maxwell, K. N.; Domchek, S. M. Cancer treatment according to

1
2
3 *BRCA1* and *BRCA2* mutations. *Nat. Rev. Clin. Oncol.* **2012**, *9*, 520-528; (f) Ström, C. E.;
4
5 Helleday, T. Strategies for the use of poly(adenosine diphosphate ribose) polymerase (PARP)
6
7 inhibitors in cancer therapy. *Biomolecules* **2012**, *2*, 635-649; (g) Davar, D.; Beumer, J. H.;
8
9 Hamieh, L.; Tawbi, H. Role of PARP inhibitors in cancer biology and therapy. *Curr. Med. Chem.*
10
11 **2012**, *19*, 3907-3921; (h) Papeo, G.; Casale, E.; Montagnoli, A.; Cirila, A. PARP inhibitors in
12
13 cancer therapy: an update. *Expert Opin. Ther. Pat.* **2013**, *23*, 503-514; (i) Ekblad, T.; Camaioni,
14
15 E.; Schüler, H.; Macchiarulo, A. PARP inhibitors: polypharmacology vs selective inhibition.
16
17 *FEBS J.* **2013**, <http://dx.doi.org/10.1111/febs.12298>.

21
22
23 (7) (a) Bryant, H. E.; Schultz, N.; Thomas, H. D.; Parker, K. M.; Flower, D.; Lopez, E.; Kyle, S.;
24
25 Meuth, M.; Curtin, N. J.; Helleday, T. Specific killing of *BRCA2*-deficient tumours with
26
27 inhibitors of poly(ADP-ribose) polymerase. *Nature* **2005**, *434*, 913-917; (b) Farmer, H.; McCabe,
28
29 N.; Lord, C. J.; Tutt, A. N.; Johnson, D. A.; Richardson, T. B.; Santarosa, M.; Dillon, K. J.;
30
31 Hickson, I.; Knights, C.; Martin, N. M.; Jackson, S. P.; Smith, G. C.; Ashworth, A. Targeting the
32
33 DNA repair defect in *BRCA* mutant cells as a therapeutic strategy. *Nature* **2005**, *434*, 917-921.

36
37
38 (8) (a) Ibrahim, Y. H.; García-García, C.; Serra, V.; He, L.; Torres-Lockhart, K.; Prat, A.; Anton,
39
40 P.; Cozar, P.; Guzmán, M.; Grueso, J.; Rodríguez, O.; Calvo, M. T.; Aura, C.; Díez, O.; Rubio, I.
41
42 T.; Pérez, J.; Rodón, J.; Cortés, J.; Ellisen, L. W.; Scaltriti, M.; Baselga, J. PI3K Inhibition
43
44 impairs *BRCA1/2* expression and sensitizes *BRCA*-proficient triple-negative breast cancer to
45
46 PARP inhibition. *Cancer Discov.* **2012**, *2*, 1036-1047; (b) Juvekar, A.; Burga, L. N.; Hu, H.;
47
48 Lunsford, E. P.; Ibrahim, Y. H.; Balmañà, J.; Rajendran, A.; Papa, A.; Spencer, K.; Lyssiotis, C.
49
50 A.; Nardella, C.; Pandolfi, P. P.; Baselga, J.; Scully, R.; Asara, J. M.; Cantley, L. C.; Wulf, G. M.
51
52 Combining a PI3K inhibitor with a PARP inhibitor provides an effective therapy for a mouse
53
54 model of *BRCA1*-related breast cancer. *Cancer Discov.* **2012**, *2*, 1048-1063.
55
56
57
58
59
60

1
2
3 (9) Bajrami, I.; Kigozi, A.; Van Weverwijk, A.; Brough, R.; Frankum, J.; Lord, C. J.; Ashworth,
4
5 A. Synthetic lethality of PARP and NAMPT inhibition in triple-negative breast cancer cells.

6
7
8 *EMBO Mol. Med.* **2012**, *4*, 1087-1096.

9
10
11 (10) Nowsheen, S.; Cooper, T.; Stanley, J. A.; Yang, E. S. Synthetic lethal interactions between
12
13 EGFR and PARP inhibition in human triple negative breast cancer cells. *PLoS ONE* **2012**, *7*,
14
15 e46614.

16
17
18 (11) (a) Mendes-Pereira, A. M.; Martin, S. A.; Brough, R.; McCarthy, A.; Taylor, J. R.; Kim, J.-
19
20 S.; Waldman, T.; Lord, C. J.; Ashworth, A. Synthetic lethal targeting of *PTEN* mutant cells with
21
22 PARP inhibitors. *EMBO Mol. Med.* **2009**, *1*, 315-322; (b) Garcia-Cao, I.; Song, M. S.; Hobbs, R.
23
24 M.; Laurent, G.; Giorgi, C.; de Boer, V. C.; Anastasiou, D.; Ito, K.; Sasaki, A. T.; Rameh, L.;
25
26 Carracedo, A.; Vander Heiden, M. G.; Cantley, L. C.; Pinton, P.; Haigis, M. C.; Pandolfi, P. P.
27
28 Systemic elevation of PTEN induces a tumor-suppressive metabolic state. *Cell.* **2012**, *149*, 49-
29
30 62.

31
32
33 (12) Williamson, C. T.; Muzik, H.; Turhan, A. G.; Zamò, A.; O'Connor, M. J.; Bebb, D. G.;
34
35 Lees-Miller, S. P. ATM deficiency sensitizes mantle cell lymphoma cells to poly(ADP-ribose)
36
37 polymerase-1 inhibitors. *Mol. Cancer Ther.* **2010**, *9*, 347-357.

38
39
40 (13) Vilar, E.; Gruber, S. B. Microsatellite instability in colorectal cancer-the stable evidence.
41
42
43 *Nature Rev. Clin. Oncol.* **2010**, *7*, 153-162.

44
45
46 (14) Brenner, J. C.; Feng, F. Y.; Han, S.; Patel, S.; Goyal, S. V.; Bou-Maroun, L. M.; Liu, M.;
47
48 Lonigro, R.; Prensner, J. R.; Tomlins, S. A.; Chinnaiyan, A. M. PARP-1 inhibition as a targeted
49
50 strategy to treat Ewing's sarcoma. *Cancer Res.* **2012**, *72*, 1608-1613.

1
2
3
4
5
6
7
8
9
10
11
12
13
14
15
16
17
18
19
20
21
22
23
24
25
26
27
28
29
30
31
32
33
34
35
36
37
38
39
40
41
42
43
44
45
46
47
48
49
50
51
52
53
54
55
56
57
58
59
60

(15) Penning, T. D.; Zhu, G. D.; Gandhi, V. B.; Gong, J.; Liu, X.; Shi, Y.; Klinghofer, V.; Johnson, E. F.; Donawho, C. K.; Frost, D. J.; Bontcheva-Diaz, V.; Bouska, J. J.; Osterling, D. J.; Olson, A. M.; Marsh, K. C.; Luo, Y.; Giranda, V. L. Discovery of the poly-(ADP-ribose) polymerase (PARP) inhibitor 2-[(R)-2-methylpyrrolidin-2-yl]-1H-benzimidazole-4-carboxamide (ABT-888) for the treatment of cancer. *J. Med. Chem.* **2009**, *52*, 514–523.

(16) (a) Jones, P.; Altamura, S.; Boueres, J.; Ferrigno, F.; Fonsi, M.; Giomini, C.; Lamartina, S.; Monteagudo, E.; Ontoria, J. M.; Orsale, M. V.; Palumbi, M. C.; Pesci, S.; Roscilli, G.; Scarpelli, R.; Schultz-Fademrecht, C.; Toniatti, C.; Rowley, M. Discovery of 2-{4-[(3S)-piperidin-3-yl]phenyl}-2H-indazole-7-carboxamide (MK-4827): a novel oral poly(ADP-ribose)polymerase (PARP) inhibitor efficacious in BRCA-1 and -2 mutant tumors. *J. Med. Chem.* **2009**, *52*, 7170–7185; (b) Jones, P.; Wilcoxon, K.; Rowley, M.; Toniatti, C. Niraparib: a poly(ADP-ribose) polymerase (PARP) inhibitor for the treatment of tumors with defective homologous recombination. *J. Med. Chem.* **2015**, *58*, 3302–3314.

(17) Thomas, H. D.; Calabrese, C. R.; Batey, M. A.; Canan, S.; Hostomsky, Z.; Kyle, S.; Maegley, K. A.; Newell, D.R.; Skalitzky, D.; Wang, L.-Z.; Webber, S. E.; Curtin, N. J. Preclinical selection of a novel poly(ADP-ribose) polymerase inhibitor for clinical trial. *Mol. Cancer Ther.* **2007**, *6*, 945–956.

(18) Menear, K. A.; Adcock, C.; Boulter, R.; Cockcroft, X. L.; Copsey, L.; Cranston, A.; Dillon, K. J.; Drzewiecki, J.; Garman, S.; Gomez, S.; Javaid, H.; Kerrigan, F.; Knights, C.; Lau, A.; Loh, V. M., Jr.; Matthews, I. T.; Moore, S.; O'Connor, M. J.; Smith, G. C.; Martin, N. M. 4-[3-(4-Cyclopropanecarbonylpiperazine-1-carbonyl)-4-fluorobenzyl]-2H-phthalazin-1-one: a novel bioavailable inhibitor of poly(ADP-ribose) polymerase-1. *J. Med. Chem.* **2008**, *51*, 6581–6591.

- 1
2
3 (19) (a) Shen, Y.; Rehman, F. L.; Feng, Y.; Boshuizen, J.; Bajrami, L.; Elliott, R.; Wang, B.;
4 Lord, C. J.; Post, L. E.; Ashworth, A. BMN673, a novel and highly potent PARP1/2 inhibitor for
5 the treatment of human cancers with DNA repair deficiency. *Clin. Cancer Res.* **2013**, *19*, 5003-
6 5015; (b) Shen, Y.; Aoyagi-Scharber, M.; Wang, B. Trapping Poly(ADP-Ribose) Polymerase. *J.*
7 *Pharmacol. Exp. Ther.* **2015**, *353*, 446-457.
- 8
9
10
11
12
13
14
15
16 (20) Wahlberg, E.; Karlberg, T.; Kouznetsova, E.; Markova, N.; Macchiarulo, A.; Thorsell, A.-
17 G.; Pol, E.; Frostell, A.; Ekblad, T.; Öncü, D.; Kull, B.; Robertson, G. M.; Pellicciari, R.;
18 Schüler, H.; Weigelt, J. Family-wide chemical profiling and structural analysis of PARP and
19 tankyrase inhibitors. *Nat. Biotechnol.* **2012**, *30*, 283-288.
- 20
21
22
23
24
25
26
27 (21) Papeo, G.; Avanzi, N.; Bettoni, S.; Leone, A.; Paolucci, M.; Perego, R.; Quartieri, F.;
28 Riccardi-Sirtori, F.; Thieffine, S.; Montagnoli, A.; Lupi R. Insights into PARP inhibitors
29 selectivity using fluorescence polarization and surface plasmon resonance binding assays. *J.*
30 *Biomol. Screen.* **2014**, *19*, 1212-1219.
- 31
32
33
34
35
36
37 (22) Yélamos, J.; Schreiber, V.; Dantzer, F. Toward specific functions of poly(ADP-ribose)
38 polymerase-2. *Trends Mol. Med.* **2008**, *14*, 169-178.
- 39
40
41
42
43 (23) Antolin, A. A.; Mestres, J. Linking off-target kinase pharmacology to the differential
44 cellular effects observed among PARP inhibitors. *Oncotarget* **2014**, *5*, 3023-3028.
- 45
46
47
48 (24) Farrés, J.; Llacuna, L.; Martin-Caballero, J.; Martínez, C.; Lozano, J. J.; Ampurdanés, C.;
49 López-Contreras, A. J.; Florensa, L.; Navarro, J.; Ottina, E.; Dantzer, F.; Schreiber, V.;
50 Villunger, A.; Fernández-Capetillo, O.; Yélamos, J. PARP-2 sustains erythropoiesis in mice by
51 limiting replicative stress in erythroid progenitors. *Cell Death Differ.* **2015**, *22*, 1144-1157.
- 52
53
54
55
56
57
58
59
60

- 1
2
3 (25) Goldberg, M. S.; Xing, D.; Ren, Y.; Orsulic, S.; Bhatia, S. N.; Sharp, P. A. Nanoparticle-
4 mediated delivery of siRNA targeting Parp1 extends survival of mice bearing tumors derived
5 from Brca1-deficient ovarian cancer cells. *Proc. Natl. Acad. Sci. U.S.A.* **2011**, *108*, 745-750.
6
7
8
9
10
11 (26) (a) Ishida, J.; Yamamoto, H.; Kido, Y.; Kamijo, K.; Murano, K.; Miyake, H.; Ohkubo, M.;
12 Kinoshita, T.; Warizaya, M.; Iwashita, A.; Mihara, K.; Matsuoka, N.; Hattori, K. Discovery of
13 potent and selective PARP-1 and PARP-2 inhibitors: SBDD analysis via a combination of X-ray
14 structural study and homology modeling. *Bioorg. Med. Chem.* **2006**, *14*, 1378–1390; (b) Hattori,
15 K.; Kido, Y.; Yamamoto, H.; Ishida, J.; Iwashita, A.; Mihara, K. Rational design of
16 conformationally restricted quinazolinone inhibitors of poly(ADP-ribose)polymerase. *Bioorg.*
17 *Med. Chem. Lett.* **2007**, *17*, 5577–5581.
18
19
20
21
22
23
24
25
26
27
28
29 (27) Eltze, T.; Boer, R.; Wagner, T.; Weinbrenner, S.; McDonald, M. C.; Thiemermann, C.;
30 Bürkle, A.; Klein, T. Imidazoquinolinone, imidazopyridine, and isoquinolindione derivatives as
31 novel and potent inhibitors of the poly(ADP-ribose) polymerase (PARP): a comparison with
32 standard PARP inhibitors. *Mol. Pharmacol.* **2008**, *74*, 1587-1598.
33
34
35
36
37
38
39 (28) (a) Varlamov, A. V.; Boltukhina, E. V.; Zubkov, F. I.; Sidorenko, N. V.; Chernyshev, A. I.;
40 Grudin, D. G. Preparative synthesis of 7-carboxy-2-R-isoindol-1-ones. *Chem. Heterocycl.*
41 *Compd.* **2004**, *40*, 22-28; (b) Medimag, R.; Marque, S.; Prim, D.; Chatti, S. 5-Amino-2-
42 furylmethylamines – appealing precursors of amino-isoindolinones? *Synthesis* **2010**, 770-774; (c)
43 Ball, M.; Boyd, A.; Churchill, G.; Cuthbert, M.; Drew, M.; Fielding, M.; Ford, G.; Frodsham, L.;
44 Golden, M.; Leslie, K.; Lyons, S.; McKeever-Abbas, B.; Stark, A.; Tomlin, P.; Gottschling, S.;
45 Hajar, A.; Jiang, J.-l.; Lo, J.; Suchozak, B. Isoindolone formation via intramolecular Diels-Alder
46 reaction. *Org. Process Res. Dev.* **2012**, *16*, 741-747; (d) Zaytsev, V. P.; Mikhailova, N. M.;
47
48
49
50
51
52
53
54
55
56
57
58
59
60

1
2
3 Airiyan, I. K.; Galkina, E. V.; Golubev, V. D.; Nikitina, E. V.; Zubkov, F. I.; Varlamov, A. V.

4
5 Cycloaddition of furfurylamines to maleic anhydride and its substituted derivatives. *Chem.*

6
7
8 *Heterocycl. Compd.* **2012**, *48*, 505-513; (e) De Cesco, S.; Deslandes, S.; Therrien, E.; Levan, D.;

9
10 Cueto, M.; Schmidt R.; Cantin, L.-D.; Mittermaier, A.; Juillerat-Jeanneret, L.; Moitessier, N.

11
12 Virtual screening and computational optimization for the discovery of covalent prolyl

13
14 oligopeptidase inhibitors with activity in human cells. *J. Med. Chem.* **2012**, *55*, 6306–6315.

15
16
17
18 (29) (a) Zubkov, F. I.; Boltukhina, E. V.; Turchin, K. F.; Borisov, R. S.; Varlamov, A. V. New
19
20 synthetic approach to substituted isoindolo[2,1-*a*]quinoline carboxylic acids via intramolecular

21
22 Diels-Alder reaction of 4-(*N*-furyl-2)-4-arylamino-butenes-1 with maleic anhydride. *Tetrahedron*

23
24 **2005**, *61*, 4099-4113; (b) Boltukhina, E. V.; Zubkov, F. I.; Nikitina, E. V.; Varlamov, A. V.

25
26 Novel approach to isoindolo[2,1-*a*]quinolines: synthesis of 1- and 3-halo-substituted 11-oxo-

27
28 5,6,6a,11-tetrahydroisoindolo[2,1-*a*]quinoline-10-carboxylic acids. *Synthesis* **2005**, 1859-1875.

29
30
31 (30) Gandhi, V. B.; Luo, Y.; Liu, X.; Shi, Y.; Klinghofer, V.; Johnson, E. F.; Park, C.; Giranda,

32
33 V. L.; Penning, T. D.; Zhu, G.-D. Discovery and SAR of substituted 3-oxoisoindoline-4-

34
35 carboxamides as potent inhibitors of poly(ADP-ribose) polymerase (PARP) for the treatment of

36
37 cancer. *Bioorg. Med. Chem. Lett.* **2010**, *20*, 1023–1026.

38
39
40 (31) Mei, T.-S.; Giri, R.; Mangel, N.; Yu, J.-Q. Pd^{II}-Catalyzed monoselective *ortho* halogenation
41
42 of C-H bonds assisted by counter cations: a complementary method to directed *ortho* lithiation.

43
44
45 *Angew. Chem. Int. Ed.* **2008**, *47*, 5215-5219.

46
47
48 (32) Jagtap, P. G.; Southan, G. J.; Baloglu, E.; Ram, S.; Mabley, J. G.; Marton, A.; Salzman, A.;

49
50 Szabo, C. The discovery and synthesis of novel adenosine substituted 2,3-dihydro-1H-isoindol-1-

1
2
3 ones: potent inhibitors of poly(ADP-ribose) polymerase-1 (PARP-1). *Bioorg. Med. Chem. Lett.*
4
5 **2004**, *14*, 81–85.

6
7
8
9 (33) Papeo, G. M. E.; Anatolievna Busel, A.; Khvat, A.; Krasavin, M. Y.; Forte, B.; Zuccotto, F.
10
11 3-oxo-2,3-dihydro-1*H*-isoindole-4-carboxamides as PARP inhibitors. Patent WO2011/006794.

12
13
14 (34) Kim, E. S.; Lee, H. S.; Kim, S. H.; Kim, J. N. An efficient InCl_3 -catalyzed hydration of
15
16 nitriles to amides: acetaldoxime as an effective water surrogate. *Tetrahedron Lett.* **2010**, *51*,
17
18 1589-1591.

19
20
21 (35) Li, J.-H.; Zhang, J.; Jackson, P. F.; Maclin, K. M. Compounds, methods and pharmaceutical
22
23 compositions for treating neural or cardiovascular tissue damage. U.S. Patent 6306889, **2001**.

24
25
26 (36) (a) Abad-Zapatero, C. Ligand efficiency indices for effective drug discovery. *Expert Opin.*
27
28 *Drug Discov.* **2007**, *2*, 469-488; (b) Abad-Zapatero, C.; Perišić, O.; Wass, J.; Bento, A. P.;
29
30 Overington, J.; Al-Lazikani, B.; Johnson, M. E. Ligand efficiency indices for an effective
31
32 mapping of chemico-biological space: the concept of an atlas-like representation. *Drug Discov.*
33
34 *Today* **2010**, *15*, 804-811.

35
36
37 (37) (a) Lord, A.-M.; Mahon, M. F.; Lloyd, M. D.; Threadgill, M. D. Design, synthesis and
38
39 evaluation *in vitro* of quinoline-8-carboxamides, a new class of poly(adenosine-diphosphate-
40
41 ribose)polymerase-1 (PARP-1) inhibitor. *J. Med. Chem.* **2009**, *52*, 868–877; (b) Gorobets, N. Y.;
42
43 Yermolayev, S. A.; Gurley, T.; Gurinov, A. A.; Tolstoy, P. M.; Shenderovich, I. G.; Leadbeater,
44
45 N. E. Difference between ^1H NMR signals of primary amide protons as a simple spectral index
46
47 of the amide intramolecular hydrogen bond strength. *J. Phys. Chem.* **2012**, *25*, 287-295.
48
49
50
51
52
53
54
55
56
57
58
59
60

1
2
3 (38) Abraham, M. H.; Abraham, R. J.; Acree, W. E., Jr.; Aliev, A. E.; Leo, A. J. An NMR
4 Method for the Quantitative Assessment of Intramolecular Hydrogen Bonding; Application to
5
6 Physicochemical, Environmental, and Biochemical Properties. *J. Org. Chem.* **2014**, *79*, 11075-
7
8 11083.
9

10
11
12
13 (39) As the K_D sensitivity limit of the fluorescence polarization assay used to evaluate the
14 biochemical potency of the inhibitors is 0.030 μM , a $K_D \geq 2 \mu\text{M}$ threshold against PARP-2 was
15 introduced to evaluate the selectivity of the compounds that reach the aforementioned assay limit
16 against PARP-1.
17
18
19
20

21
22 (40) The 4,4-difluorocyclohexyl moiety was chosen in light of its purported superior metabolic
23 stability compared to the corresponding unsubstituted cyclohexyl derivative. See, for example:

24
25 (a) Dorr, P.; Westby, M.; Dobbs, S.; Griffin, P.; Irvine, B.; Macartney, M.; Mori, J.; Rickett, G.;
26
27 Smith-Burchnell, C.; Napier, C.; Webster, R.; Armour, D.; Price, D.; Stammen, B.; Wood, A.;

28
29 Perros, M. Maraviroc (UK-427,857), a Potent, Orally Bioavailable, and Selective Small-
30
31 Molecule Inhibitor of Chemokine Receptor CCR5 with Broad-Spectrum Anti-Human
32
33 Immunodeficiency Virus Type 1 Activity. *Antimicrob. Agents Chemother.* **2005**, *49*, 4721-4732;

34
35 (b) Kuduk, S. D.; Chang, R. K.; DiPardo, R. M.; Di Marco, C. N.; Murphy, K. L.; Ranson, R.
36
37 W.; Reiss, D. R.; Tang, C.; Prueksaritanont T.; Pettibone, D. J.; Bock, M. G. Bradykinin B_1
38
39 receptor antagonists: An α -hydroxy amide with an improved metabolism profile. *Bioorg. Med.*
40
41
42
43
44
45
46
47
48
49
50
51
52
53
54
55
56
57
58
59
60
Chem. Lett. **2008**, *18*, 5107–5110.

51 (41) Robichaud, J.; Black, W. C.; Thérien, M.; Paquet, J.; Oballa, R. M.; Bayly, C. I.; McKay, D.
52
53 J.; Wang, Q.; Isabel, E.; Léger, S.; Mellon, C.; Kimmel, D. B.; Wesolowski, G.; Percival, M. D.;
54
55 Massé, F.; Desmarais, S.; Falguyret, J.-P.; Crane, S. N. Identification of a nonbasic, nitrile-

1
2
3 containing cathepsin K inhibitor (MK-1256) that is efficacious in a monkey model of
4 osteoporosis. *J. Med. Chem.* **2008**, *51*, 6410–6420.
5
6
7

8
9 (42) Boundra, M. T.; Bolin, C.; Chiker, S.; Fouquin, A.; Zaremba, T.; Vaslin, L.; Biard, D.;
10 Cordelières, F. P.; Mégnin-Chanet, F.; Favoudon, V.; Fernet, M.; Pennaneach, V.; Hall, J. PARP-
11 2 depletion results in lower radiation cell survival but cell line specific differences in poly(ADP-
12 ribose) levels. *Cell. Mol. Life Sci.* **2015**, *72*, 1585-1597.
13
14
15
16
17

18
19 (43) Karlberg, T.; Hammarström, M.; Schütz, P.; Svensson, L.; Schüler, H. Crystal Structure of
20 the Catalytic Domain of Human PARP2 in Complex with PARP Inhibitor ABT-888.
21
22
23
24 *Biochemistry* **2010**, *49*, 1056-1058.
25
26

27
28 (44) Colombo, M.; Riccardi-Sirtori, F.; Rizzo, V. A fully automated method for accurate mass
29 determination using high-performance liquid chromatography with a quadrupole/orthogonal
30 acceleration time-of-flight mass spectrometer. *Rapid Commun. Mass Spectrom.* **2004**, *18*, 511-
31 517.
32
33
34
35
36

37
38 (45) Felder, E. R.; Badari, A.; Disingrini, T.; Mantegani, S.; Orrenius, C.; Avanzi, N.; Isacchi,
39 A.; Salom, B. The generation of purinome-targeted libraries as a means to diversify ATP-
40 mimetic chemical classes for lead finding. *Mol. Diversity* **2012**, *16*, 27-51.
41
42
43
44

45
46 (46) Licensed by: GraphPad Software, Inc. 7825 Fay Avenue, Suite 230 La Jolla, CA 92037
47
48
49 USA.
50

51
52 (47) Leslie, A. G. W. Integration of macromolecular diffraction data. *Acta Crystallogr., Sect. D:*
53
54
55
56
57
58
59
60 *Biol. Crystallogr.* **1999**, *55*, 1696–1702.

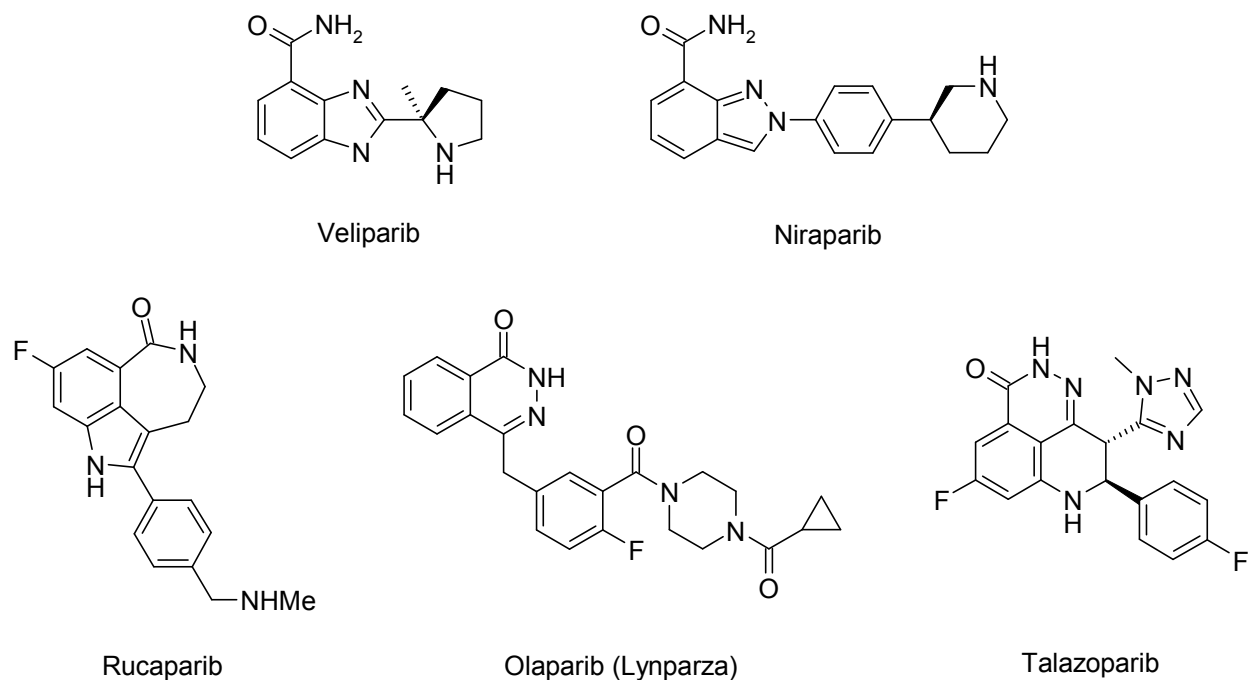
1
2
3 (48) Bailey, S. The CCP4 suite: programs for protein crystallography. *Acta Crystallogr., Sect. D:*
4
5 *Biol. Crystallogr.* **1994**, *50*, 760–763.
6
7

8
9 (49) Murshudov, G. N.; Vagin, A. A.; Dodson, E. J. Refinement of Macromolecular Structures
10
11 by the Maximum-Likelihood Method. *Acta Crystallogr., Sect. D: Biol. Crystallogr.* **1997**, *53*,
12
13 240-255.
14
15

16
17 (50) Emsley, P.; Cowtan, K. Coot: model-building tools for molecular graphics. *Acta*
18
19 *Crystallogr., Sect. D: Biol. Crystallogr.* **2004**, *60*, 2126–2132.
20
21

22
23 (51) Beria, I.; Ballinari, D.; Bertrand, J. A.; Borghi, D.; Bossi, R. T.; Brasca, M. G.; Cappella, P.;
24
25 Caruso, M.; Ceccarelli, W.; Ciavolella, A.; Cristiani, C.; Croci, V.; De Ponti, A.; Fachin, G.;
26
27 Ferguson, R. D.; Lansen, J.; Moll, J. K.; Pesenti, E.; Poster, H.; Perego, R.; Rocchetti, M.;
28
29 Storici, P.; Volpi, D.; Valsasina, B. Identification of 4,5-dihydro-1*H*-pyrazolo[4,3-*h*]quinazoline
30
31 derivatives as a new class of orally and selective polo-like kinase 1 inhibitors. *J. Med. Chem.*
32
33 **2010**, *53*, 3532-3551.
34
35
36

37
38 (52) Kerns, E. H.; Di, L.; Petusky, S.; Farris, M.; Ley, R.; Jupp, P. Combined application of
39
40 parallel artificial membrane permeability assay and Caco-2 permeability assays in drug
41
42 discovery. *J. Pharm. Sci.* **2004**, *93*, 1440-1453.
43
44
45
46
47
48
49
50
51
52
53
54
55
56
57
58
59
60



28 **Figure 1.** Examples of PARP inhibitors clinical candidates

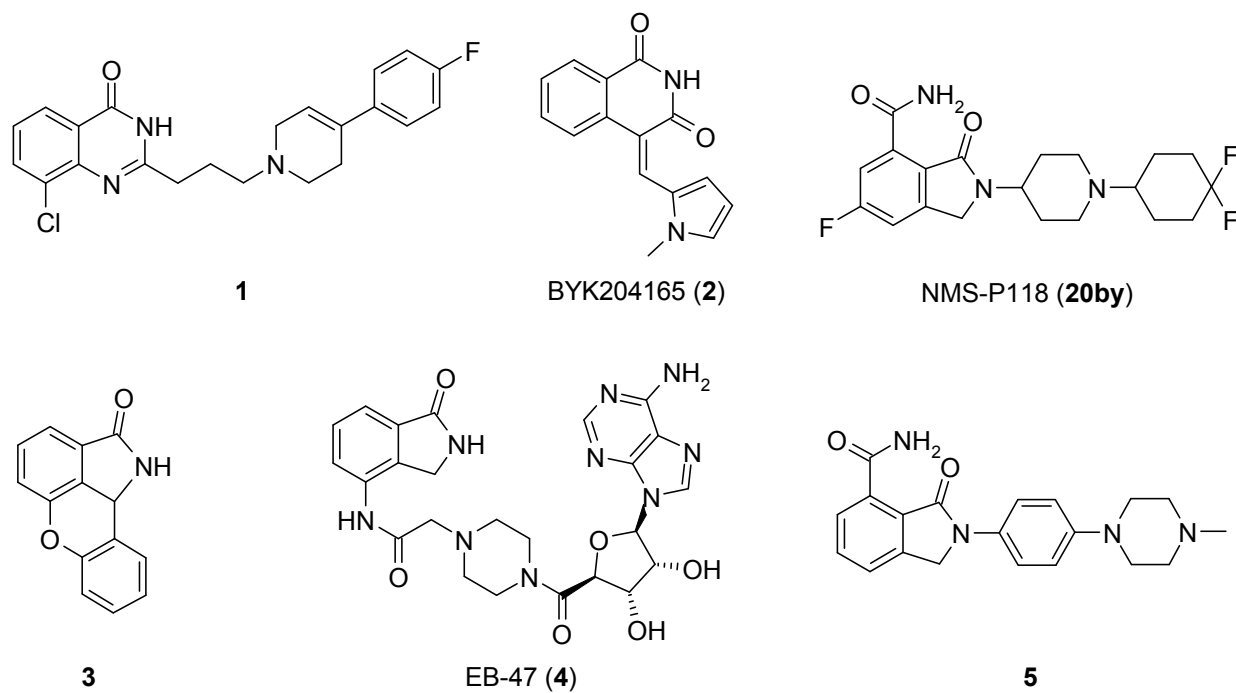
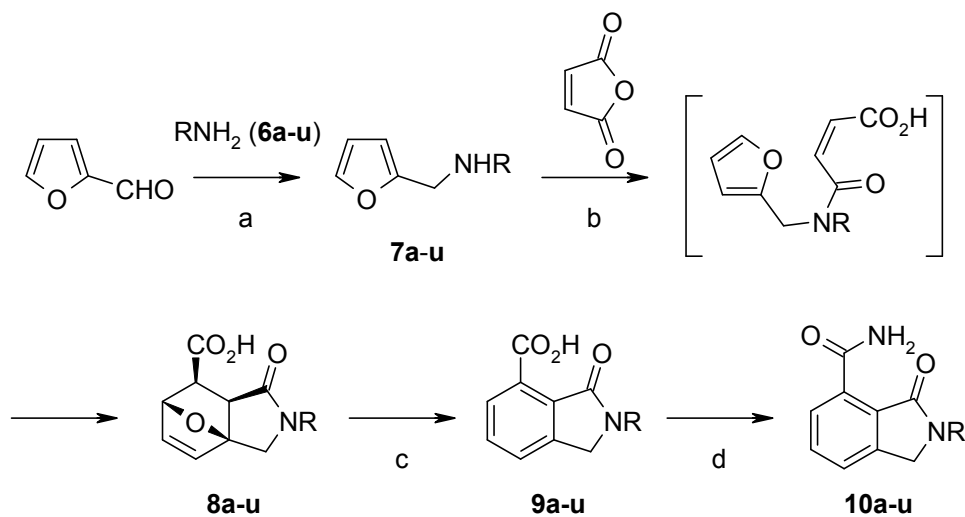


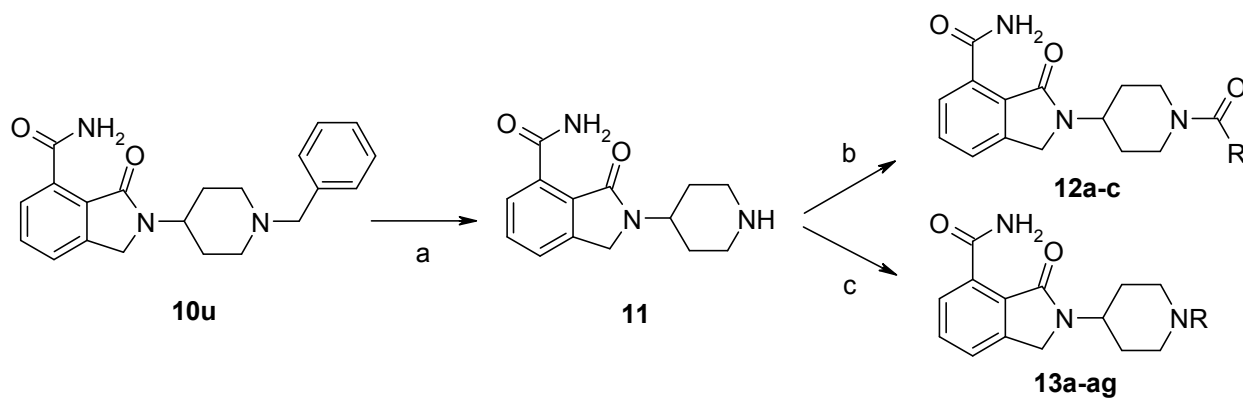
Figure 2. PARP-1 Selective inhibitors (**1**, **2**), NMS-P118 (**20by**) and isoindolinone-containing compounds (**3-5**)

Scheme 1A. Isoindolinones synthesis via intramolecular Diels-Alder reaction^a



^a Conditions: (a) RNH₂ (**6**), dioxane or toluene (Dean-Stark), reflux then NaBH₄, ethanol, rt; (b) maleic anhydride, THF, rt or toluene, reflux; (c) concentrated aqueous hydrochloric acid, reflux; (d) HOBt·NH₃, EDCI·HCl, DIEA, DMF, rt.

Scheme 1B. Elaboration of the piperidin-4-yl- moiety of intermediate **11**^a



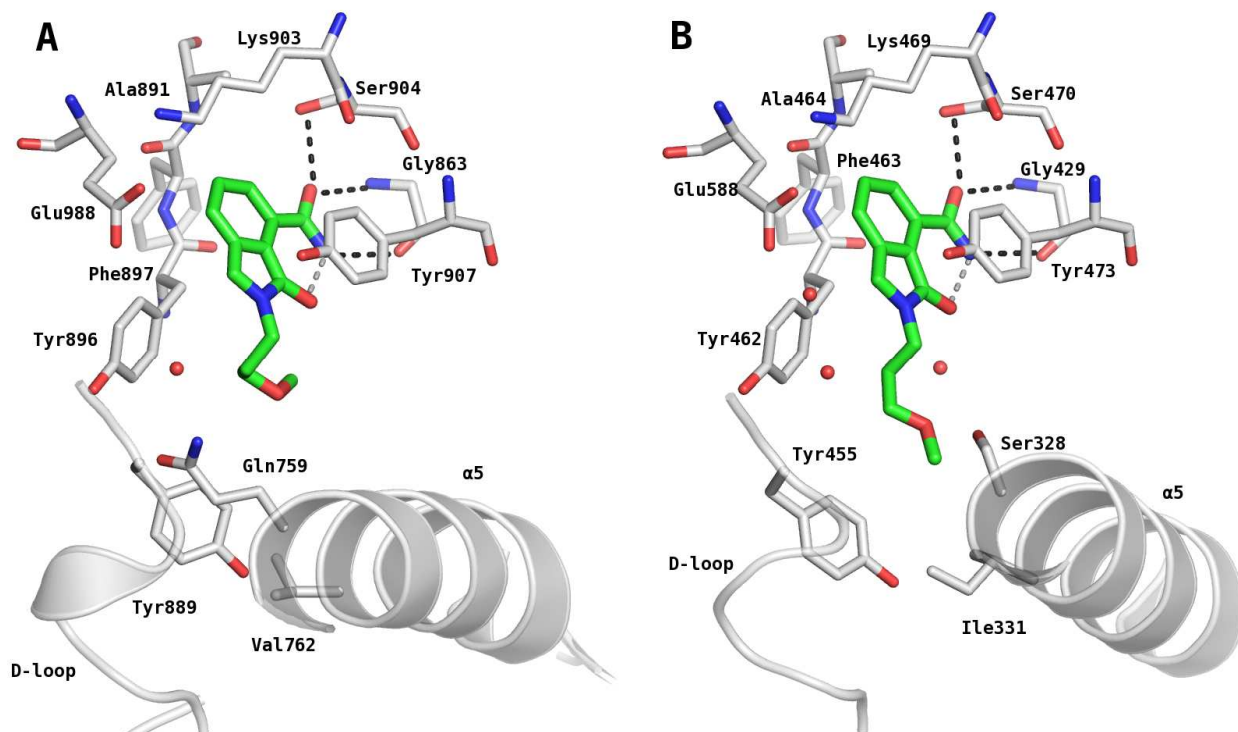


Figure 3. Co-crystal structures of **10b** with hPARP-1 (A) (PDB code 4ZZZ) and hPARP-2 (B) (PDB code 4ZZX) catalytic domain at 1.9 and 1.7 Å resolution, respectively.

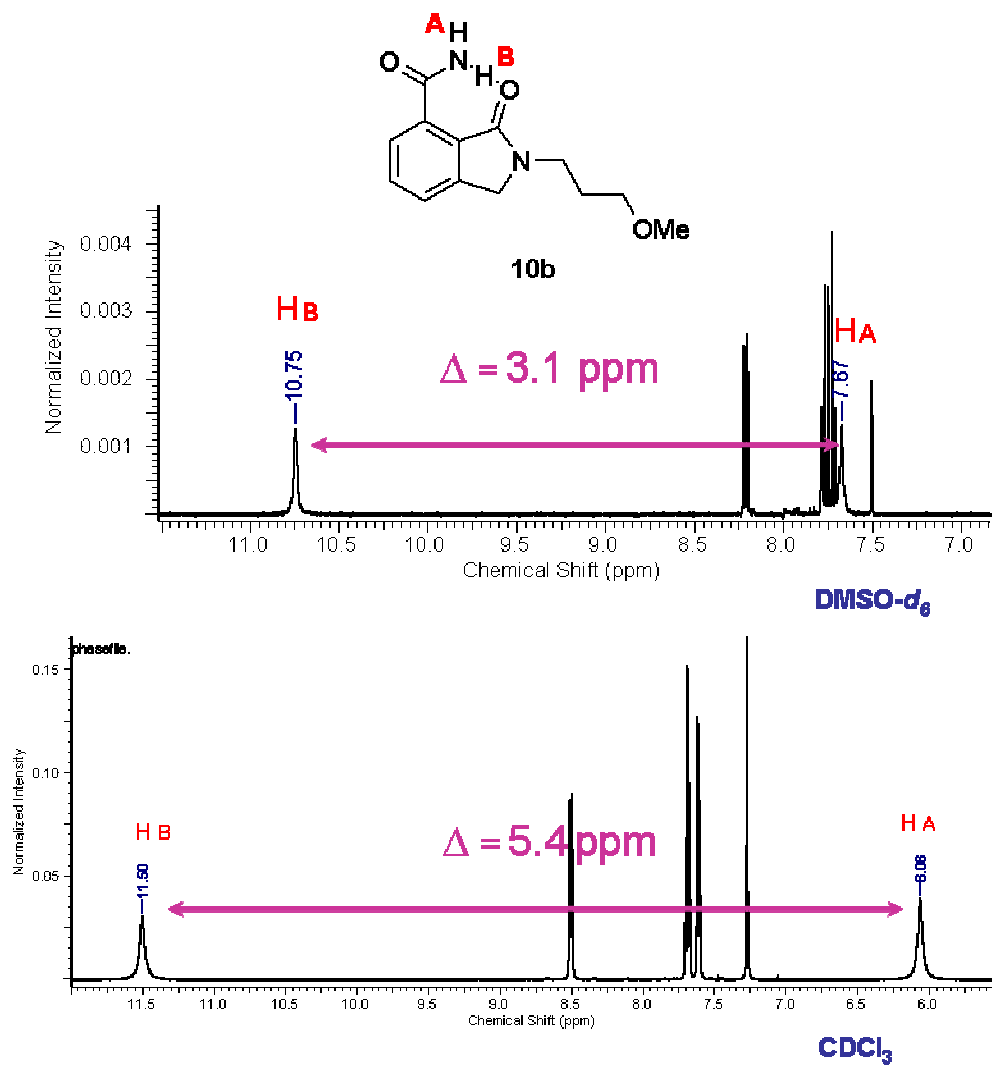


Figure 4. Downfield portion of ^1H NMR spectra of a 3 mM solution of **10b** in $\text{DMSO-}d_6$ (**A**) and CDCl_3 (**B**) showing the $\Delta\delta$ of the two amide protons.

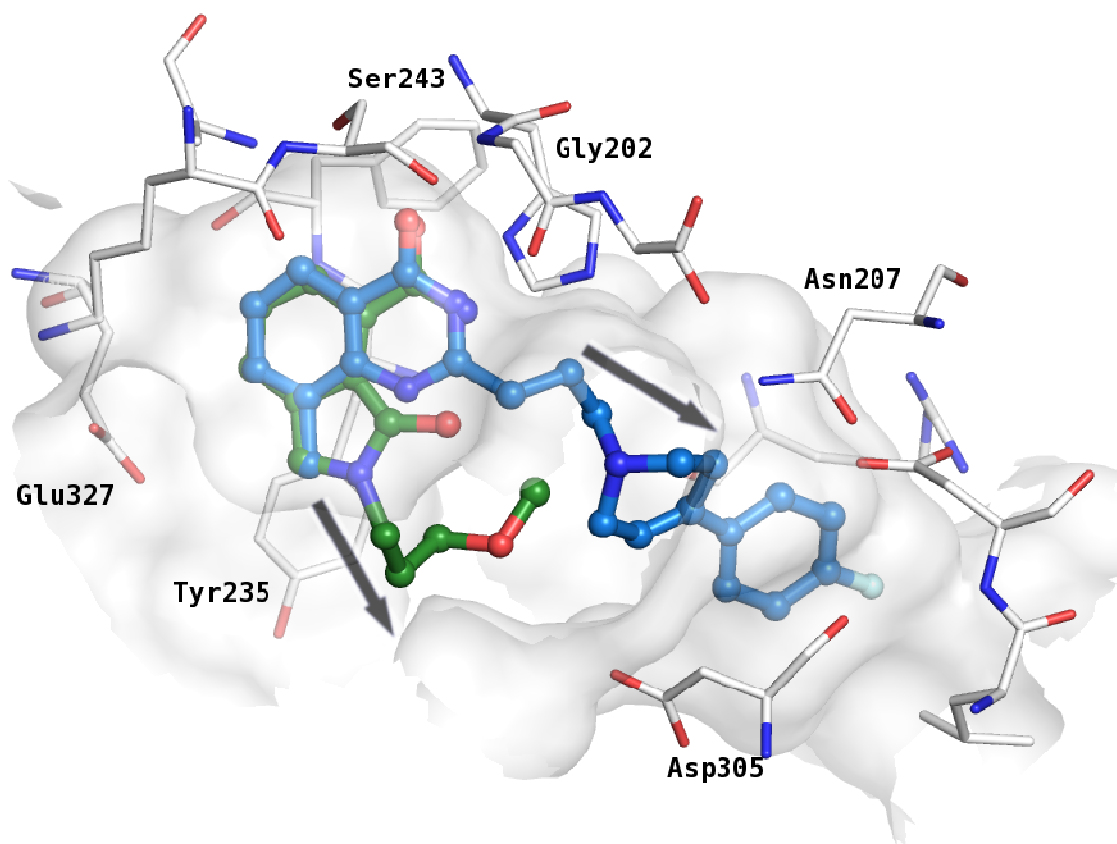


Figure 5. Overlay of co-crystal structures of **10b** (green carbon atoms PDB code 4ZZZ) and quinazolinone **1** (light blue carbon atoms, PDB code 1UK0) in the hPARP-1 binding site. Grey arrows indicate the direction of substituents departing from the nicotinamide-mimic scaffolds.

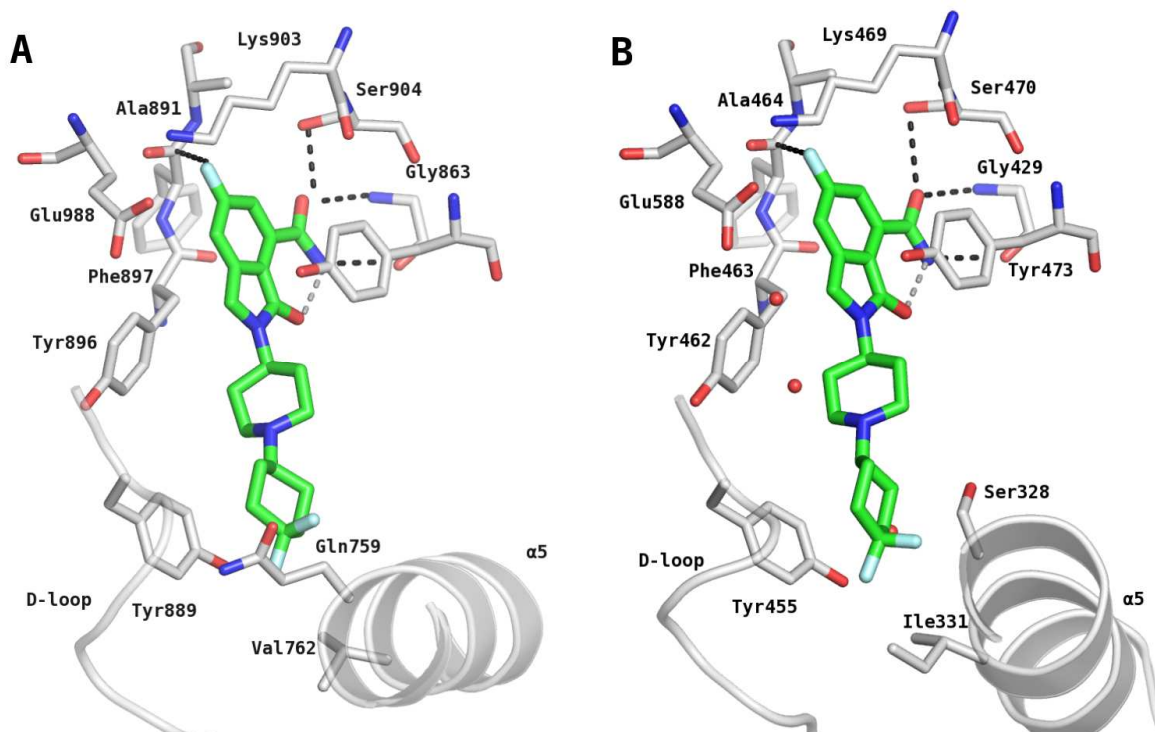


Figure 6. Co-crystal structures of **20by** with hPARP-1 (**A**) (PDB code 5A00) and hPARP-2 (**B**) (PDB code 4ZZY) catalytic domain at 2.7 and 2.2 Å resolution, respectively.

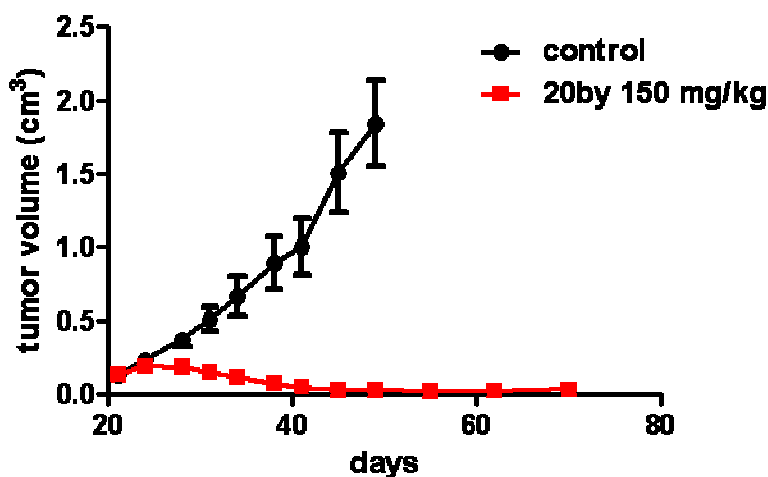


Figure 7. Anti-tumor efficacy of **20by** in BRCA mutated breast cancer model in mice. Mice carrying subcutaneous MDA-MB-436 human breast carcinoma were treated with either vehicle or **20by** orally administered. Mice were treated once a day for 28 days starting from day 20. Data are represented as mean \pm SEM.

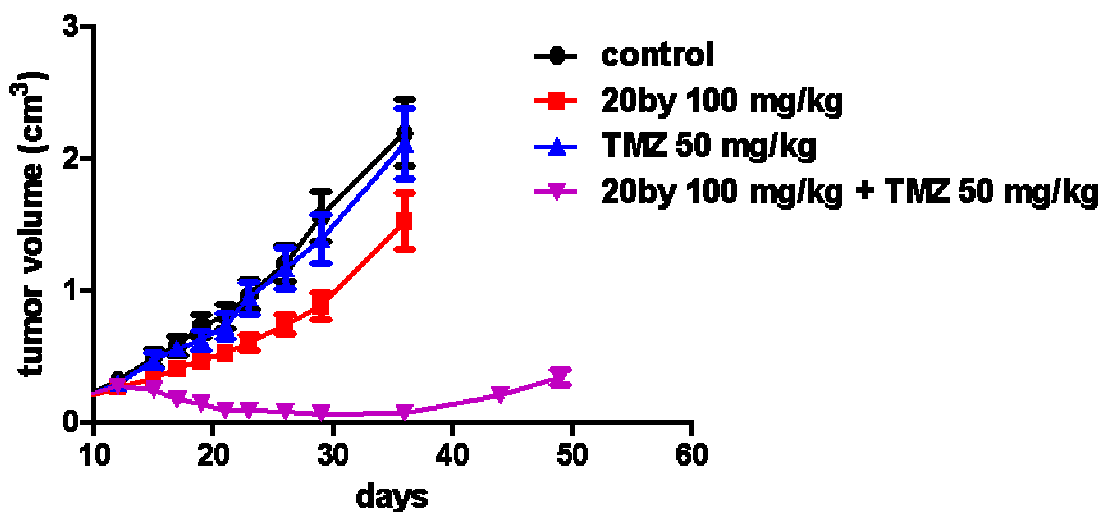


Figure 8. Anti tumor efficacy of 20by in combination with temozolomide 20by was administered to male athymic nu/nu mice carrying subcutaneously Capan-1 pancreatic cancer, orally once daily for 12 days at the dose of 100 mg/kg, starting on day 9. Temozolomide (TMZ) was administered at a dosage of 50 mg/kg for 5 days starting from day 11. Data are represented as mean \pm SEM.

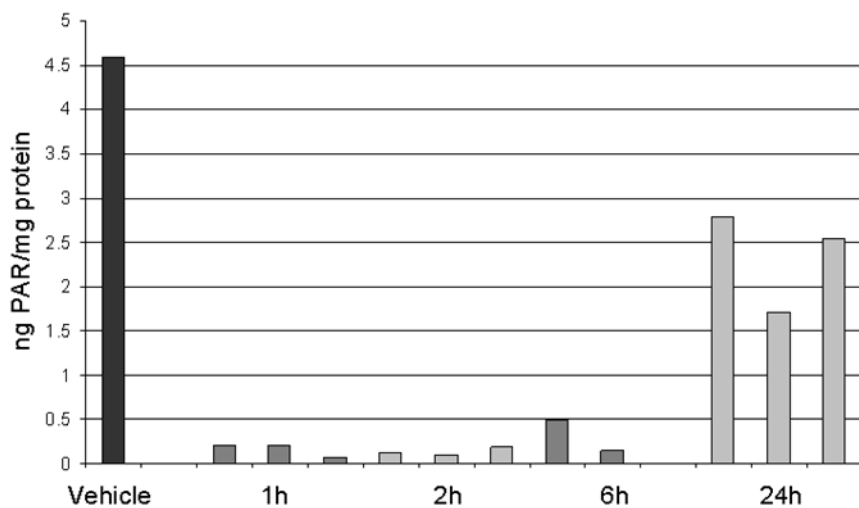
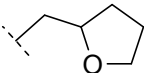
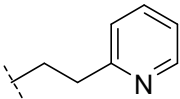
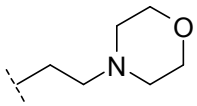
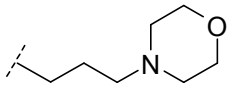
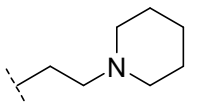
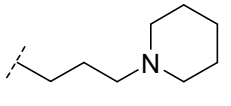
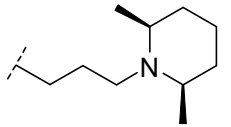
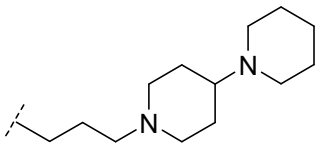
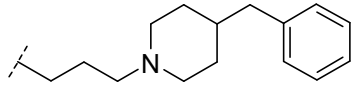
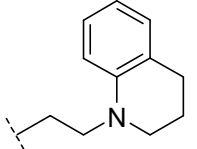
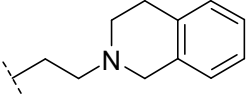
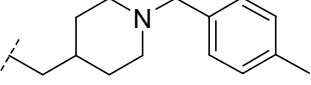
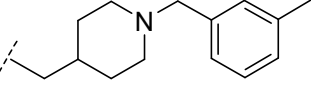
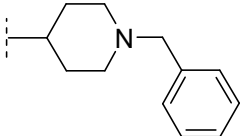


Figure 9. In vivo inhibition of PAR activity. Mice were treated with a single oral dose of **20by** (100 mg/kg) and intratumoral levels of PAR were assessed by ELISA at 1, 2, 6 and 24 hours after dosing. Each bar represents an individual tumor from an individual animal.

Table 1. Isoindolinones preliminary SAR investigation.

					
Cpd #	R	PARP-1 K_D (μM) ^a	PARP-2 K_D (μM) ^a	PARP-2 K_D / PARP-1 K_D ³⁹	PAR IC_{50} (μM) ^a
10a	-(CH ₂) ₂ CH ₃	0.084	0.422	5	1.14
10b	-(CH ₂) ₃ OCH ₃	0.087	0.125	1.4	5.30
10c	-(CH ₂) ₂ OCH ₃	0.220	-	-	-
(±)-10d		0.760	-	-	-
10e	-(CH ₂) ₂ OH	0.090	0.575	6.4	-
10f	-CH ₂ C ₆ H ₅	0.320	-	-	-
10g	-(CH ₂) ₂ C ₆ H ₅	0.032	0.178	5.6	-
10h	-(CH ₂) ₃ C ₆ H ₅	0.033	0.286	8.7	-
10i		< 0.030 ^b	< 0.030	1	-

10j		0.160	-	-	-
10k		0.035	5.870	168	2.15
10l		0.290	-	-	-
10m		< 0.030	3.360	> 112	0.20
<i>cis</i> -10n		0.330	-	-	-
10o		2.590	-	-	-
10p		0.049	0.670	14	-
10q		0.056	0.420	7.5	-

10r		< 0.030	5.776	> 193	2.25
10s		0.031	1.112	36	-
10t		< 0.030	2.600	> 87	0.04
10u		0.050	> 10	> 200	2.00

^a K_D and IC_{50} values are reported as the mean of 2-3 experiments.

^b Fluorescence polarization displacement assay sensitivity limit (see ref. 21).

Table 2. *In vitro* ADME parameters and PK data of compound **10t**.

ADME parameters	PK parameters			
		10 mg/kg	10 mg/kg	
		IV administration	Oral administration	
Solubility pH 7 (μM)	> 225	C_{max} (μM)	4.9 ± 0.4	0.03 ± 0.0
Permeability PAMPA				
Papp				
[10^{-6} cm/s]	50.0 (20.8)	AUC_{∞} ($\mu\text{M}\cdot\text{h}$)	2.0 ± 0.2	0.02 ± 0.0
(% in membrane)				
PPB ^c (%)	98	CL (mL/min/kg)	230.0 ± 27.5	
Intrinsic CL				
(mL/min/kg)	14	V_{ss} (L/kg)	3.4 ± 0.2	
HLM ^d				
		$t_{1/2}$ (h)	0.2 ± 0.0	nm ^e
		F^f (%)		< 1

^a Harlan Nu/Nu Mice; $n = 3$ animals per study.

1
2
3 ^b Dosed iv (intravenous administration): in situ prepared **10t** hydrochloride in 5% dextrose;
4
5
6 dosed per os (oral administration): 0.5% methocel.
7

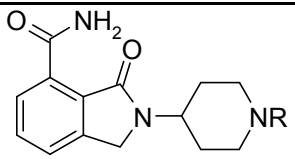
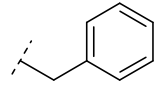
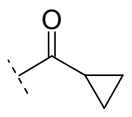
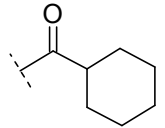
8
9 ^c Plasma protein binding.
10

11
12 ^d Human liver microsomes.
13

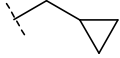
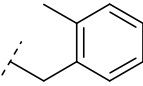
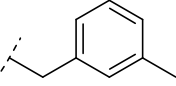
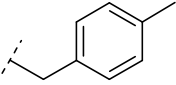
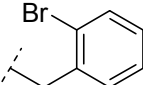
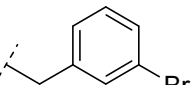
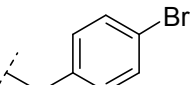
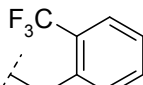
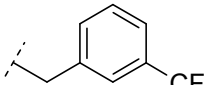
14
15 ^e nm: not measurable.
16

17
18 ^f Bioavailability.
19
20
21
22
23
24
25
26
27
28
29
30
31
32
33
34
35
36
37
38
39
40
41
42
43
44
45
46
47
48
49
50
51
52
53
54
55
56
57
58
59
60

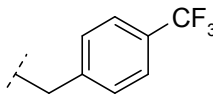
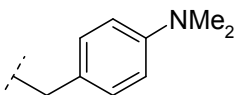
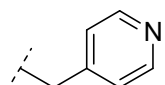
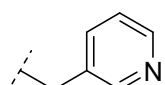
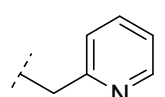
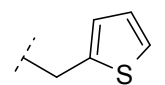
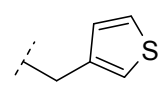
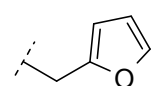
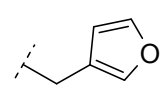
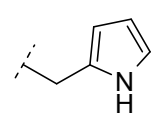
Table 3. Piperidin-4-yl substituted isoindolinones SAR investigation.^a

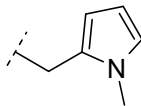
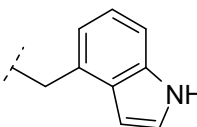
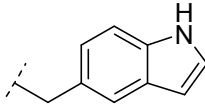
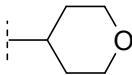
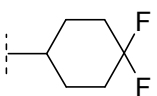
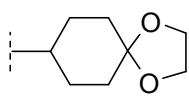
					
Cpd #	R	PARP-1 K _D (μM) ^b	PARP-2 K _D (μM) ^b	PARP-2 K _D / PARP-1 K _D ³⁹	HeLa IC ₅₀ (μM) ^b
10u		0.050	> 10	> 200	2.00
12a		0.250	-	-	-
12b		0.150	-	-	-
12c		0.350	-	-	-
13a	-CH ₃	< 0.030 ^c	0.033	-	-
13b	-CH ₂ CH ₃	< 0.030	0.340	-	-
13c	-CH(CH ₃) ₂	< 0.030	0.075	-	-
13d	-CH ₂ CH(CH ₃) ₂	< 0.030	0.264	-	-

1
2
3
4
5
6
7
8
9
10
11
12
13
14
15
16
17
18
19
20
21
22
23
24
25
26
27
28
29
30
31
32
33
34
35
36
37
38
39
40
41
42
43
44
45
46
47
48
49
50
51
52
53
54
55
56
57
58
59
60

13e		< 0.030	0.441	-	-
13f	-(CH ₂) ₂ OCH ₃	0.113	-	-	-
13g		0.042	> 10	> 238	1.10
13h		< 0.030	8.714	> 290	9.90
13i		< 0.030	8.991	> 300	0.11
13j		0.034	6.916	203	> 10
13k		0.053	2.289	43	-
13l		< 0.030	2.425	> 81	6.00
13m		0.41	-	-	-
13n		0.046	> 10	> 217	3.00

1
2
3
4
5
6
7
8
9
10
11
12
13
14
15
16
17
18
19
20
21
22
23
24
25
26
27
28
29
30
31
32
33
34
35
36
37
38
39
40
41
42
43
44
45
46
47
48
49
50
51
52
53
54
55
56
57
58
59
60

13o		0.054	3.627	67	-
13p		0.039	> 10	> 256	6.60
13q		0.050	> 10	> 200	5.40
13r		0.072	6.804	> 95	13.40
13s		0.042	> 10	> 238	0.37
13t		< 0.030	1.435	-	-
13u		< 0.030	3.700	> 123	1.00
13v		< 0.030	1.698	-	-
13z		< 0.030	0.583	-	-
13aa		< 0.030	0.983	-	-

1 2 3 4 5 6 7 8 9	13ab		0.050	> 10	> 200	1.60
10 11 12 13 14 15 16	13ac		0.034	2.510	74	-
17 18 19 20 21 22	13ad		< 0.030	3.017	> 100	0.10
23 24 25 26	13ae		< 0.030	> 10	> 330	0.56
27 28 29 30 31 32	13af		< 0.030	3.937	> 131	0.15
33 34 35 36 37 38	13ag		0.132	-	-	-

39
40
41
42
43
44
45
46
47
48
49
50
51
52
53
54
55
56
57
58
59
60

^a Intermediate **11** (Scheme 1B) was not tested as already reported not to be selective against PARP-2 (see ref. 30 for details).

^b K_D and IC_{50} values are reported as the mean of 2-3 experiments.

^c Fluorescence polarization displacement assay sensitivity limit (see ref. 21).

Table 4. *In vitro* ADME parameters of selected piperidin-4-yl substituted isoindolinones.

Cpd #	Solubility pH 7 (μM)	Permeability		
		PAMPA Papp [10^{-6} cm/s] (% in membrane)	PPB ^a (%)	CL (mL/min/kg) HLM ^b
13i	94	50.0 (31.0)	94	8
13ad	106	41.8 (36.1)	98	12
13af	> 225	28.8 (9.6)	85	7

^a Plasma protein binding.

^b Human liver microsomes.

Table 5. PK data of selected piperidin-4-yl substituted isoindolinones.

Cpd #	PK data ^a iv						PK data ^a per os				
	dose ^b : (mg/kg)	C_{max} (μ M)	AUC_{∞} (μ M·h)	CL (mL/min/kg)	V_{ss} (L/kg)	$t_{1/2}$ (h)	dose ^c : (mg/kg)	C_{max} (μ M)	AUC_{∞} (μ M·h)	$t_{1/2}$ (h)	F^d (%)
13i	10	9.7 ±	8.2 ±	57.8 ± 13.0	2.2 ± 0.2	0.5 ±	10	1.1 ±	0.8 ±	nm ^e	15
		0.9	1.8			0.1		0.2	0.2		
13ad	4	2.0 ±	1.8 ±	110.0 ± 40.8	4.9 ± 0.8	0.7 ±	10	1.0 ±	3.7 ±	1.7 ±	80
		0.1	0.9			0.5		0.3	0.4		
13af	10	6.8 ±	26.3 ±	17.1 ± 2.5	3.4 ± 0.3	2.8 ±	10	3.6 ±	21.0 ±	2.9 ±	80
		0.6	4.0			0.1		0.5	3.1		

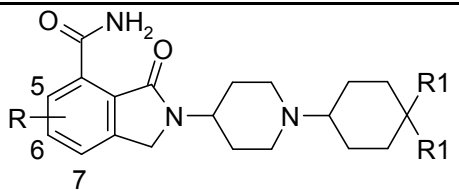
^a Harlan Nu/Nu Mice; $n = 3$ animals per study.

^b Dosed iv (intravenous administration): 5% Tween 80 in 5% dextrose for **13i**, PEG 400 in 5% dextrose for **13ad** and 10% Tween 80 in 5% dextrose for **13af**.

^c Dosed per os (oral administration): 0.5% methocel.

^d Bioavailability.

^e nm: not measurable.

Table 6. SAR investigation of phenyl substituted isoindolinones.


Cpd #	R	R1	PARP-1 K _D (μM) ^a	PARP-2 K _D (μM) ^a	PARP-2 K _D / PARP-1 K _D ³⁹	HeLa IC ₅₀ (μM) ^a
13af	H	F	< 0.030 ^b	3.937	> 131	0.15
20ay	5-F	F	1.880	-	-	-
20by	6-F	F	< 0.030	2.500	> 83	0.04
20cy	7-F	F	0.080	> 10	> 125	1.90
20dy	6-Cl	F	< 0.030	> 10	> 333	0.50
20bx	6-F	Cl	< 0.030	> 10	> 333	0.09

^a K_D and IC₅₀ values are reported as the mean of 2-3 experiments.

^b Fluorescence polarization displacement assay sensitivity limit (see ref. 21).

Table 7. ^1H NMR chemical shifts difference between amide protons of selected isoindolinones.^a

Cpd #	$\Delta\delta$ (ppm)
13af	3.07
20ay	0.24
20by	2.92
20cy	2.84
20dy	2.82

^a ^1H NMR spectra were recorded in $\text{DMSO-}d_6$ at 25 °C and 3 mM concentration.

Table 8. K_D values and dissociation equilibrium constants for PARP-1 and PARP-2 catalytic domain determined with Biacore T-100.

Cpd #	PARP-1 CD ^a		PARP-2 CD ^a	
	K_D (μM) ^b	$t_{1/2}$ (min) ^b	K_D (μM) ^b	$t_{1/2}$ (min) ^b
olaparib	0.00024 \pm 0.00012	51.12 \pm 1.10	0.00028 \pm 0.00013	17.40 \pm 0.30
veliparib	0.0017 \pm 0.0003	1.53 \pm 0.02	0.0058 \pm 0.0004	1.10 \pm 0.10
13af	0.0157 \pm 0.0005	1.68 \pm 0.028	1.219 \pm 0.305	0.07 \pm 0.0006
13c	0.075 \pm 0.007	0.2 \pm 0.06	0.118 \pm 0.031	0.2 \pm 0.068
20by	0.0086 \pm 0.0011	3.27 \pm 0.11	1.389 \pm 0.383	0.08 \pm 0.0008

^a CD: catalytic domain.

^b Reported values are the average and standard deviation of three independent experiments.

Table 9. Anti-proliferative activity on tumor cell lines.^a

Cpd #	IC ₅₀ (μM)		
	MDA-MB-436 (BRCA1 deficient)	Mcf-7	MIA-PACA
20by	0.14	>10	>10
13af	0.60	>10	>10

^a Cells were exposed to different doses of the indicated compounds for 10-14 days, after which colonies were counted and. IC₅₀ values were calculated.

Table 10. *In vitro* ADME parameters and PK data of compound **20by**.

ADME parameters		PK parameters					
		mouse ^a			rat ^b		
		iv ^c	oral ^c		iv ^d	oral ^d	
		10 mg/kg		10 mg/kg		100 mg/kg	
Solubility pH 7 (μM)	194	C_{max} (μM)	5.6 ± 0.1	5.2 ± 0.6	6.0 ± 0.7	2.8 ± 0.3	17.7 ± 1.1
Permeability PAMPA Papp [10 ⁻⁶ cm/s] (% in membrane)	29.1 (10.0)	AUC _∞ (μM·h)	20.7 ± 2.3	19.7 ± 5.2	40.0 ± 8.0	34 ± 2.9	251.0 ± 30.5
PPB ^e (%)	78	CL (mL/min/kg)	19.3 ± 2.3		10.8 ± 2.4		
CL (mL/min/kg) HLM ^f	5	V _{ss} (L/kg)	3.9 ± 0.1		3.5 ± 0.6		

CL (mL/min/kg)	5	$t_{1/2}$ (h)	3.3 ± 0.1	3.1 ± 0.1	4.7 ± 1.2	3.9 ± 0.1	nm ^g
rat hepatocytes		F^h (%)	95			87	65

^a Harlan Nu/Nu Mice; $n = 3$ animals per study.

^b Sprague Dawley Rat; $n = 3$ animals per study.

^c Dosed iv (intravenous administration): 10% Tween 80 in 5% dextrose; dosed per os (oral administration): 0.5% methocel.

^d Dosed iv (intravenous administration): 20% DMSO + 40% PEG 400 in 5% dextrose; dosed per os (oral administration): 0.5% methocel.

^e Plasma protein binding.

^f Human liver microsomes.

^g nm: not measurable.

^h Bioavailability

Table of Contents Graphic.

